Distribution Agreement

In presenting this thesis or dissertation as a partial fulfillment of the requirements for an advanced degree from Emory University, I hereby grant to Emory University and its agents the non-exclusive license to archive, make accessible, and display my thesis or dissertation in whole or in part in all forms of media, now or hereafter known, including display on the world wide web. I understand that I may select some access restrictions as part of the online submission of this thesis or dissertation. I retain all ownership rights to the copyright of the thesis or dissertation. I also retain the right to use in future works (such as articles or books) all or part of this thesis or dissertation.

Signature:

_____ _____

Yan Hong Date

Mutant Huntingtin Impairs Astrocytic Secretion

By

Yan Hong
Doctor of Philosophy

Graduate Division of Biological and Biomedical Sciences
Neuroscience

_____
Xiao-Jiang Li, M.D, Ph.D
Advisor

_____
Shi-Hua Li, M.D, Ph.D
Co-advisor

_____ _____
John Hepler, Ph.D Malu Tansey, Ph.D
Committee Member Committee Member

_____ _____
Thomas Kukar, Ph.D Lary Walker, Ph.D
Committee Member Committee Member

Accepted:

_____
Lisa A. Tedesco, Ph.D.
Dean of the James T. Laney School of Graduate Studies

_____
Date

Mutant Huntingtin Impairs Astrocytic Secretion

By

Yan Hong

M.D., Jinzhou Medical University, 2006

M.S., Dalian Medical University, 2010

Advisor: Xiao-Jiang Li, M.D., Ph.D.

Co-advisor: Shi-Hua Li, M.D.

An abstract of
A dissertation submitted to the Faculty of the
James T. Laney School of Graduate Studies of Emory University
in partial fulfillment of the requirements of the degree of
Doctor of Philosophy
in Graduate Division of Biological and Biomedical Sciences
Neuroscience
2017

Abstract

Mutant Huntingtin Impairs Astrocytic Secretion

By Yan Hong

Huntington's disease (HD) is a fatal, inherited, neurodegenerative disorder that affects one in every 10,000 Americans. To date, there is no effective treatment, in part because the pathogenic mechanism driving the disease is not fully understood. Expansion of a polyglutamine (polyQ) repeat in the N-terminal region of the HD protein, huntingtin (Htt), is the molecular basis of the disease. Although neuronal cells are preferentially degenerated in HD, the function of glial cells is also affected by mutant huntingtin (mHtt). Astrocytes and other glial cells can release a variety of functional cellular vesicles into the extracellular space to support the normal function and survival of neighboring neurons. My thesis work focused on two types of important vesicles, brain-derived neurotrophic factor (BDNF)-containing dense-core vesicles and heat shock protein-containing exosomes. Exosomes are small membranous vesicles that are secreted by multiple cell types and carry protein and genetic materials for cell-cell communication. Whether mHtt affects astrocytic secretion in the HD brain remains unknown. We used full-length HD knock-in (KI) mice to investigate the effect of mHtt on astrocytic secretion. Our results found that mHtt binds Rab3a, a small GTPase localized on membranes of dense-core vesicles, to affect its GTP/ GDP exchange; this impairs the docking of dense-core vesicles in HD astrocytes, resulting in decreased release of BDNF. Importantly, overexpression of Rab3a rescues impaired BDNF vesicle docking and secretion from astrocytes and alleviates HD early neuropathology in the HD KI mouse brain. Our results also demonstrated that mHtt reduces the expression of αB-crystallin, a small heat shock protein that mediates exosome secretion, in astrocytes. This effect reduces exosome secretion in HD brains, which could be alleviated by overexpression of αB-crystallin. These findings have revealed new pathological pathways that affect astrocytic secretion and contribute to non-cell-autonomous neurotoxicity in HD.

Mutant Huntingtin Impairs Astrocytic Secretion

By

Yan Hong

M.D., Jinzhou Medical University, 2006

M.S., Dalian Medical University, 2010

Advisor: Xiao-Jiang Li, M.D., Ph.D.

Co-advisor: Shi-Hua Li, M.D.

A dissertation submitted to the Faculty of the
James T. Laney School of Graduate Studies of Emory University
in partial fulfillment of the requirements of the degree of
Doctor of Philosophy
in Graduate Division of Biological and Biomedical Sciences
Neuroscience
2017

ACKNOWLEDGMENTS

I would like to thank my advisor, Dr. Xiao-Jiang Li, for his support and guidance throughout my graduate school career. He gave me the opportunity to study the role of mutant htt in astrocyte, which was not only interesting to me, but also had the potential to make a novel impact on the field. I would also like to thank my co-advisor, Dr. Shi-Hua Li, who provided valuable help and advice in technical aspects of experiments during my time in the lab. I thank both of my advisors for helping advance my career as a scientist. I will always remember the wonderful time we had in your house in holidays. I would also like to thank my committee members, Drs. John Hepler, Thomas Kukar, Malu Tansey, Lary Walker, who were very easy to work with and gave me helpful advice. They were crucial for the success of my work, and it was a pleasure to work with them. I would also like to thank the past and present lab members of the Li lab for their friendship and scientific expertise. I want to thank the entire faculty and staff in the Neuroscience program and the Department of Human Genetics. Of course, I would like to thank my parents, my grandmother, and other family members who have always encouraged me to pursue my dreams. They were almost 8000 miles away, but I could chat with them online when I missed them. Last but not least, I would like to thank my husband, Ting Zhao, who is also my lab member and my best friend. He is an amazing scientist and always gives me confidence and help when I need it. This work could not have been accomplished without his love and encouragement.

Table of Contents

Chapter 1: General Introduction……..... 1

1.1 Polyglutamine Disease.…… 2

1.2 Huntington's Disease…… 3

1.3 Glial Dysfunction in Huntington's Disease……..... 6

1.4 Neurotrophic Factors in Huntington's Disease……. 9

1.5 Exocytosis in Astrocytes…….. 11

1.6 Rab proteins in Huntington's Disease…….. 13

1.7 Roles of Exosomes in Neuron-Glia Communication…….15

1.8 Dissertation Goals……..17

Chapter 2: Materials and Methods…….. 27

2.1 Animals…….. 28

2.2 Antibodies and Reagents…… 28

2.3 Primary Cultures……..... 29

2.4 Preparation of ACM…… 29

2.5 Enzyme-Linked Immunosorbent Assays (ELISA)……. 30

2.6 Western Blotting……. 30

2.7 Glutamate Measurement…… 30

2.8 RT-qPCR.……... 31

2.9 Knockdown Assay……. 31

2.10 Stereotaxic Injection of Virus…….. 31

2.11 Preparation of Brain Slices……... 32

2.12 Rab3 GTPase Activity Assay……32

2.13 Total Internal Reflection Fluorescence (TIRF) microscopy……..... 33

2.14 Immunoprecipitation……. 34

2.15 Immunofluorescence Staining…….. 34

2.16 ATP Assay…… 35

2.17 Purification of Exosomes……. 35

2.18 Electron Microscopy and Immunogold Labeling……..... 36

2.19 Chromatin Immunoprecipitation (ChIP)…….. 37

2.20 Statistical Analyses…….. 37

Chapter 3: Mutant Huntingtin Impairs BDNF Release from Astrocytes by Disrupting Conversion of Rab3a-GTP into Rab3a-GDP…… 38

3.1 Abstract……. 39

3.2 Introduction…… 40

3.3 Results…… 41

3.4 Discussion…….. 50

Chapter 4: Mutant Huntingtin Inhibits αB-crystallin Expression and Impairs Exosome Secretion From Astrocytes…… 73

4.1 Abstract……... 74

4.2 Introduction……. 74

4.3 Results…… 76

4.4 Discussion…….. 83

Chapter 5: General Conclusions and Future Directions…….. 103

5.1 Summary……..104

5.2 Future Directions……109

5.3 Conclusions…… 112

References……116

List of Tables and Figures

Chapter 1: General Introduction

Table 1.1 Poly Q disease…….. 18

Figure 1.1 Poly Q expansion ……19

Figure 1.2 Huntingtin protein……....21

Figure 1.3 BDNF sources for MSNs…….23

Figure 1.4 Synthesis, storage and release of BDNF …….25

Chapter 3: Mutant Huntingtin Impairs BDNF Release from Astrocytes by Disrupting Conversion of Rab3a-GTP into Rab3a-GDP

Figure 3.1 BDNF secretion from HD astrocytes is reduced…… 55

Figure 3.2 Transcription or translation of BDNF is not changed in the HD astrocytes... 57

Figure 3.3 MHtt associates with Rab3a in astrocytes…….. 59

Figure 3.4 Reduced association between Rab3-GAP1 and Rab3a by mHtt results in increased GTP-Rab3a in HD astrocytes…….. 61

Figure 3.5 Overexpression of Rab3a rescues defective release of BDNF from HD astrocytes……. 63

Figure 3.6 Overexpression of Rab3a rescues the deficient release of ATP from HD

astrocytes……. 65

Figure 3.7 Defective docking of BDNF- and ATP-containing vesicles is rescued by Rab3a overexpression in HD astrocytes…….. 67

Figure 3.8 Overexpression of Rab3a reduces reactive astrocytes in the striatum of HD140Q KI mice…… 69

Figure 3.9 Proposed model for the decreased dense core vesicles released from HD astrocytes…… 71

Chapter 4: Mutant Huntingtin Inhibits αB-crystallin Expression and Impairs Exosome Secretion From Astrocytes

Figure 4.1 mHtt is not present in the exosomes released by cultured astrocytes……..87

Figure 4.2 Astrocytic exosomes reduce mHtt aggregate in the striatum of HD KI mice……..89

Figure 4.3 Exosome secretion is decreased from primary astrocyte cultures……...91

Figure 4.4 N-terminal fragments of mHtt impairs exosome secretion from cultured astrocytes……...93

Figure 4.5 mHtt decreases exosome secretion from KI mouse striatum……...95

Figure 4.6 mHtt impairs αB-crystallin expression both in cultured astrocytes and in the striatum…… 97

Figure 4.7 Sp1 mediates αB-crystallin expression in astrocytes…….. 99

Figure 4.8 Overexpression of αB-crystallin rescues defective exosome secretion from KI astrocytes……..101

Chapter 5: General Conclusions and Future Directions

Figure 5.1 Proposed model for the decreased astrocytic secretion…….114

Chapter 1

General Introduction

1.1 Polyglutamine disease

Polyglutamine (PolyQ) diseases represent a family of nine neurodegenerative disorders including Huntington's disease (HD), spinocerebellar ataxia (SCA) 1, 2, 3, 6, 7, 17, spinal and bulbar muscular atrophy (SBMA) and dentatorubral-pallidoluysian atrophy (DRPLA) (Li and Li, 2006; Zoghbi and Orr, 2000). PolyQ diseases are inherited, fatal neurodegenerative disorders caused by an expansion of a trinucleotide (CAG) repeat, encoding a polyQ tract, in the exonic regions of specific genes. These genes encode huntingtin, ataxin-1, ataxin-2, ataxin-3, CACNA1A, ataxin-7, TATA-binding protein, androgen receptor, and atrophin-1. All of these polyQ diseases are dominantly inherited, with the exception of SBMA, which is the only X-linked, recessively inherited polyQ disease (**Table 1.1**).

PolyQ diseases share several common features. First, polyQ diseases are late-onset disorders. Symptoms of these diseases usually appear in middle age and progressively worsen until death. A juvenile or early onset form also occurs for these polyQ diseases and is usually associated with more than 60 CAG repeats. Thus, the longer polyQ tracts lead to a greater severity of diseases presentation and a younger age of onset (Weber et al., 2014).

Second, although mutant polyQ proteins are ubiquitously expressed throughout the body, neurons are extremely sensitive to the toxicity of expanded polyQ proteins, and only specific types of neurons degenerate in each polyQ disease. For example, HD is characterized by the preferential loss of striatal medium spiny neurons (MSNs) (Ross and Tabrizi, 2011). SCAs mostly lead to degeneration of Purkinje neurons in the cerebellum (Zoghbi and Orr, 2000). SBMA is the X-linked, recessively inherited disease in the

polyQ disease family, and leads to motor neuron loss in the spinal cord and brain stem (Soukup et al., 2009). DRPLA is characterized by neuronal degeneration in the cerebellum (Schilling et al., 1999b). These differences suggest that the pathogenesis of polyQ diseases is highly protein context-dependent.

Finally, all polyQ diseases show aggregates formed by misfolded protein in patient brains, which are a pathological hallmark of the polyQ diseases (**Fig. 1.1**). The cellular location of the aggregates is also protein context-dependent. Whether aggregates are toxic or have a protective role remains controversial. For example, mutant Htt (mHtt) aggregates were mainly found in the nucleus and neuropil of postmortem HD patient brains (DiFiglia et al., 1997; Gutekunst et al., 1999). MHtt aggregates that accumulate in the nuclei and neuropil of cells interfere with gene transcription and axonal transport, respectively. However, emerging evidence shows that mHtt intranuclear aggregates are not directly correlated with neuronal death, because aggregate-containing neurons are also seen in non-degenerating regions. Also, emerging evidence shows that mHtt aggregates are not correlated with cell death in several HD animal models (Takahashi et al., 2008; Cisbani et al., 2012), suggesting that polyQ aggregates are either non-toxic or protective.

1.2 Huntington's disease

Huntington's disease (HD) was first described in the medical literature in 1872 by Dr. George Huntington. HD is the most common polyQ disorder, affecting approximately 5-10 individuals per 100,000 in worldwide populations (Harper, 1992; Driver-Dunckley E, 2007). It is caused by a polyglutamine (polyQ>37) expansion in the protein Huntingtin

(htt) (The Huntington's Disease Collaborative Research Group, 1993; Kremer et al., 1994). The average age of onset is 40 years, and death usually occurs 15-20 years after the onset of symptoms. The age of onset is inversely correlated with repeat length, and the presence of more than 60 CAG repeats results in juvenile HD, in which symptoms occur before the age of 20 (Duyao et al., 1993; Turmaine et al., 2000). HD symptoms consist of movement disorders (chorea), body weight loss, cognitive deficit, and psychiatric problems. To date, there is no effective treatment for HD, in part because the pathogenic mechanism driving the disease is not fully understood.

HD is caused by a mutation in the huntingtin gene located on chromosome 4 (The Huntington's Disease Collaborative Research Group, 1993). The polyQ domain begins at the 18th amino acid. Normal individuals usually have 11–34 glutamine residues, but HD patients contain more than 37 glutamines. Two proline-rich domains follow the polyQ domain. Htt also contains multiple HEAT (**H**untingtin, elongation factor 3 (**E**F3), a subunit of protein phosphatase 2**A** and **T**OR1) repeats that are also found in other cytoplasmic proteins, and may be involved in cytoplasmic-nuclear transport. HEAT repeats also form an α-helical structure that is important for protein-protein interactions, suggesting that huntingtin may function as a scaffold protein and facilitate protein complex formation. Unlike other large proteins of similar size, Htt is completely soluble, and normally is a cytoplasmic protein (Dragatsis et al., 2000). Htt is expressed ubiquitously, with the highest expression levels in the testes and brain, and the protein plays roles in clathrin-mediated endocytosis, vesicle transport, transcriptional regulation, and cell survival (Harjes and Wanker, 2003; Cattaneo et al., 2005; Brandstaetter et al., 2014). MHtt induces neuronal death by disrupting gene expression, axonal transport, and

mitochondrial functions (Crook et al., 2011; Tsunemi et al., 2012; Li et al., 2001) (**Fig. 1.2**).

The polyglutamine expansion is proposed to cause toxic gain of function. The PolyQ expansion results in abnormal association of htt with a variety of proteins, which may cause pathological changes in HD (Li and Li, 2004). For example, mHtt binds more strongly to several nuclear transcription factors, such as specificity protein 1 (Sp1), which, as a result, inhibits the association of Sp1 with the promoter of its target genes, and disrupts the transcriptional activity of genes that are important for neuronal function and survival (Chen-Plotkin et al., 2006; Li et al., 2002). Moreover, mHtt impairs mitochondrial function by binding to the TIM23 complex in the inner membrane of mitochondria to suppress mitochondrial protein import, which leads to neuronal death (Yano et al., 2014). Furthermore, htt normally associates with huntingtin-associated protein 1 (Hap1) in the cytoplasm. Hap1 forms a complex with htt and P150, a subunit of dynactin. This htt/Hap1/P150 complex is necessary for the transport of brain-derived neurotrophic factor (BDNF)-containing vesicles in neurons. Since striatal neurons are unable to produce BDNF, exogenous BDNF derived from cortical and substantia nigral neurons are vital for survival of striatal neurons. MHtt binds more strongly to Hap1 and P150, causing decreased association of the htt/Hap1/P150 complex with microtubules, which perturbs the trafficking of BDNF-containing vesicles, and consequently decreases neurotrophic support to striatal neurons (Gauthier et al., 2004). Alternatively, several studies demonstrate that a loss of function mechanism may contribute to disease pathogenesis. For example, a HD knockout mouse model shows cell degeneration and embryonic lethality (Duyao et al., 1995; Nasir et al., 1995; Zeitlin et al., 1995).

Inactivation of the HD gene in the brain and testis leads to neurodegeneration and sterility in mice (Dragatsis et al., 2000). Taken together, the above evidence indicates that HD is caused by both loss and gain of function.

1.3 Glial Dysfunction in Huntington's disease

Glia, which make up 90% of brain cells, contribute to the formation, operation and adaptation of neural circuitry (Allen et al., 2009). In mammals, glial cells are classified into astrocytes, microglia, and oligodendrocytes. The functions of glia include maintaining ionic balance in the extracellular space, supporting neurotransmission, and insulating axons to accelerate electrical communication. Emerging evidence suggests that glia may play important roles in the pathogenesis of a broad range of neurological diseases (Kim and de Vellis, 2005; Lobsiger and Cleveland, 2007; Shin et al., 2005).

HD is characterized by selective neurodegeneration that preferentially occurs in striatal medium spiny neurons. In addition to cell-autonomous toxicity in neuronal cells, mHtt-mediated dysfunction of glial cells is likely to play an important role in the pathogenesis of HD. Recent studies in different HD mouse models have demonstrated that dysfunction of astrocytes and oligodendrocytes leads to neuronal vulnerability and disease progression (Shin et al., 2005; Bradford et al., 2009; Tong et al., 2014; Huang et al. 2015). Furthermore, microstructural changes are found in the white matter of the corpus callosum in HD patient brains (Rosas et al., 2009), suggesting that mHtt impairs the integrity of oligodendrocytes in humans.

Astrocytes are the largest cell population in the central nervous system (CNS) and play essential roles in promoting neuronal survival and plasticity, removing toxic

materials, providing gliotransmitters to neurons through neuronal–glial interactions, and regulating the blood-brain barrier in the CNS (Molofsky et al., 2012; Pekny et al., 2016). Accumulation of mHtt in striatal astrocytes is found in the brains of HD patients and animal models, suggesting that mHtt disrupts normal processes in astrocytes. Indeed, glutamate uptake is decreased in HD mice compared to WT mice due to reduced expression of astroglial glutamate transporter (GLT-1) in brains of R6/2 mice, a HD transgenic mouse model that expresses mHtt exon1 (Lievens et al., 2001). This finding was confirmed by a subsequent study that further demonstrated neuronal excitotoxicity caused by reduction of GLT-1 expression in cultured astrocytes (Shin et al., 2005). Importantly, a transgenic mouse model expressing mHtt carrying 160Q specifically in astrocytes shows multiple HD-like symptoms, including body weight loss, motor function deficits, and shorter lifespans, indicating that expression of mHtt in astrocytes is sufficient to cause neuropathology (Bradford et al., 2009). Recent studies show that symptom onset in HD transgenic and knock-in mouse models is associated with decreased K^+ channel (Kir4.1) expression in astrocytes (Tong et al., 2014). Overexpression of the Kir4.1 channel in striatal astrocytes by viral injection normalizes extracellular K^+, ameliorates aspects of MSN dysfunction and attenuates some motor phenotypes in HD knock-in mouse models. These findings suggest that astrocyte dysfunction might be a possible pathogenic mechanism for the selective degeneration of MSNs in the striatum.

Microglia are resident macrophages in the brain and are implicated in several neurodegenerative diseases (EI Khoury et al., 2008; Klegeris et al., 2007; Sargsyan et al., 2005). In normal conditions, microglia are resting; however, under stressful conditions,

microglia are activated, sense signals, and migrate to damaged sites. The role of microglia in neuronal injury is debated, because they not only release neuroprotective molecules such as neurotrophins to support neuron survival, but they also secrete neurotoxic molecules such as nitric oxide (NO) and proinflammatory cytokines. In the brains of HD patients and mouse models, mHtt aggregates are found in dysregulated microglial cells featuring thick and distorted processes (Simmons et al., 2007). Activation of microglia can be observed at the presymptomatic stage of HD (Tai et al., 2007), suggesting that microglial activation is an early pathological event in the progression of the disease that potentially correlates with HD pathogensis. In addition, expression of inducible nitric oxide synthase (iNOS, a key player in inflammation) is found in microglia at the symptomatic stage of HD mice (Tabrizi et al., 2000). Therefore, microglial activation may play adverse roles in different stages of HD.

Oligodendrocytes produce the myelin sheaths that electrically insulate axons of CNS neurons, leading to rapid and efficient propagation of nerve signals. Oligodendrocyte dysfunction and defective myelination are found in a variety of neurodegenerative diseases (Bankston et al., 2013). In HD patients, myelin breakdown is found at the presymptomatic stage (Bartzokis et al., 2007), which correlates with cognitive decline and motor deficits (Bohanna et al., 2011). In HD mouse models, although HD knock-in mice do not show obvious neuronal loss, axonal degeneration is an early pathologic event (Li et al., 2001). In HD transgenic monkeys, axonal degeneration is also found in the absence of cell body degeneration (Wang et al., 2008). It remains unknown whether axon degeneration is caused by the expression of mHtt in axonal processes or in oligodendrocytes, the latter of which leads to defective myelination that

makes axons more susceptible to degeneration. To answer this question, Huang and colleagues (Huang et al., 2015) generated a transgenic mouse model that selectively expresses N-terminal mHtt with 150Q in oligodendrocytes under the proteolipid protein (PLP) promoter; the mice showed obvious axonal degeneration and early-onset phenotypes including body weight loss, impaired rotarod performance, and reduced lifespan, providing strong evidence that mHtt in oligodendrocytes contributes to neuronal toxicity. Furthermore, the researchers found that mHtt abnormally affects the transcriptional activity of Myelin Regulatory Factor (MYRF), which is a recently identified transcription factor activating and maintaining the expression of myelin genes in mature oligodendrocytes. These findings suggest that mHtt-induced dysfunctional oligodendrocytes contribute to the pathogenesis of HD.

1.4 Neurotrophic factors in Huntington's disease

Neurotrophic factors (NTFs) are a family of secreted growth factors that support neuronal survival and function in the CNS. Traditionally, the NTF family includes three sub-families: (1) neurotrophins, including nerve growth factor (NGF) (the first identified NTF), brain-derived neurotrophic factor (BDNF), neurotrophin-3 (NT-3) and neurotrophin-4 (NT-4); (2) glial cell line-derived neurotrophic factors (GDNFs); (3) ciliary neurotrophic factor (CNTF) and neuropoietic cytokines, such as interleukin-6 (IL-6), IL-11, and IL-27. Recently, a new family of NTFs was reported to include cerebral dopamine neurotrophic factor (CDNF) and mesencephalic astrocyte-derived neurotrophic factor (MANF) (Huang and Reichardt, 2001; Airaksinen and Saarma, 2002; Bauer et al., 2007; Palgi et al., 2009).

Among all the NTFs, BDNF is most studied in HD. It has been found that

administering BDNF to the striatum of HD mice by an osmotic minipump prevented the death of striatal neurons (Canals et al., 2004), suggesting that delivering exogenous BDNF or increasing endogenous BDNF production has therapeutic potentials for HD. BDNF is widely expressed in the adult mammalian brain, and has been shown to promote the survival of all types of neurons. BDNF has eight 5′ untranslated exons (I–VIII) and one protein-coding exon (IX) (Aid et al., 2007) in rodents and humans. It is first synthesized in the endoplasmic reticulum (ER). After passing through the Golgi apparatus, it is packaged into dense-core vesicles, and is trafficked mainly through regulated secretory pathway.

A large number of studies demonstrate that BDNF is decreased in HD mouse models before the onset of symptoms. For example, presymptomic 9-month-old transgenic mice (YAC72) expressing full-length mHtt show 30% less protein levels of BDNF in the cerebral cortex than their wild-type littermates (Zuccato et al., 2001), and mRNA levels of BDNF are reduced in the cerebral cortex of YAC72 mice beginning at the age of 3 months (Hermel et al., 2004), suggesting that the decrease in BDNF in HD models is attributed to the reduction of transcription. Wild-type htt mediates BDNF gene transcription by inhibiting the repressor element 1/neuron-restrictive silencer element (RE1/NRSE) within BDNF promoter II (Zuccato et al., 2001, 2005), whereas mHtt fragments in HD mouse models inhibit transcription of BDNF by altering the activities of promoters III and IV. The mechanism underlying the reduction in BDNF transcription is proposed to be that mHtt disrupts the association between transcription factors and BDNF promoters (Zuccato et al., 2001, 2003, 2005).

The striatum is the brain region that is preferentially and most severely affected in

HD, and like other neurons, striatal neurons require BDNF for their activity and survival. However, striatal neurons are unable to produce endogenous BDNF, and therefore rely on exogenous BDNF released from cortical neurons (**Fig. 1.3**). Several studies have shown that the loss of BDNF support from other brain regions could be one of the pathological mechanisms driving the course of HD. Htt is predominantly found in the cytoplasm of neurons, and is enriched in compartments containing vesicle-associated proteins (DiFiglia et al., 1995). It has been demonstrated that wild-type htt enhances the transport of BDNF-containing vesicles along microtubules in mammalian cells (Gauthier et al., 2004). However, mHtt impairs the transport velocity of BDNF-containing vesicles in knock-in cells (Gauthier et al., 2004). BDNF is stored in dense-core vesicles that are transported along microtubules, and it is eventually secreted following a variety of depolarization stimuli in neurons (Lu, 2003; Dieni et al., 2012). It has been demonstrated that mHtt disrupts microtubule-dependent transport of BDNF-containing vesicles in cortical neurons, suggesting deficient cortical neuron-derived BDNF for the striatum, which may contribute to the selective loss of striatal neurons in HD (Toro et al., 2006).

Beside BDNF, other NTFs have also been implicated in polyQ diseases. For example, NGF levels are significantly lower in HD patients than in normal subjects (Tasset et al., 2012); NT-3and NT-4 prevent the death of striatal neurons in a HD mouse model (Perez-Navarro et al., 2000); CNTF has been used in a clinical trial for HD, but showed somewhat disappointing results (Bloch et al., 2004). Taken together, these findings suggest that NTFs contribute to HD pathogenesis, and provide potential therapeutic strategies for HD.

1.5 Exocytosis in astrocytes

Astrocytes and other glial cells can release a variety of transmitters into the extracellular space using different mechanisms: (1) release through channels (Pasantes Morales and Schousboe, 1988) and functional unpaired connexons on the cell surface (Cotrina et al., 1998; Iglesias et al., 2009); (2) release through transporters (Szatkowski et al., 1990); and (3) release through Ca^{2+}-dependent exocytosis (Parpura et al., 1994), such as amino acids, nucleotides and peptides.

Here, we focus on the potential role of Ca^{2+}-dependent exocytosis from astrocytes. Exocytosis participates in cell-cell communication, and consists of four distinct steps: recruitment of secretory vesicles to the release site, docking of secretory vesicles to the plasma membrane, priming, and stimulus-dependent fusion of secretory vesicles to the plasma membrane (Jahn et al., 2012). Chemicals released through a Ca^{2+}-dependent exocytosis mechanism from astrocytes include glutamate, nucleotides, and peptides. Glutamate is synthesized within astrocytes as a by-product of the tricarboxylic acid (TCA) cycle (Hertz et al., 1999). The synthesized glutamate can be transported into vesicles via proton-dependent vesicular glutamate transporters (VGLUTs). Astrocytes release glutamate when the vesicles fuse with the plasma membrane. This fusion process is mediated by synaptotagmin 4 and SNARE proteins: syntaxin 1, synaptobrevin 2 and synaptosome-associated protein of 23 kDa (SNAP-23) (Westergaard et al., 1996).

Second, astrocytes can release nucleotides through exocyotosis, such as adenosine 5′-triphosphate (ATP). ATP is produced by glycolysis and oxidative phosphorylation. Intracellular ATP provides energy for a variety of processes, and extracellular ATP is an intercellular signaling molecule. Cultured astrocytes under the electron microscope show

large, ATP-containing dense-core vesicles (Coco et al., 2003). Nitric oxide causes increased cytoplasmic Ca^{2+}, which induces the release of ATP into the extracellular space (Bal-Price et al., 2002). To study the quantal nature of ATP release from astrocytes, Pangrsic et al treated astrocytes with quinacrine, a compound that fluorescently labels endogenous ATP-containing vesicles (Pangrsic et al., 2007). Under total internal reflection fluorescence (TIRF) microscopy, quinacrine shows that punctate staining, which represents ATP-containing vesicles, rapidly fades in the presence of increased intracellular Ca^{2+} levels, suggesting that ATP is released by Ca^{2+}-dependent exocytosis (Pryazhnikov and Khiroug, 2008).

Finally, astrocytes can release peptides via exocytosis machinery, such as atrial natriuretic peptide (ANP) and BDNF. In contrast to amino acids and ATP, which are loaded into vesicles by membrane transporters, peptides such as ANP and BDNF enter vesicles via the synthetic secretory pathway (Dannies, 1999). The pro-peptides are synthetized in the ER, and then enter the Golgi apparatus from which vesicles containing concentrated and sorted peptides bud off. Subsequently, these vesicles transport from the Golgi apparatus to the plasma membrane, where they dock and fuse with the plasma membrane in response to increased cytosolic Ca^{2+} levels (**Fig. 1.4**).

1.6 Rab proteins in Huntington's disease

Exocytosis is regulated by a number of proteins including Rab proteins, which are are small (21-25 kDa) monomeric GTP-binding molecules (GTPase), and are the largest branch of the Ras superfamily. In humans, the Rab family consists of almost 70 members that may serve as major factors between transport vesicles and the plasma membrane.

Rabs are associated with cyclical activation and inactivation in the form of a GTP-bound/active state regulated by GEFs (guanine nucleotide exchange factors) and a GDP-bound/inactive state regulated by GAPs (GTPase activating proteins) between the membranes and cytoplasm (Bucci et al., 2014).

Rab11 is the most characterized molecule among all the Rabs. The numbers of Rab11 isoforms vary among species. For instance, Rab11 in drosophila has no isoform, whereas three isoforms, Rab11a, Rab11b and Rab25, are identified in vertebrates, suggesting more sophisticated functions of Rab11 in more complex animals (Casanova et al., 1999; Cox et al., 2000). Rab11 is associated with recycling endosomes, and regulates vesicular trafficking through recycling of the endosomal compartment and early endosomes (EEs) to the trans-Golgi network (TGN) and plasma membrane (Ullrich et al., 1996; Ren et al., 1998; Wilcke et al., 2000). Dominant-negative Rab11 expressed in the striatum and the cortex of wild-type mice causes neuropathology and motor dysfunction, suggesting that defective Rab11 activity is pathogenic in vivo (Li et al., 2009).

Rab11 has been implicated in a number of diseases, such as Alzheimer's disease, HD, and cancers (Bhuin et al., 2015). Htt plays a key role in manipulating Rab11 vesicles, such as movement of Rab11-containing vesicles within axons; however, mHtt disrupts Rab11-dependent endosomal recycling. Rab11 is involved in synaptic dysfunction prior to the onset of HD symptoms. Inhibition of Rab11 function in the fibroblasts of HD patients impairs vesicle formation from recycling endosomes (Li et al., 2009). Conversely, Rab11 overexpression ameliorates synaptic dysfunction, rescues neurodegeneration, and extends lifespan in a Drosophila model of HD. These results suggest that disruption of Rab11-mediated endosome recycling mediated by mHtt may

contribute to the early neuropathology observed in HD (Power et al., 2012).

In addition to Rab11, dysfunction of other Rab family members is also proposed to be involved in HD pathogenesis. Rab5 is an important regulator of the early endocytic pathway in mammalian cells (Bucci et al., 1992; Stenmark et al., 1994). Htt indirectly interacts with Rab5 via HAP40 to regulate endocytosis (Pal et al., 2006). It has been reported that inhibition of Rab5 enhances polyglutamine toxicity, whereas overexpression of Rab5 attenuates toxicity in HD cell and Drosophila models. In addition, Rab8 participates in vesicles trafficking from the Golgi complex to the plasma membrane. Optineurin, an adaptor protein associated with the Golgi complex, links Rab8 to huntingtin, and this complex is required for post-Golgi trafficking (Sahlender et al., 2005). Loss of normal htt function in HD may disrupt the Rab8-dependent trafficking pathway. Taken together, multiple Rab proteins are likely to be involved in the pathogensis of HD, and elucidating adverse effect of mHtt on the function of Rab proteins may provide new insights into etiology of HD.

1.7 Roles of exosomes in neuron-glia communication

Exosomes are endosome-derived small membranous vesicles (40-100nm) secreted by various types of cell, and they can be isolated from conditioned cell culture media or body fluids. Exosome biogenesis involves the inward budding of multivesicular bodies (MVB) to form intraluminal vesicles (ILV). Exosomes are released by fusion of MVBs with the plasma membrane followed by secretion of the ILVs into the extracellular space (Théry et al., 2002). Functions of these vesicles include cell-cell communication, removing unwanted proteins, and pathogens transmission between cells. Exosomes

contain a set of proteins that are conserved across different cell types. Typical exosome-containing proteins are the tetraspanin family, cytoskeletal proteins, heat-shock proteins, metabolic enzymes of glucose metabolism, flotillin-1, and those involved in transport and fusion. (Théry et al., 2011).

In the CNS, all brain cells have been reported to secrete exosomes into the extracellular environment. Neuronal exosomes may influence glutamatergic synaptic activity (Lachenal et al., 2011). Emerging evidence shows that proteins associated with neurodegenerative diseases, such as the β-amyloid peptide in Alzheimer's disease and α-synuclein in Parkinson's disease, have been identified in neuronal exosomes, which is a mechanism underlying the spread of toxic proteins in the brain (Bellingham et al., 2012; Wang et al., 2017). Oligodendrocyte-derived exosomes include galactocerebroside, sulfatide, and cholesterol (Krämer-Albers et al., 2007). Neuronal signals trigger exosome release from oligodendrocytes by elevating intracellular Ca^{2+} levels in oligodendrocytes. After internalization by neurons, these oligodendrocyte-derived exosomes are beneficial for axonal outgrowth. On the other hand, astrocytic exosomes carry neuroprotective cargoes, such as Hsp/Hsc70 and HspB1, which are involved in maintaining the homeostasis of recipient neurons (Taylor et al., 2007; Nafar et al., 2016). Microglia are the resident macrophages of the CNS. Microglia-derived exosomes, containing monocarboxylate transporter 1 and glycolytic enzymes, may deliver energy substrates to neurons (Potolicchio et al., 2005). Microglia also can take up and degrade exosomes released by oligodendrocytes. Under specific pathological conditions, these exosomes may transfer antigens to microglia to induce inflammatory responses (Kettenmann et al., 2011; Bianco et al., 2009). Thus, studying exosomes in the CNS will advance

understanding of the spreading of toxic misfolded proteins, and may open up a new avenue for treatment of neurological disorders.

1.8 Dissertation Goals

Although HD is characterized by the selective degeneration of striatal medium-size spiny neurons, it is necessary to understand how mHtt affects the function of non-neuronal cells to fully understand the pathobiology of HD. Astrocytes are the largest cell population in the CNS, and they support neuronal survival partly by providing vesicles containing neurotrophic factors and heat shock proteins. Although it has been reported that mHtt disrupts normal astrocytic functions, whether mhtt affects astrocytic secretion remains unknown. Since striatal neurons cannot produce BDNF, BDNF released by astrocytes in the striatum should be important to protect the neighboring neurons from mHtt toxicity in HD brains. Consistent with this perspective, emerging evidence shows that exosomes secreted from astrocytes contain neuroprotective cargoes that could support the survival of neurons (Taylor et al., 2007; Nafar et al., 2016). The current dissertation project seeks to determine whether mHtt at endogenous levels affects astrocytic secretion, and if so, what are the mechanisms underlying the deficient release of functional vesicles? Specifically, I hypothesize that mHtt impairs the release of dense-core vesicles and exosomes from astrocytes, which reduces trophic supports for neurons and contributes to the pathogenesis of HD. In this study, I used primary culture, brain slice, and HD KI and transgenic mouse models to examine the effect of mHtt on astrocytic secretion.

Table 1.1

Poly Q Disease	Disease Protein	Normal PolyQ Repeats	Mutant PolyQ Repeats	**Brain regions most affected**
Huntington's diseasae (HD)	Huntingtin	6-34	36-121	Striatal medium spiny neurons
Spinocerebellar ataxia 1 (SCA1)	Ataxin-1	6-44	39-82	Cerebellar Purkinje cells
Spinocerebellar ataxia 2 (SCA2)	Ataxin-2	15-31	36-63	Cerebellar Purkinje cells
Spinocerebellar ataxia 3 (SCA3)	Ataxin-3	12-41	62-84	Cerebellar dentate neurons, spinal cord and brain stem
Spinocerebellar ataxia 6 (SCA6)	CACNA1A	4-18	21-33	Cerebellar Purkinje cells
Spinocerebellar ataxia 7 (SCA7)	Ataxin-7	4-35	37-306	Cerebellar Purkinje cells
Spinocerebellar ataxia 17 (SCA17)	TATA-binding protein (TBP)	25-42	47-63	Cerebellar Purkinje cells
Spinal and bulbar muscular atrophy (SBMA)	Androgen receptor	9-36	38-62	Anterior horn and bulbar neurons, dorsal root ganglia
Dentatorubral-pallidoluysian atrophy (DRPLA)	Atrophin-1	6-36	49-84	Cerebellum, cerebral cortex, basal ganglia

Figure 1.1

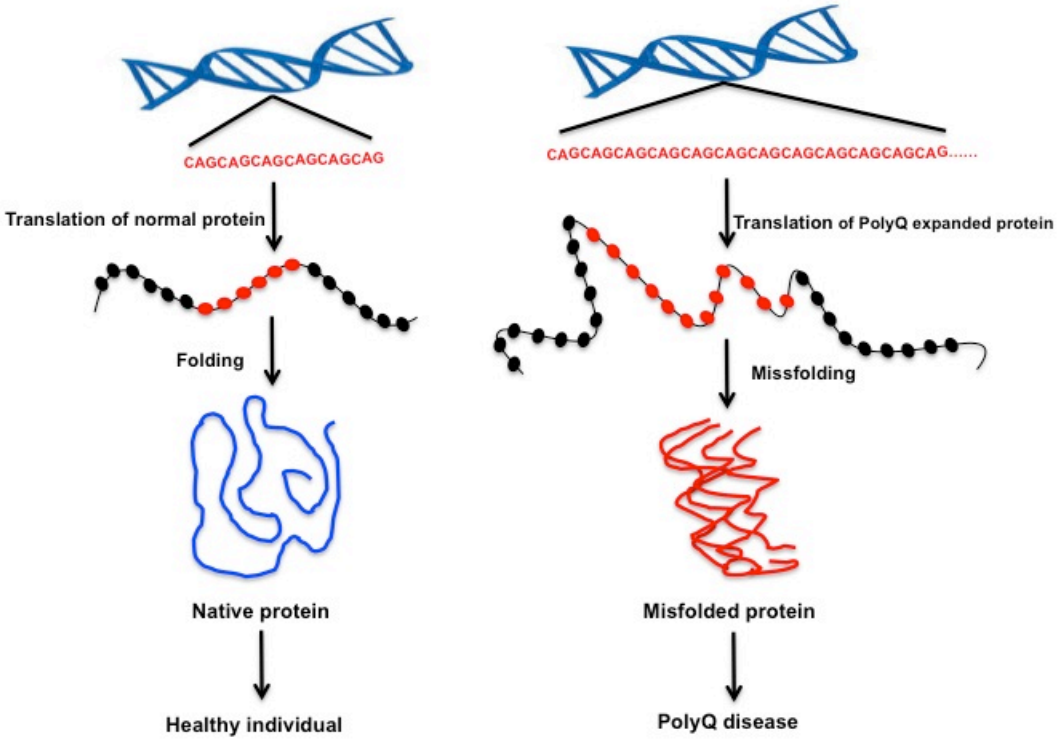
CAGCAGCAGCAGCAGCAG
Translation of normal protein
Folding
Native protein
Healthy individual
CAGCAGCAGCAGCAGCAGCAGCAGCAGCAGCAG.....
Translation of PolyQ expanded protein
Missfolding
Misfolded protein
PolyQ disease

Figure 1.1 PolyQ expansion

PolyQ diseases are caused by an expansion of a trinucleotide (CAG) repeat, encoding a polyQ tract, in the exonic regions of specific genes. Aggregates formed by misfolded proteins in patient brains are a pathological hallmark of the polyQ diseases.

Figure 1.2

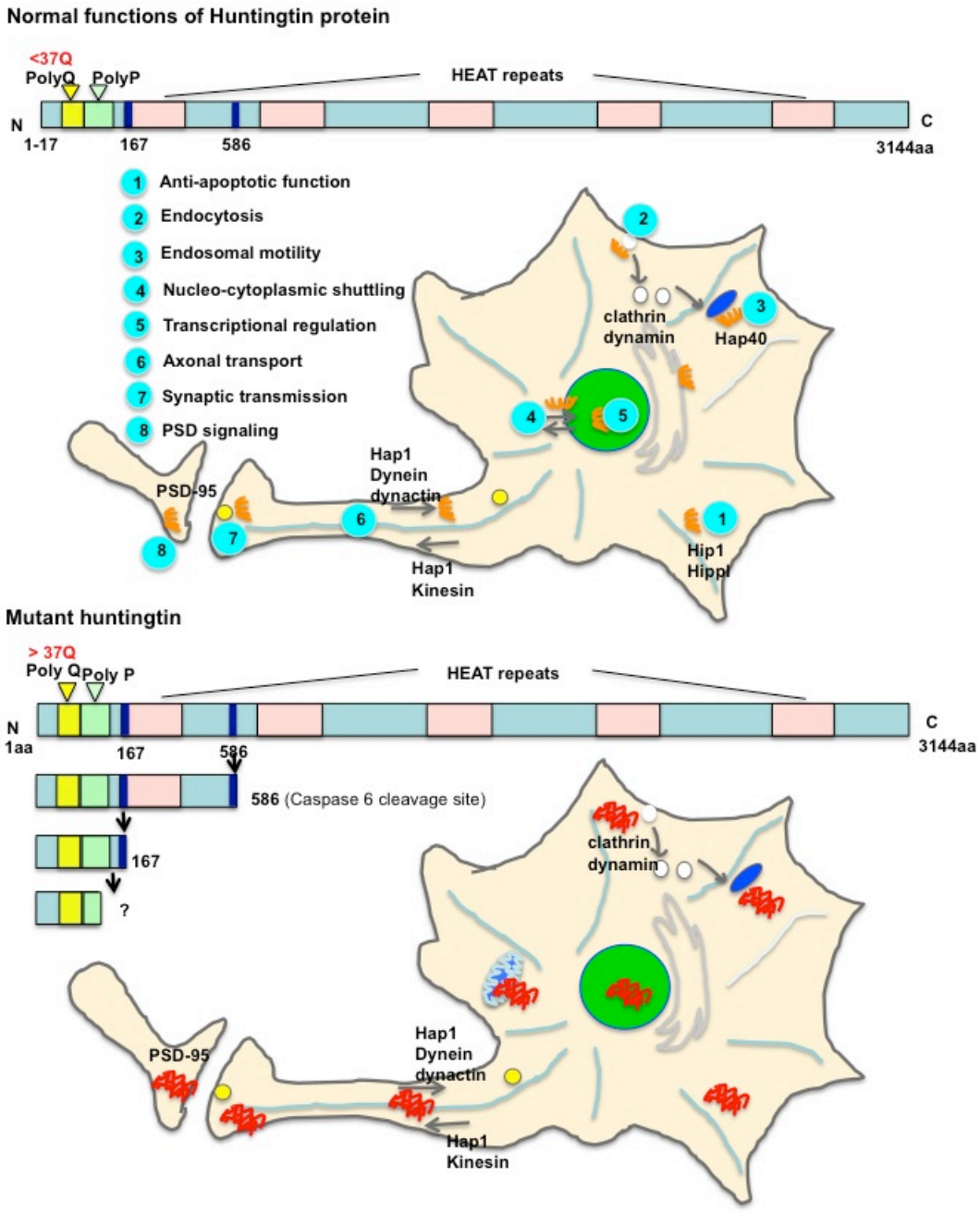
Normal functions of Huntingtin protein
<37Q
PolyQ
PolyP
HEAT repeats
N
C
1-17
167
586
3144aa
1 Anti-apoptotic function
2 Endocytosis
3 Endosomal motility
4 Nucleo-cytoplasmic shuttling
5 Transcriptional regulation
6 Axonal transport
7 Synaptic transmission
8 PSD signaling
clathrin
dynamin
Hap40
Hap1
Dynein
dynactin
PSD-95
Hap1
Kinesin
Hip1
Hippl
Mutant huntingtin
> 37Q
Poly Q
Poly P
HEAT repeats
N
1aa
167
586
3144aa
586 (Caspase 6 cleavage site)
167
?
clathrin
dynamin
Hap1
Dynein
dynactin
PSD-95
Hap1
Kinesin

Figure 1.2 Huntingtin protein

The huntingtin protein (htt) is a large protein including 3144 amino acids. The polyQ domain (yellow) begins at the 18th amino acid. Normal individuals usually have less than 37Q, but HD patients contain more than 37Q. Two proline-rich domains (green) follow the polyQ domain. Htt also contains multiple HEAT repeats (pink), which may be involved in cytoplasmic-nuclear transport. Htt plays multiple roles in neurons (1-8). Mutant huntingtin (mHtt) cleavage resulting in N-terminal fragments containing the polyglutamine expansion is a key step in HD pathogenesis. MHtt induces neuronal death by disrupting gene expression, axonal transport, and mitochondrial functions.

Figure 1.3

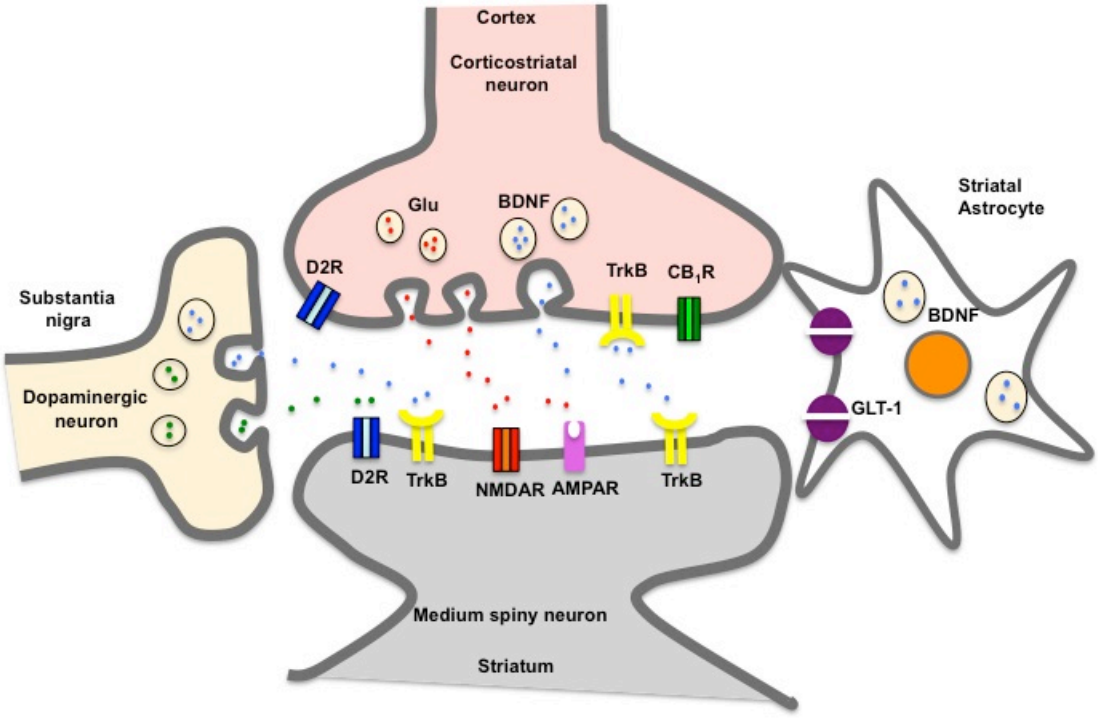
Cortex
Corticostriatal neuron
Glu
BDNF
D2R
TrkB
CB1R
Striatal Astrocyte
Substantia nigra
BDNF
Dopaminergic neuron
GLT-1
D2R
TrkB
NMDAR
AMPAR
TrkB
Medium spiny neuron
Striatum

Figure 1.3 BDNF sources for MSNs

Striatal neurons require BDNF for their activity and survival. However, striatal neurons are unable to produce endogenous BDNF, and therefore rely on exogenous BDNF (blue dots) released from cortical neurons (pink), substantia nigral neurons (yellow), and striatal astrocytes (white).

Figure 1.4

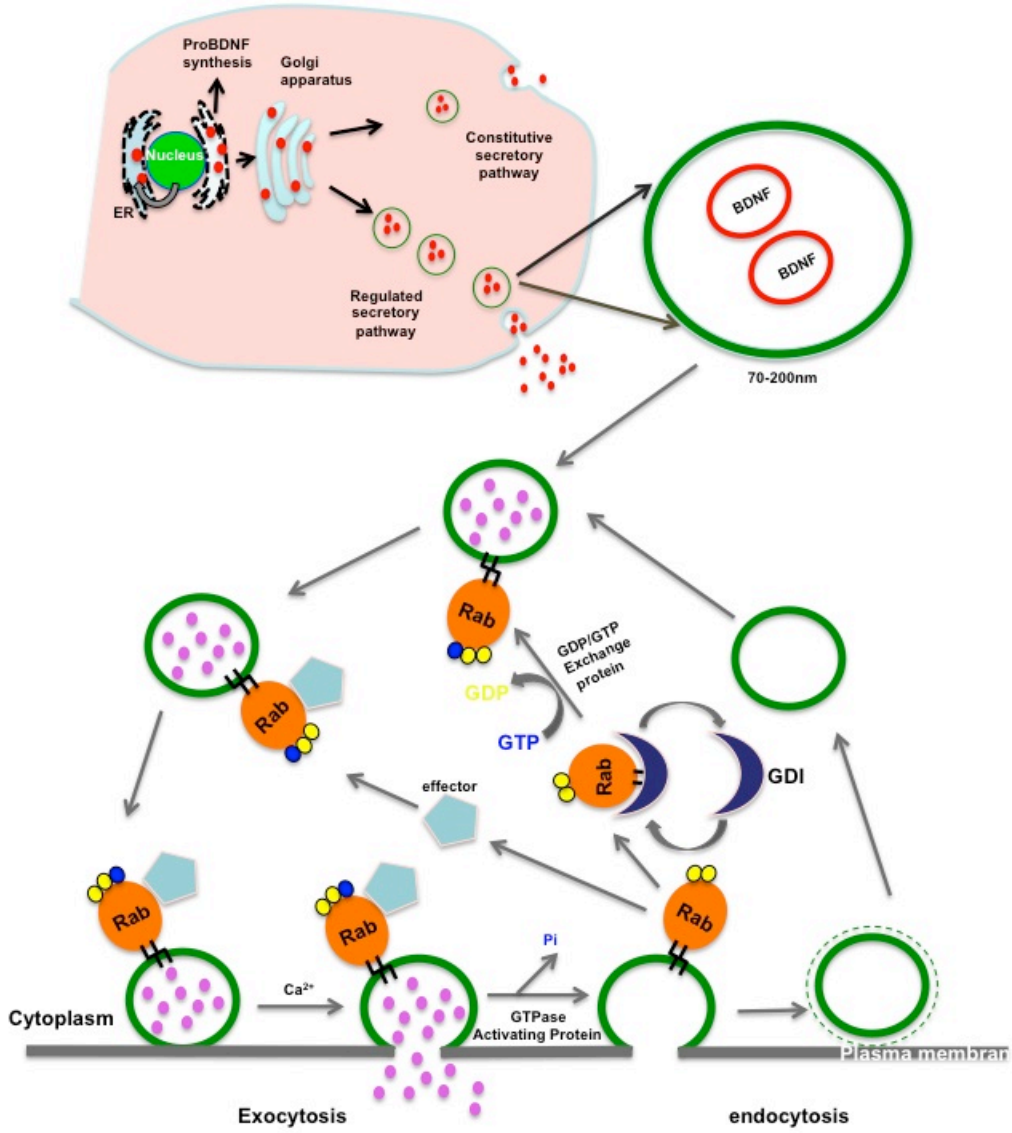
ProBDNF synthesis
Golgi apparatus
Nucleus
ER
Constitutive secretory pathway
Regulated secretory pathway
BDNF
BDNF
70-200nm
Rab
GDP/GTP Exchange protein
GDP
GTP
GDI
effector
Rab
Rab
Rab
Rab
Ca2+
Pi
GTPase Activating Protein
Cytoplasm
Plasma membran
Exocytosis
endocytosis

Figure 1.4 Synthesis, storage and release of BDNF

BDNF is first synthesized in the endoplasmic reticulum (ER). After passing through the Golgi apparatus, it is packaged into dense-core vesicles, and is trafficked mainly through regulated secretory pathway along microtubules. It is eventually secreted following a variety of depolarization stimuli, which is regulated by Rab-mediated exocytosis.

Chapter 2
Materials and Methods

This chapter was published in part as: Yan Hong, Ting Zhao, Xiao-Jiang Li, and Shi-Hua Li (2016) The Journal of Neuroscience 36:8790-801. Xiao-Jiang Li and Shi-Hua Li helped with the experimental design. Xiao-Jiang Li played a key role in the preparation of the manuscript

2.1 Animals

KI mice were kindly provided by Dr. Michael Levine of the University of California, Los Angeles (Hickey et al., 2008). GFAP-Htt transgenic (TG) mice with 160Q were generated previously by our laboratory (Bradford et al., 2009). Mice were maintained at the Emory University animal facility. Both male and female pups from these mice were used for primary cultures. Male and female adult mice of different ages were used for viral injection and brain-slice preparation. This study was performed in strict accordance with the recommendations in the *Guide for the Care and Use of Laboratory Animals* of the National Institutes of Health. The protocol was approved by the Committee on the Ethics of Animal Experiments of Emory University (permit number 2002557).

2.2 Antibodies and reagents.

Antibodies used were anti-expanded polyQ (1C2) (Millipore, MAB1574), anti-Htt (mEM48), anti-Rab3a (BD Biosciences, 610379), anti-GTP-Rab3a (NewEast Biosciences, 26920), anti-Rab3-GAP1 (Proteintech, 21663-1-AP), anti-V5 (Life Technologies 46-0705), anti-TrkB (Cell Signaling, 80E3), anti-phospho-TrkB (Epitomics, 2149-1), anti-BDNF (Santa Cruz, sc-546), and anti-Actin (Sigma, A5060), anti-GFAP (Millipore, MAB360), anti-NeuN (Millipore, ABN78), anti-Alix (Millipore, ABC40), anti-flotillin-1 (Millipore, MAB1118), anti-αB-crystallin (abcam, ab13496), anti-Hsc70 (Santa Cruz, sc7298), anti-Hsp90 (Cell signalling, 4874S), anti-GM130 (BD, 610822), anti-GRP78 (Santa Cruz, sc-1051), anti-CD9 (GeneTex GTX80172). Secondary antibodies were HRP-labeled donkey anti-mouse, donkey anti-rabbit, donkey anti-mouse Alexa Fluor 488 or 594, and donkey anti-rabbit Alexa Fluor 488 or 594 from Jackson

ImmunoResearch. Proteinase inhibitor cocktail, phorbol 12-myristate 13-acetate (PMA), Adenosine 5'-triphosphate (ATP) Bioluminescent Assay Kit and quinacrine dihydrochloride were purchased from *Sigma*. Rab3-V5 adenovirus was purchased from SignaGen Laboratories (SL174810). The Glutamate Assay Kit was purchased from BioVision. αB-crystallin adenovirus was purchased from SignaGen Laboratories (SL170680). Chromatin Immunoprecipitation (ChIP) Assay kit was purchased from Millipore.

2.3 Primary cell cultures.

The brains of postnatal (day 1-3) male and female mouse pups were used for culturing cortical astrocytes. Following dissection, the cortex was subjected to 0.3mg/ml papain digestion. Cell suspension was filtered through 70-μm nylon cell strainers (Fisher Scientific). Microglia and oligodendrocytes were removed from cultures at DIV14 by shaking. Remaining cells were detached with 0.25% trypsin and plated for the following experiments. For cortical neuron cultures, cortical neurons were prepared from postnatal day 0 murine pups. The cortex was digested with 0.3mg/ml papain. Cell suspension was filtered through 40-μm nylon cell strainers (Fisher Scientific) to remove debris. Neurons were plated at 1×10^6 on poly-D-lysine coated 6-well plates and cultured in Neurobasal-A medium supplemented with B27 and glutamine (Invitrogen).

2.4 Preparation of astrocyte-conditioned medium (ACM).

Primary astrocytes (DIV 25) were cultured at a density of 2 x 10^6 in 6-well plates and treated with 28 mM KCL for 30 min at 37°C. The culture medium was collected for measuring released BDNF via ELISA.

2.5 Enzyme-linked immunosorbent assays (ELISA).

Levels of BDNF were determined by a BDNF ImmunoAssay System **(**Promega) following the manufacturer's protocol. Briefly, samples or standards (100 µl) were added to 96-well plates, incubated at 4°C overnight, and washed extensively, followed by a 2 h incubation with the anti-BDNF antibody and a 1 h incubation with anti-IgY HRP conjugate plus substrate for signal development. The absorbance was recorded at 450 nm on a plate reader (Microplate Reader, BioTek). The amount of BDNF in each sample was calculated based on the standard curve prepared in the same experiment.

2.6 Western blotting.

Primary cultures or brain tissues were homogenized in ice-cold NP-40 buffer containing a protease inhibitor mixture (Pierce Protein Biology Products, Thermo Scientific) and 100µM PMSF. Samples were boiled for 5min in SDS/β-mercaptoethanol (BME) protein loading dye and run on 4–12% Tris-Glycine gels purchased from Invitrogen (catalog #EC60385). Proteins were transferred to a nitrocellulose membrane in Tris-Glycine buffer. After blocking, blots were probed with Rab3a or other primary antibodies overnight. The Western blots were developed using the ECL Prime Chemiluminescence kit (GE Healthcare).

2.7 Glutamate measurement.

Glutamate release from astrocytes was determined by a Glutamate Assay Kit (BioVision) following the manufacturer's protocol. Briefly, each culture medium was diluted in the

assay buffer. Samples or standards (50 µl) were added to 96-well plates. Reaction Mix (100 µl) was added to each well containing the glutamate standard and test samples. Reactions were incubated for 30 min at 37°C and protected from light. Measured OD was at 450 nm in a microplate reader (BioTek). The amount of glutamate in each sample was calculated based on the standard curve prepared in the same experiment.

2.8 RT-qPCR.

Total RNA was isolated from WT, TG, and KI astrocytes. Reverse transcription reactions were performed with 1.5 µg of total RNA using the Superscript III First-Strand Synthesis System (Invitrogen). One microliter of cDNA was combined with 10 µl SYBR Select Master Mix (Applied Biosystems) and 1 µl of each primer in a 20 µl reaction. The reaction was performed in a thermal cycler (Eppendorf, RealPlex Mastercycler).

2.9. Knockdown assay.

Rab3a siRNA duplexes and negative control siRNA were purchased from OriGene (SR402766). The following combination of oligonucleotides was used to target the Rab3a gene: CGACUAUAUGUUCAAGAUCCUGATC, GGAGUCAUUUAAUGCAGUGCAGGAC, CGCAGUCCUUGACAUUAAAGAGAAT.

2.10 Stereotaxic injection of virus.

Male adult mice were used for Rab3-V5 or αB-crystallin adenoviral and control GFP adenoviral injections. Heads of the animals were placed and fixed in a stereotaxic frame

(David Kopf Instruments, Model 1900) equipped with a digital manipulator and a UMP3-1 Ultra pump. The mice were kept deeply anesthetized as assessed by monitoring pinch withdrawal and respiration rate. Animals were injected in the striatum (0.6 mm anterior to bregma, 2.0 mm lateral to the midline, 3.5 mm ventral to dura). The injections were performed at a rate of 0.2 ml/min. The needle was left in place for 10 min after each injection to minimize the upward flow of viral solution after raising the needle. Rab3a-V5 was allowed to be expressed for 21-30 days *in vivo* before slicing the brains. For exosome injection, astrocytic exosomes were suspended in PBS. A total of 8 μl were injected into two sites of striatum in one hemisphere (0.6/0.4 mm anterior to bregma, 2.0 mm lateral to the midline, 3.5 mm ventral to dura) in 9-month-old KI mice with 4 μl for each site. PBS injection served as a control in the other side of the same mouse. Seven days after injection, the mouse brains were examined using immunocytochemistry.

2.11 Preparation of brain slices.

Brains from male mice were immersed in chilled artificial cerebral spinal fluid (ACSF), and then were cut with the vibratome into 250-mm coronal slices containing striatum. To stimulate BDNF release from the brain slices, 56 mM of KCl were added to the ACSF.

2.12 Rab3 GTPase activity assay.

GST-Rab3a was loaded with 20 μCi of [γ-^{32}P]-GTP (5000 Ci/mmol, Amersham Pharmacia Biotech) in 40 μl of loading buffer (20 mM Tris pH 7.6, 5 mM EDTA, and 0.1 mM DTT) for 15 min at room temperature. The loading reaction was stopped by adding 2 μl of 0.4 M $MgCl_2$. Five μl of preloaded GTPase was diluted in assay buffer (20 mM Tris

pH 7.6, 1 mM GTP, 1 mg/ml BSA and 0.1 mM DTT) to yield a final volume of 50 μl. The total amount of [γ-^{32}P]-GTP-loaded GTPase was measured by removing 5 μl of the loading sample (t_0) into 1 ml of ice-cold dilution buffer (50 mM Tris pH 7.6, 50 mM NaCl, 5 mM $MgCl_2$). WT or KI astrocyte lysates without Rab3-GAP1 were then added to the assay and incubated with [γ-^{32}P]-GTP labeled GST-Rab3A for various periods of time at room temperature. Rab3-GAP1 in astrocyte lysate was immunoprecipitated by Rab3-GAP1 antibody. After 30, 60, and 90 min, 5 μl of sample was removed and diluted into 1 ml of ice-cold dilution buffer. At each time, the samples were filtered through nitrocellulose filters (Millipore) to trap the γ-^{32}P-labeled GTPase, and the radioactivity retained on the filters was determined by scintillation counting.

2.13 Total internal reflection fluorescence microscopy.

A Total internal reflection fluorescence (TIRF) microscope (GE Healthcare Life Sciences, GE DeltaVision OMX Blaze) was used to study vesicles docking near the plasma membrane. Astrocytes were plated onto poly-L-lysine-coated coverslips and then transfected with BDNF fused to RFP. After 48 h of transfection, docking of BDNF-RFP vesicles was examined by TIRF microscope, which allows selective imaging of a ~100-nm region beneath the plasma membrane. Quinacrine dihydrochloride often serves as a fluorescent marker for intracellular ATP-enriched vesicles (Akopova et al., 2012). Living astrocytes were treated with phorbol 12-myristate 13-acetate (PMA) for 15 min at 37^{o}C. Quinacrine staining was performed by incubating living astrocytes with 1 μM quinacrine dihydrochloride for 15 min at room temperature. Quinacrine fluorescence in living astrocytes after stimulation was examined with a Nikon A1R confocal microscope. To

examine ATP-containing vesicles, astrocytes were treated with quinacrine dihydrochloride for 15 min at room temperature. Images were acquired by the TIRF microscope every 200 ms. The number of plasma membrane-docked vesicles was counted at the entire cell surface in the evanescent field by Fiji.

2.14 Immunoprecipitation.

Cells were harvested and lysed in ice-cold 0.5% Triton X-100/PBS solution with protease inhibitor mixture and 100 mM PMSF on ice. The lysates were centrifuged at 16,000×g for 15 min. Protein concentrations were measured with BCA assay (Thermo Fisher Scientific). A total of 300 μg of samples were precleared with protein A agarose beads (Sigma-Aldrich), and huntingtin and Rab3a-V5 proteins were immunoprecipitated with 1C2 and anti-V5 antibodies, respectively, at 4°C overnight. Protein A agarose beads were added to capture the immunoprecipitates for 1 h at 4°C. Ice-cold lysis buffer was used to wash beads three times. Proteins from the immunoprecipitates and inputs were subjected to Western blotting.

2.15 Immunofluorescence staining.

Cultured astrocytes were fixed with 4% paraformaldehyde for 8-10 min. Mouse brains were sliced at 10 μm thickness with a cryostat at -20°C, mounted onto gelatin-coated sides, and fixed with 4% paraformaldehyde for 10 min. Fixed samples were blocked with 3% BSA/0.2% Triton X-100 for 30 min at room temperature. Following incubation of fixed samples with primary antibodies at 4^{o}C overnight and washes, fluoroconjugated secondary antibodies and Hoechst nuclear dye were added to the samples for staining.

Images were acquired with an Imager Z1 microscope or an Olympus FV1000 inverted microscope. Quantitative analysis of GFAP staining was performed using the method in our previous studies (Yang et al., 2015). Briefly, NIH ImageJ software was used to measure GFAP immunostaining intensity. Colored images obtained with a 63× objective were converted to eight-bit black-and-white images. The "Threshold" function was used to adjust the background to highlight GFAP-specific staining. The same threshold was applied to all images analyzed. Finally, the "Measure" function was used to quantify GFAP staining intensity in each image. Each group had 7 to 10 images per section and 8 sections per group were examined.

2.16 ATP assay.

ATP levels in astrocyte culture medium were analyzed by an ATP bioluminescence assay kit (Sigma-aldrich) and a luminometer (BioTek) according to the manufacturer's instructions. Briefly, WT, KI, and Rab3a-overexpressed KI astrocytes were treated with PMA for 15 min at 37^{o}C. Each culture medium was harvested for ATP assay. Each sample was run in duplicate and assayed within 5–10 min of collection.

2.17 Purification of exosomes.

Exosomes were prepared from culture medium as described previously (Théry et al., 2006). Briefly, the culture medium of astrocytes was replaced with medium containing exosome-free FBS. After 24 h incubation, culture supernatants were harvested and centrifuged sequentially at 300 × g for 10 min, 2000 × g for 10 min, 10,000 × g for 30 min, and 100,000 × g for 70 min. The pellet was resuspended in cold PBS and then

centrifuged 100,000 × g for 70 min. The pellet containing exosomes was resuspended in appropriate buffers. All centrifugations were performed at 4 °C.

Exosomes from mouse brain tissues were prepared as described previously (Perez-Gonzalez et al., 2012; Polanco et al., 2016). In brief, the striatum were dissected from HD KI and age-and gender-matched wild-type controls. These tissues were gently chopped before being treated with 20 units/ml papain in Hibernate A solution for 15 min at 37 °C. The reaction was stopped with 2 volumes of cold Hibernate A solution containing 1×protease inhibitor cocktail. The tissues were gently disrupted by pipetting with a 10 ml pipette, followed by a series of differential centrifugation as described above. The supernatant from the 10,000 g centrifugation step was filtered through a 0.22 μm syringe filter and centrifuged at 100,000 g for 70 min at 4 °C to pellet exosomes. The pellet was then resuspended in cold PBS and was centrifuged at 100,000 g for 70 min. The washed pellet was resuspended in 2 ml of 0.95 M sucrose in 20 mM HEPES, then added to a centrifuge tube containing continuous sucrose gradients (from bottom 2.0 M, 1.65 M, 1.3 M, 0.95M, 0.6M to 0.25M on top, 2 ml each gradient). The continuous sucrose gradients were centrifuged at 200,000 g for 16 h at 4 °C. The original six 2 ml fractions were collected and resuspended in 8 ml ice-cold PBS, followed by 100,000 g centrifugation for 70 min at 4 °C. Finally, pellets were resuspended in appropriate buffers.

2.18 Electron Microscopy and Immunogold Labeling.

Exosomes prepared as described above were deposited on collodion-carbon-coated grids and fixed with 2% paraformaldehyde. The exosomes were permeabilized with 0.1% saponin, followed by immunolabeling with an antibody to CD9 and secondary antibody

conjugated with 10-nm gold particles. The exosomes were negatively stained with uranyl acetate and analyzed with a transmission electron microscope.

2.19 Chromatin Immunoprecipitation (ChIP).

ChIP assay with semiquantitative PCR were performed as described in previously (Bradford et al., 2009). Astrocyte lysates were used along with reagents from the Millipore Chromatin Immunoprecipitation (ChIP) Assay kit. After cross-linking, rabbit anti-Sp1 was used to precipitate the Sp1-DNA complex. Rabbit IgG was used as a control antibody. PCR was conducted with primers to amplify the enhancer region of the mouse αB-crystallin gene (forward 5'AAG ATT CCA GTC CCT GCC CAG 3'; reverse 5' TCA CTA GCT CTC TGT CCA CAC C 3'). PCNA (forward 5' TCC TAA GGA TGG AAA CTG CAG CCT 3'; reverse 5' ATA GGC GAG GGG CAT CAC GG 3'). PCR with the precipitates by rabbit IgG or without template served as negative controls.

2.20 Statistical analyses.

Statistical analyses were performed with unpaired two-tailed Student's t-tests. Results are expressed as means ± SEM. P value < 0.05 was considered significant. Statistical significance level was set as follows: $*P < 0.05$, $**P < 0.01$, $***P < 0.001$.

Chapter 3

Mutant Huntingtin Impairs BDNF Release from Astrocytes by Disrupting Rab3a GTP/GDP Exchange

This chapter presents work published as: Yan Hong, Ting Zhao, Xiao-Jiang Li, and Shi-Hua Li (2016) The Journal of Neuroscience 36:8790-801. Yan Hong performed all of the experiments in this chapter. Yan Hong and Ting Zhao performed TIRF microscopy together. Xiao-Jiang Li and Shi-Hua Li helped with the experimental design. Xiao-Jiang Li played a key role in the preparation of the manuscript.

3.1 Abstract

Brain-derived neurotrophic factor (BDNF) is essential for neuronal differentiation and survival. We know that BDNF levels decline in the brains of patients with Huntington's disease (HD), a neurodegenerative disease caused by the expression of mutant huntingtin protein (mHtt), and furthermore that administration of BDNF in HD mice is protective against HD neuropathology. BDNF is produced in neurons, but astrocytes are also an important source of BDNF in the brain. Nonetheless, whether mHtt affects astrocytic BDNF in the HD brain remains unknown. Here we investigated astrocytes from HD140Q knock-in mice and uncovered evidence that mHtt decreases BDNF secretion from astrocytes, which is mediated by exocytosis in astrocytes. Our results demonstrate that mHtt associates with Rab3a, a small GTPase localized on membranes of dense-core vesicles, and prevents GTP-Rab3a from binding to Rab3-GAP1, disrupting the conversion of GTP-Rab3a into GDP-Rab3a and thus impairing the docking of BDNF vesicles on plasma membranes of astrocytes. Importantly, overexpression of Rab3a rescues impaired BDNF vesicle docking and secretion from HD astrocytes. Moreover, ATP release and the number of ATP-containing dense-core vesicles docking are decreased in HD astrocytes, suggesting that the exocytosis of dense-core vesicles is impaired by mHtt in HD astrocytes. Further, Rab3a overexpression reduces reactive astrocytes in the striatum of HD140Q knock-in mice. Our results indicate that compromised exocytosis of BDNF in HD astrocytes contributes to the decreased BDNF levels in HD brains and underscores the importance of improving glial function in the treatment of HD

3.2 Introduction

Huntington's disease (HD) is characterized by selective neurodegeneration, although the mutant HD protein (mHtt) is expressed in both neuronal and glial cells throughout the brain (Ross and Tabrizi, 2011; Saxena and Caroni, 2011). Despite the lower vulnerability of glial cells in HD brains, emerging evidence shows that mHtt affects the function of astrocytes. For example, mHtt decreases the levels of both EAAT2 (GLT-1) and Kir4.1 in astrocytes, which consequently increases neuronal excitotoxicity (Shin et al., 2005; Bradford et al., 2009; Tong et al., 2014). The consensus has been that dysfunctional astrocytes contribute to the pathogenesis of HD (Chan and Surmeier, 2014).

Brain-derived neurotrophic factor (BDNF), a neurotrophic factor stored in dense-core vesicles, is decreased in the brains of HD patients, as well as animal models (Zuccato et al., 2001; Hermel et al., 2004). A causal relationship between the reduction of BDNF and neuropathology in HD has been proposed (Lu et al., 2005; Zuccato and Cattaneo, 2007) and is supported by the finding that increasing BDNF levels ameliorates the neuropathology and phenotypes of HD animals (Zuccato et al., 2005; Giralt et al., 2011). The decreased BDNF in neuronal cells was found to be due to the effect of mHtt on the transcriptional expression of BDNF (Zuccato et al., 2001) and its axonal transport from cortical neurons to the striatum (Gauthier et al., 2004), implicating neuronal BDNF dysfunction in HD pathogenesis. Astrocytes are also an important source of BDNF (Miyamoto et al., 2015). BDNF is released from astrocytes via exocytosis to support the neighboring neurons and regulate their functions (Wu et al., 2008; Parpura and Zorec, 2010; Quesseveur et al., 2013). However, whether mHtt affects astrocytic BDNF production or secretion in the HD brain remains unknown. A previous study found that

overexpressing mHtt in cultured astrocytes decreased BDNF levels by sequestering BDNF transcriptional factors into mHtt aggregates (Wang et al., 2012). Considering that very few mHtt aggregates are formed in astrocytes in the HD brains that express mHtt at the endogenous level (Shin et al., 2005), we wanted to investigate whether mHtt at the endogenous level can affect BDNF production or secretion in astrocytes.

We used both full-length HD140Q knock-in (KI) and GFAP- Htt transgenic (TG) mouse models to investigate the effect of mHtt on astrocytic BDNF. In these mouse models, full-length mHtt with 140Q is expressed at the endogenous level in knock-in mice (Menalled et al., 2003), and N-terminal Htt (1–208 aa) with 160Q is expressed at levels similar to endogenous Htt (Bradford et al., 2009). Using primary astrocytes and brain-slice cultures, we found that secreted BDNF from HD astrocytes is reduced, and that this reduction stems from impaired docking of BDNF vesicles attributable to an abnormal association between mHtt and Rab3a in HD astrocytes. More importantly, overexpression of Rab3a improves docking of BDNF-containing vesicles and BDNF release from HD astrocytes. Moreover, overexpression of Rab3a ameliorated reactive astrocytes in the striatum of full-length HD140Q knock-in mice, which is an early HD pathology. Our findings suggest a new mechanism behind the reduced BDNF levels in HD brains and indicate the importance of improving the function of astrocytes in the treatment of HD.

3.3 Results

mHtt at endogenous levels impairs BDNF secretion from astrocytes

To examine whether BDNF secretion from astrocytes is affected by mHtt in KI mice, we

measured BDNF secretion by cultured astrocytes from WT, KI, and TG mice. TG mice were used because the expression of N-terminal mHtt under the control of the GFAP promoter in these mice is astrocyte-specific (Bradford et al., 2009). Using ELISA to directly detect BDNF in the cell culture medium following 28 mM KCL stimulation, we found that primary astrocytes from either TG (n = 6 independent experiments, p = 1.6381E-05) or KI (n = 4 independent experiments, p = 0.0208) mice release less BDNF into culture medium than do astrocytes from WT astrocytes (**Fig. 3.1*A***). To verify whether mHtt affects BDNF release in astrocytes in the presence of neuronal cells, we also measured BDNF release from brain slices of TG mice in which mHtt expression is restricted to astrocytes. We found that brain slices from TG mice released less BDNF than slices from WT mice (**Fig. 3.1*A*.** n = 3 independent experiments, p = 0.0449), which also suggests that the expression of mHtt in astrocytes affects BDNF secretion. Nevertheless, BDNF release from brain slices of N171-82Q mice that express N-terminal mHtt primarily in neurons is unchanged compared with WT brain slices, further indicating that mHtt selectively impairs BDNF secretion from astrocytes (**Fig. 3.1*A*.** n = 3 independent experiments, p = 0.1489).

To show the functional consequences of reduced BDNF release, we treated WT neurons with either WT or KI astrocyte-conditioned medium (ACM) for 10 min to induce phosphorylation of TrkB, as binding of BDNF to TrkB receptors leads to TrkB phosphorylation (Duman et al., 2012), so the extent of TrkB phosphorylation (p-TrkB) reflects BDNF levels in the ACM. Consistently, we found that neurons treated with KI ACM showed reduced p-TrkB levels (p-TrkB/Actin) compared with those treated with WT ACM (**Fig. 3.1*B*.** n = 4 independent experiments, p = 0.0157). This result further

supports our observation that BDNF levels are reduced in KI ACM compared with WT ACM. To verify that mHtt specifically impairs dense core vesicle release in astrocytes, we also measured glutamate release from astrocytes. This glutamate is stored in small synaptic-like clear-core vesicles. The glutamate measurement assay showed no significantly decreased levels of glutamate in TG astrocyte culture medium (Student's t-test, n = 5 independent experiments, p = 0.1027) or in KI astrocyte culture medium (Student's t-test, n = 6 independent experiments, p = 0.3647) compared with WT astrocyte culture medium **(Fig. 3.1*C*)**. Collectively, our results indicate that mHtt at endogenous levels impairs BDNF secretion from astrocytes.

mHtt does not affect the generation of BDNF in HD astrocytes

To explore the mechanism behind the decreased BDNF secretion from HD astrocytes, we first examined BDNF production in cultured astrocytes, as previous studies suggested that overexpressing mHtt influenced BDNF transcription and translation in astrocytes (Wang et al., 2012). We performed a qRT-PCR assay using BDNF-specific primers and found that levels of different BDNF mRNA isoforms are not significantly changed in TG or KI astrocytes compared with WT astrocytes (**Fig. 3.2*A*,*B***). Moreover, using western blotting and BDNF-specific antibody, we found no significant changes in either mature BDNF (mBDNF) or precursor of BDNF (pro-BDNF) in cultured astrocytes from TG or KI mice (**Fig. 3.2*C*,*D***). These results suggest that mHtt at the endogenous level does not affect BDNF mRNA or protein levels.

mHtt binds to Rab3a in astrocytes

Since BDNF synthesis was unchanged, we reasoned that the decreased BDNF protein secretion might be due to decreased exocytosis of BDNF vesicles. Rab3 is a small GTPase comprising four isoforms (Rab3 a-d) (Takai et al., 1996). Rab3a, the isoform highly enriched in the brain, is localized on membranes of secretory vesicles, including synaptic vesicles and dense core vesicles, and mediates the exocytosis of vesicles (Tsuboi et al., 2006). Although Rab3a is expressed in astrocytes (Maienschein et al., 1999), its function in astrocytes remains elusive. We used Rab3a siRNA to knock down Rab3a expression in cultured WT astrocytes and found that knocking down Rab3a results in the defective release of BDNF and ATP, another cargo in dense core vesicles, from astrocytes (**Fig. 3.3*A,B.*** BDNF release, $n = 3$ independent experiments, $p = 0.0353$; ATP release, $n = 5$ independent experiments, $p = 0.0142$). These findings suggest that Rab3a plays an important role in dense core vesicle-mediated secretion from astrocytes.

Given that mHtt binds a variety of proteins to affect intracellular trafficking (Li et al., 2004), we wanted to know whether mHtt binds Rab3a and affects its mediated BDNF secretion from astrocytes. To test this hypothesis, we performed a co-immunoprecipitation (Co-IP) assay using an antibody (1C2) to selectively precipitate mHtt and found that mHtt could coprecipitate with Rab3a from cultured KI astrocyte lysates (**Fig. 3.3*C***), but not from cultured KI neuronal lysates (**Fig. 3.3*D***). These results indicate that mHtt specifically binds to Rab3a in astrocytes. Using an antibody to precipitate Rab3a, we noticed that more degraded mHtt than full-length mHtt was coprecipitated with Rab3a (**Fig. 3.3*E***). This result suggests that N-terminal mHtt is likely to affect the function of Rab3a. To confirm the interaction of N-terminal mHtt with Rab3a, we *in vitro* synthesized N-terminal mHtt (1-212 amino acids) with 150Q and then

incubated the product with purified GST-Rab3a. This *in vitro* binding assay also showed an association between mHtt and Rab3a (**Fig. 3.3*F*)**. Since GTP-Rab3a is an active form of Rab3a for exocytosis, we immunoprecipitated mHtt from KI astrocytes and found it also interacts with GTP-Rab3a (**Fig. 3.3*G***). Together, our results suggest that Rab3a plays a critical role in BDNF secretion in astrocytes, and the association between mHtt and Rab3a may contribute to the impaired BDNF release from HD astrocytes.

mHtt binds GTP-Rab3a to prevent its association with Rab3-GAP in astrocytes

The ability to associate/dissociate GTP and GDP is essential for the function of Rab3a in dense core vesicle docking (Van et al., 2007). Given the increased binding of mHtt to GTP-Rab3a, we wanted to know whether mHtt disrupts the conversion of GTP-Rab3a into GDP-Rab3a (GTP/GDP-Rab3a exchange), which could result in altered levels of GTP-Rab3a. Using western blotting with a GTP-Rab3a-specific antibody, we found that GTP-Rab3a protein levels were indeed increased in KI astrocytes (**Fig. 3.4*A***), supporting the idea that mHtt inhibits the conversion of GTP-Rab3a. As Rab3-GAP binds GTP-Rab3a and then converts the active GTP bound form to the inactive GDP bound form (Burstein et al., 1993), we examined whether mHtt could reduce the association of GTP-Rab3a with Rab3-GAP1, the catalytic subunit of Rab3-GAP. Indeed, we found that the association between GTP-Rab3a and Rab3-GAP1 is significantly reduced in astrocytes from KI mice compared with WT astrocytes (**Fig. 3.4*B,C*.** n = 4 independent experiments, $p = 0.0041$). In addition, we observed the same result in protein lysates from KI corpus callosum, a brain region enriched in glial cells (**Fig. 3.4*B,C*.** n = 4 independent experiments, $p = 0.0106$). Western blotting using a Rab3-GAP1-specific antibody

showed that there is no difference in Rab3-GAP1 levels between WT and KI astrocytes, ruling out the possibility that the increased GTP-Rab3a is caused by a reduction of Rab3-GAP1 (**Fig. 3.4*D***). We also used an *in vitro* assay to measure GTP-Rab3a activity. In this assay, Rab3-GAP1 was removed from WT and KI astrocyte lysates by immunodepletion to examine the direct effect of mHtt in astrocyte lysates on purified Rab3a for its GTPase activity to incorporate [γ-^{32}P]-GTP (**Fig. 3.4*E***). The result revealed no difference between WT and KI lysates, suggesting that mHtt in KI lysates does not directly affect the GTPase activity of Rab3a, but disrupts GTP/GDP-Rab3a exchange by interfering with the association between GTP-Rab3a and Rab3-GAP1.

Overexpression of Rab3a in HD astrocytes rescued deficits of BDNF secretion

If mHtt binds Rab3a to inhibit GTP/GDP-Rab3a exchange, overexpression of Rab3a should antagonize this inhibition and the related decrease in BDNF release. We therefore generated adenoviral vector to overexpress Rab3a-V5 in cultured astrocytes from KI mice. Immunofluorescent staining and western blotting of these cells verified the expression of Rab3a-V5 (**Fig. 3.5*A,B***). Using stereotaxic techniques, we injected Rab3a-V5 adenovirus into the striatum of TG mice and confirmed the expression of Rab3a-V5 via western blotting (**Fig. 3.5*C***). It is important to see whether overexpressed Rab3a could increase BDNF release in HD astrocytes, so we isolated mouse brain slices 30 days after stereotaxic injection. TG mouse brain slices containing the striatum area were prepared and incubated in ACSF, immediately followed by stimulation with 56 mM KCL for 30 min to trigger BDNF release, and the ACSF in the culture dish was harvested and used for ELISA (**Fig. 3.5*D***). Similar to cultured KI astrocytes (n = 3 independent

experiments, $p = 0.0056$), the BDNF secretion from TG brain slices is also increased after viral Rab3a-V5 injection ($n = 3$ independent experiments, $p = 0.0464$) compared with control virus-infected TG mice (**Fig, 3.5*E***). Moreover, this increased BDNF release is further supported by the increased levels of p-TrkB found in cultured WT neurons that were incubated with ACM from Rab3a overexpressing KI astrocytes (**Fig. 3.5*F*.** $n = 5$ independent experiments, $p = 0.0292$). These results demonstrated that defective BDNF secretion from HD astrocytes could be rescued by overexpressing Rab3a.

Overexpression of Rab3a rescued the defective release of ATP from HD astrocytes

Since BDNF is not the only cargo in dense core vesicles, we also examined whether mHtt also impairs the release of ATP, which is stored in dense core vesicles. Quinacrine often serves as a fluorescent marker for intracellular ATP-enriched vesicles. After PMA treatment, quinacrine staining was performed by incubating living cultured astrocytes with quinacrine for 15 min at room temperature. Quinacrine staining results showed that ATP levels are higher in KI astrocytes compared with WT astrocytes after stimulation, perhaps because the reduced release of ATP increased the intracellular accumulation of ATP. Importantly, these increased ATP levels are attenuated by overexpression of Rab3a in KI astrocytes (**Fig. 3.6*A,B*.** WT vs. KI, WT = 12 cells, KI = 14 cells, $p = 0.0204$; KI vs. KI+Rab3a-V5, KI = 14 cells, KI+Rab3a-V5 = 15 cells, $p = 0.0068$). We next measured the released ATP in culture medium after stimulation. ATP release was decreased in KI astrocyte culture medium, and overexpression of Rab3a could restore the release of ATP from KI astrocytes (**Fig. 3.6*C*.** $n = 5$ independent experiments, WT vs. KI,

p = 0.00006; KI vs. KI+Rab3a-V5, p = 0.0125). These results indicated that overexpressing Rab3a could also rescue the defective ATP release from HD astrocytes.

Perturbed Rab3a GTP-GDP exchange leads to impaired docking of dense core vesicles in KI astrocytes

Disruption of GTP/GDP-Rab3a exchange is reported to cause defective docking of dense-core vesicles in mammalian chromaffin cells (Van et al., 2007). To explore whether the disrupted GTP/GDP- Rab3a exchange by mHtt influences docking of BDNF-containing dense-core vesicles in HD astrocytes, we used TIRF microscopy (TIRFM) to examine the vesicle docking in cultured astrocytes. We transfected BDNF-RFP into cultured WT and KI astrocytes and quantified BDNF-containing vesicles docking on astrocytic plasma membranes. The numbers of BDNF docking vesicles are significantly decreased in KI astrocytes (n = 16 cells, p = 0.0043) compared with WT astrocytes (n = 11 cells). Moreover, the impaired docking could be rescued by overexpressing Rab3a in KI astrocytes (n = 8 cells, p = 0.0275) compared with KI astrocytes (n = 16 cells) (**Fig. 3.7*A,C***). It is well known that Rab3a is a membrane protein of dense-core vesicles that carry not only BDNF but also other kinds of cargoes, such as ATP in astrocytes (Pangrsic et al., 2007). The disruption of BDNF vesicle docking implies that mHtt probably perturbs the docking of all dense-core vesicles in KI astrocytes. We performed fluorescent labeling of endogenous ATP with quinacrine dihydrochloride (Pangrsic et al., 2007); indeed, fewer docked ATP-containing vesicles were observed in KI (n = 13 cells, p = 0.0435) than in WT (n = 16 cells) astrocytes (**Fig. 3.7*B,D***). Moreover, overexpressing

Rab3a (n = 15 cells, p = 0.0226) could rescue the defective docking compared with KI astrocytes (n = 13 cells) without overexpression of Rab3a (**Fig. 3.7*B*,*D***).

Overexpression of Rab3a reduces reactive astrocytes in the striatum of HD140Q knock-in mice

In HD KI mouse brains, the elevated staining of GFAP, an astrocyte marker, reflects reactive astrocytes in the absence of neuronal loss (Yu et al., 2003), which represents an early HD pathological event. To examine whether overexpression of Rab3a would decrease HD-related pathology in vivo, we injected Rab3a-V5 adenovirus into the striatum of HD140Q KI mice. This Rab3a-V5 adenovirus expresses Rab3a under the control of the CMV promoter. After 21 days, we performed immunofluorescent staining and observed the preferential transduction of Rab3a-V5 adenovirus into astrocytes (**Fig. 3.8*A***), which is in agreement with previous findings that adenovirus preferentially infects glia in vivo (Iino et al., 2001; Yue et al., 2005). We then performed stereotaxic injection of Rab3a and GFP adenovirus into different sides of the striatum in the same animal ((**Fig. 3.8*B***). Compared with GFP adenovirus injection, immunofluorescent staining showed that GFAP expression level is significantly decreased in the Rab3a-V5 injection side (**Fig. 3.8*C***). We also examined NeuN-positive neuronal cells and mutant Htt aggregates, but did not see differences between adenoviral Rab3a-V5 and GFP injection sides (**Fig. 3.8*C,D***). Thus, overexpression of Rab3a could selectively decrease reactive astrocytes in HD KI mouse model. Based on these findings, we propose that mHtt binds Rab3a to affect its GTP/GDP exchange and impairs the docking of dense-core vesicles in HD astrocytes, resulting in decreased release of BDNF (**Fig. 3.9**).

3.4 Discussion

Decreased BDNF levels in HD brains are believed to play a critical role in HD pathogenesis (Zuccato et al., 2007). While previous studies have focused on the effect of mHtt on neuronal BDNF, our findings demonstrate that mHtt in astrocytes can also affect BDNF release, yielding new insight into the decreased BDNF levels in HD brain.

Given the fact that over 70% of cells in the striatum are astrocytes, the role of astrocytes in the striatum is vitally important. Astrocytes have a wide range of functions to support neuronal cells, including the reuptake of neurotransmitters and release of growth factors. MHtt was found to reduce the transcription of an important neurotransmitter transporter, glutamate transporter (GLT-1) (Bradford et al., 2009) in astrocytes, which may contribute to the increased glutamate levels and excitotoxic neuronal death in the brains of HD mice (Espey et al., 1998; Liévens et al., 2001; Behrens Pet al., 2002; Hassel et al., 2008; Estrada-Sánchez et al., 2009; Bradford et al., 2010; Wolfram-Aduan et al., 2014). Our findings indicate that mHtt can also affect the secretion of neurotrophic factors of astrocytes. Astrocytic secretion of neurotrophic factors in supporting neuronal function and survival is a well-studied subject (Quesseveur et al., 2013). BDNF is reported to play an important role in neuronal development and survival, and decreased BDNF levels in neurodegenerative diseases, including HD, Parkinson's disease, and Alzheimer's disease, have been proposed as a major player in neuronal death (Zuccato et al., 2007; Howells et al., 2000; Lee et al., 2005). Elucidating the mechanism behind the decreased BDNF in these diseases could help us find ways to restore BDNF levels in diseased brains, providing new therapeutic targets for HD, as well as other neurodegenerative diseases.

In the present study, using primary cultures and mouse brain slice models from HD mice, we found that mHtt at the endogenous level was able to compromise BDNF secretion from HD astrocytes but not from HD neurons. This idea is supported by the fact that brain slices from the N171-82Q mouse model, in which N-terminal Htt with 82Q is primarily expressed in neuronal cells (Schilling et al., 1999a), do not show defective BDNF release. Additionally, cultured astrocytes and brain slices from TG mice that express mHtt selectively in astrocytes show defective release of BDNF. This selectivity is likely due to the specific binding of mHtt to Rab3a in astrocytes, but not in neurons. Although it remains to be investigated how mHtt selectively binds Rab3a in astrocytes, we can speculate that astrocyte-specific molecules, proteins, and post-translational modifications may contribute to this selective binding, given that mHtt can associate with a large number of proteins and its function is regulated by complex post-translational modifications. Our studies also indicate that N-terminal mHtt fragments can affect the secretion of BDNF. This is because immunoprecipitation results show that N-terminal mHtt binds Rab3a and that TG mice expressing N-terminal mHtt show defective BDNF release from their astrocytes.

On the other hand, we found no changes in BDNF mRNA and protein levels in cultured astrocytes from astrocyte-specific transgenic HD or HD knock-in mice. This finding differs from an earlier report that showed that BDNF mRNA in cultured astrocytes was decreased by overexpressed N-terminal mHtt via adenoviral infection (Wang et al., 2012). This discrepancy may be due to different expression levels of mHtt. In our studies, we used astrocytes that express endogenous full-length mHtt or N-terminal mHtt at a level similar to endogenous Htt.

Rab3 undergoes functional conversion between active and inactive forms, which is essential for vesicle docking and exocytosis in cells (Darchen et al., 2000; Schlüter et al., 2004; Van et al., 2007; Tsuboi et al., 2006). It has been reported that Rab3 is located on the membrane of synaptic vesicles and dense-core vesicles regulating vesicle exocytosis in neurons; however, the location and function of Rab3 in astrocytes remains unknown. Although electron microscopy studies have shown that astrocytes contain both dense-core vesicles and synaptic-like clear-core vesicles, whether the exocytosis of these vesicles is mediated by different mechanisms is currently unknown (Parpura, et al., 2010). Despite this, we know that BDNF is packed in dense-core vesicles in astrocytes in a similar manner as in neurons, which requires GTP/GDP-Rab3a exchange (Parpura et al., 2010). We found that the association of mHtt with Rab3a perturbs this exchange. First, we detected an increased level of GTP-Rab3a in KI astrocytes, which may be the result of the impaired GTP/GDP-Rab3a exchange. Second, our results demonstrate that the binding of mHtt to GTP-Rab3a inhibits the association of GTP-Rab3a with Rab3-GAP1. Previous studies showed that Rab27 and Rab3 sequentially regulate dense-core vesicles exocytosis in human sperm cells (Bustos et al., 2012). However, we did not find the association of mHtt with Rab27 by immunoprecipitation (data not shown). These results suggest that the disruption of the GTP/GDP-Rab3a exchange causes the deficient release of BDNF from HD astrocytes by binding mHtt to Rab3a. More importantly, we found that overexpressing Rab3a significantly improved vesicle docking and BDNF release from HD astrocytes.

Previous studies also showed that overexpression of Rab3a increases vesicle docking (Martelli et al., 2000), and conversely, disruption of GTP/GDP-Rab3 exchange inhibits vesicle docking (van Weering et al., 2007). Using TIRFM, we found a reduced number of BDNF-containing docking vesicles underneath the plasma membranes of KI astrocytes, which was increased through Rab3a overexpression. This result also supports the notion that disrupting conversion of Rab3-GTP to Rab3-GDP suppresses vesicle docking. Because BDNF is not a unique cargo for dense-core vesicles (Parpura et al., 2010), we examined ATP release and the docking of ATP-containing dense-core vesicles. Consistently, we found defective ATP secretion and less docking of ATP-containing dense-core vesicles, which are also rescued by Rab3a overexpression. Therefore, our results indicate that mHtt impairs the docking of dense-core vesicles by intervening in the conversion of GTP/GDP-Rab3a in astrocytes. The defective docking of dense-core vesicles in astrocytes could impair the release of BDNF, ATP, and other molecules, which can synergistically contribute to HD pathology. In support of this idea, overexpressing Rab3a in the striatum in HD140Q knock-in mice can reduce reactive astrocytes, an early neuropathology event in HD KI mouse brains. We did not observe that overexpressed Rab3a influences mHtt aggregates, also suggesting that the rescue effect is due to the antagonistic effect on the abnormal association of mHtt with Rab3a rather than a direct effect on the expression of mutant Htt.

Substances like BDNF released from astrocytic dense-core vesicles are well known to play broad roles in neuronal survival and excitability, as well as astrocyte-neuron communication. Our findings provide new insight into the decreased secretion of BDNF from HD astrocytes in which mHtt is expressed at endogenous levels. Our

findings also suggest that mHtt could affect other functions of astrocytes or the secretion of different molecules via a similar mechanism. Furthermore, our finding that Rab3a overexpression can rescue the defective docking, increase BDNF secretion, and ameliorate reactive astrocytes in vivo suggests that improving the exocytosis function of astrocytes could be beneficial to the treatment of HD.

Figure 3.1

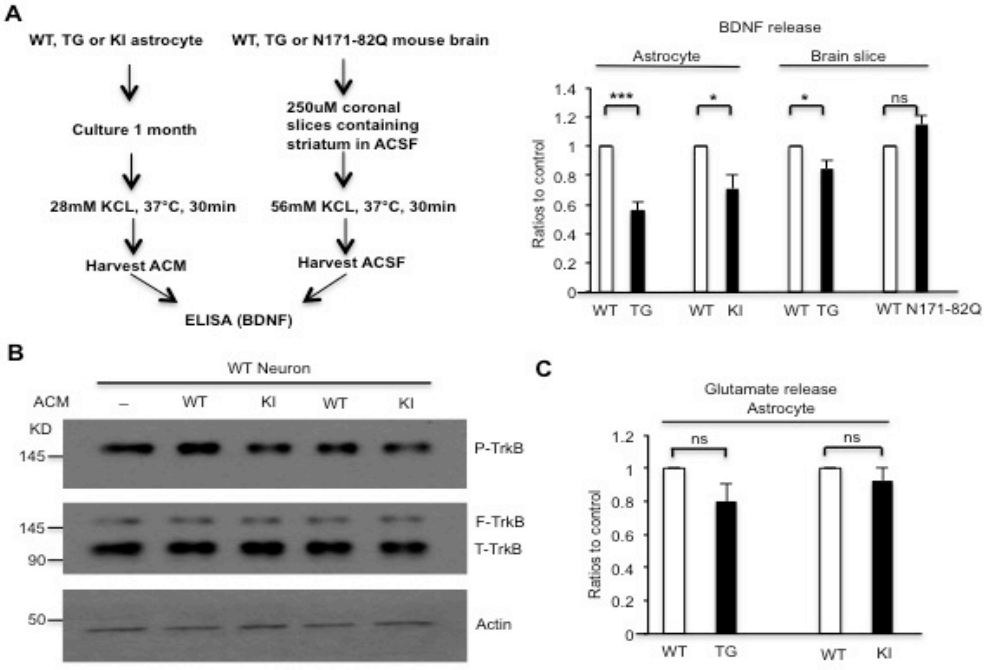
A
WT, TG or KI astrocyte
WT, TG or N171-82Q mouse brain
Culture 1 month
250uM coronal slices containing striatum in ACSF
28mM KCL, 37°C, 30min
56mM KCL, 37°C, 30min
Harvest ACM
Harvest ACSF
ELISA (BDNF)
BDNF release
Astrocyte
Brain slice
Ratios to control
WT TG
WT KI
WT TG
WT N171-82Q
B
WT Neuron
ACM
–
WT
KI
WT
KI
KD
145
P-TrkB
145
90
F-TrkB
T-TrkB
50
Actin
C
Glutamate release
Astrocyte
Ratios to control
WT
TG
WT
KI

Figure 3.1.

BDNF secretion from HD astrocytes is reduced. ***A,*** ELISA assay showed that cultured primary astrocytes from TG (Student's t-test, n = 6 independent experiments, p = 1.6381E-05) and KI (Student's t-test, n = 4 independent experiments, p = 0.0208) mice release less BDNF than astrocytes from WT mice. ELISA results also indicated that BDNF secretion is decreased from brain slices of TG mice compared with WT mice (Student's t-test, n = 3 independent experiments, p = 0.0449). However, BDNF secretion is unchanged from brain slices of N171-82Q mice compared with WT mice (Student's t-test, n = 3 independent experiments, p = 0.1489). ***B*****,** WT neurons were treated with astrocyte-conditioned medium (ACM) containing released BDNF from WT or KI astrocytes, and then analyzed via Western blotting to examine p-TrkB levels. p-TrkB is decreased in KI ACM-treated neurons, confirming decreased BDNF in KI ACM. ***C***, Glutamate measurement assay showing no significant reduction in glutamate release in cultured astrocytes from TG mice (Student's t-test, n = 5 independent experiments, p = 0.1027) or KI mice (Student's t-test, n = 6 independent experiments, p = 0.3647) compared with WT astrocytes. *$p < 0.05$, **$p < 0.01$, *** $p < 0.001$, ns, not significant.

Figure 3.2

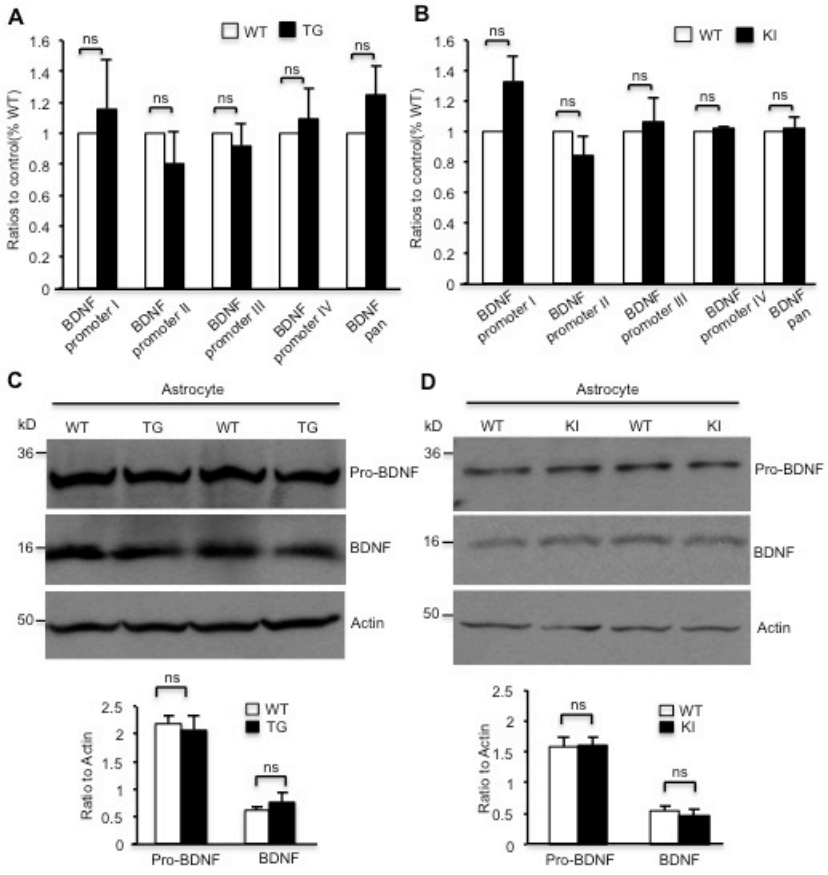
A
WT
TG
Ratios to control(% WT)
ns
BDNF promoter I
BDNF promoter II
BDNF promoter III
BDNF promoter IV
BDNF pan
B
WT
KI
Ratios to control(% WT)
C
Astrocyte
kD
WT
TG
WT
TG
36
Pro-BDNF
16
BDNF
50
Actin
Ratio to Actin
Pro-BDNF
BDNF
D
Astrocyte
WT
KI
WT
KI

Figure 3.2.

Transcription or translation of BDNF is not changed in the HD astrocytes. ***A-B***, RT-qPCR results revealing no significant reduction in BDNF mRNA levels in cultured astrocytes from TG mice (***A***, Student's t-test, n = 5 independent experiments; BDNF transcripts generated by different promoters are indicated: BDNF promoter I, p = 0.5844; BDNF promoter II, p = 0.3669; BDNF promoter III, p = 0.5765; BDNF promoter IV, p = 0.67; BDNF promoter pan, p = 0.2406) or KI mice (***B***, Student's t-test, n = at least 5 independent experiments; BDNF promoter I, p = 0.0688; BDNF promoter II, p = 0.2283; BDNF promoter III, p = 0.6892; BDNF promoter IV, p = 0.0809; BDNF promoter pan, p = 0.7733) compared with WT astrocytes. ***C-D***, Western blotting revealing similar mature BDNF (mBDNF) and pro-BDNF levels in cultured astrocytes from TG (***C***), KI (***D***), and WT mice. Quantifying ratios of pro-BDNF or mBDNF to actin in TG astrocytes (***C***, Student's t-test; pro-BDNF, n = 8 independent experiments, p = 0.6983; mBDNF, n = 8 independent experiments, p = 0.4087) and KI astrocytes (***D*****,** Student's t-test; pro-BDNF, n = 8 independent experiments, p = 0.8801; mBDNF, n = 5 independent experiments, p = 0.6349). ns, not significant.

Figure 3.3

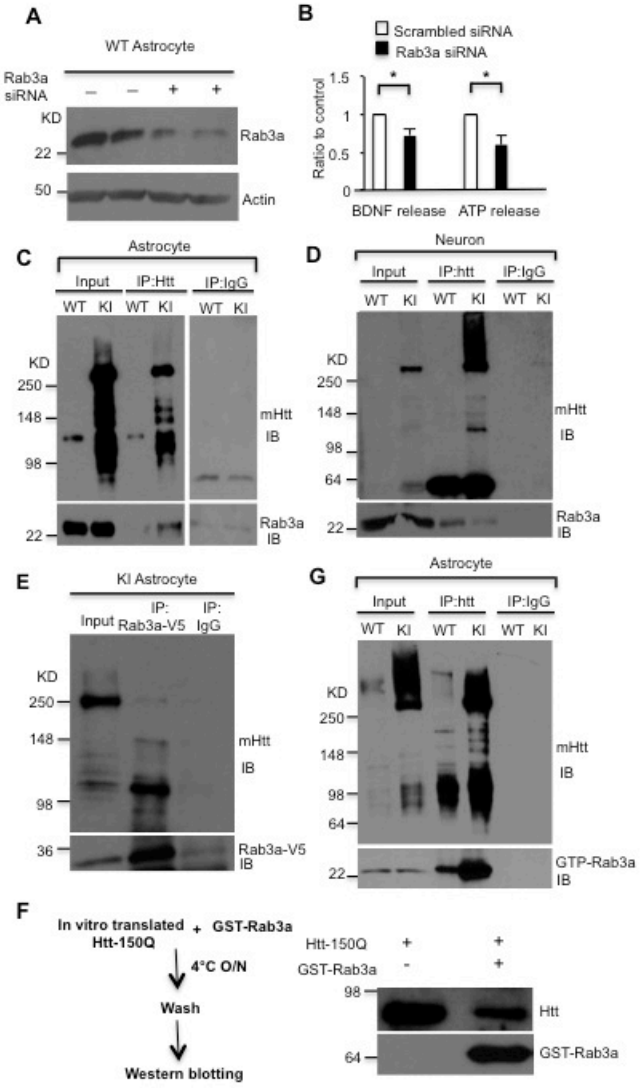
A
WT Astrocyte
Rab3a siRNA
– – + +
KD
22
Rab3a
50
Actin
B
Scrambled siRNA
Rab3a siRNA
Ratio to control
1.5
1
0.5
0
*
*
BDNF release
ATP release
C
Astrocyte
Input
IP:Htt
IP:IgG
WT KI WT KI WT KI
KD
250
148
98
22
mHtt IB
Rab3a IB
D
Neuron
Input
IP:htt
IP:IgG
WT KI WT KI WT KI
KD
250
148
98
64
22
mHtt IB
Rab3a IB
E
KI Astrocyte
Input
IP: Rab3a-V5
IP: IgG
KD
250
148
98
36
mHtt IB
Rab3a-V5 IB
G
Astrocyte
Input
IP:htt
IP:IgG
WT KI WT KI WT KI
KD
250
148
98
64
22
mHtt IB
GTP-Rab3a IB
F
In vitro translated Htt-150Q
+ GST-Rab3a
4°C O/N
Wash
Western blotting
Htt-150Q + +
GST-Rab3a - +
98
64
Htt
GST-Rab3a

Figure 3.3.

MHtt associates with Rab3a in astrocytes. ***A***, Knocking down Rab3a via siRNA in WT astrocytes. ***B***, ELISA results showing that downregulation of Rab3a inhibits the release of BDNF and ATP from WT astrocytes compared with scrambled siRNA transfected astrocytes. (Student's t-test, BDNF release, $n = 3$ independent experiments, $p = 0.0353$; ATP release, $n = 5$ independent experiments, $p = 0.0142$). ***C-D,*** Association of mHtt with Rab3a is detected in cultured KI astrocytes (***C***) but not in cultured KI neurons (***D***). Endogenous mHtt in KI astrocytes or KI neurons was immunoprecipitated by 1C2 antibody, and the immunoprecipitates were probed with antibody to Rab3a. IP with IgG served as a control. ***E*****,** Association of mHtt with Rab3a-V5 was detected in cultured KI astrocytes infected with Rab3a-V5 adenovirus. Rab3a was immunoprecipitated by anti-V5 antibody, and the immunoprecipitates were probed with antibodies to 1C2 to detect mHtt. IP with IgG served as a control. ***F*****,** *in vitro* binding assay showed that *in vitro* translated Htt (1-212 amino acid) with 150Q binds to purified GST-Rab3a. ***G***, Binding of mHtt to GTP-Rab3a was found in cultured HD KI astrocytes. 1C2 antibody was used to immunoprecipitate endogenous mHtt in HD KI astrocytes, and the immunoprecipitates were probed with the antibody specific to GTP-Rab3a. $*p < 0.05$.

Figure 3.4

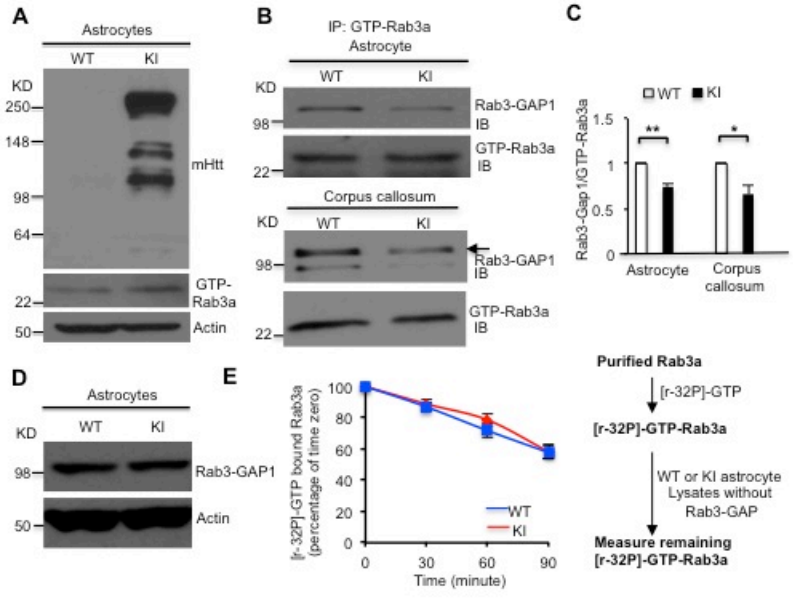
A
Astrocytes
WT
KI
KD
250
148
98
64
22
50
mHtt
GTP-Rab3a
Actin
B
IP: GTP-Rab3a
Astrocyte
WT
KI
KD
98
22
Rab3-GAP1 IB
GTP-Rab3a IB
Corpus callosum
WT
KI
KD
98
22
Rab3-GAP1 IB
GTP-Rab3a IB
C
WT
KI
Rab3-Gap1/GTP-Rab3a
1.5
1
0.5
0
**
*
Astrocyte
Corpus callosum
D
Astrocytes
WT
KI
KD
98
50
Rab3-GAP1
Actin
E
[r-32P]-GTP bound Rab3a (percentage of time zero)
100
80
60
40
20
0
0
30
60
90
Time (minute)
WT
KI
Purified Rab3a
[r-32P]-GTP
[r-32P]-GTP-Rab3a
WT or KI astrocyte Lysates without Rab3-GAP
Measure remaining [r-32P]-GTP-Rab3a

Figure 3.4.

Reduced association between Rab3-GAP1 and Rab3a by mHtt results in increased GTP-Rab3a in HD astrocytes. ***A***, GTP-Rab3a protein levels were increased in cultured KI astrocytes (Student's t-test, n = 3 independent experiments, p = 0.0402). ***B-C***, Association between GTP-Rab3a with Rab3-GAP1 is decreased in both cultured KI astrocytes (***C*****,** Student's t-test, n = 4 independent experiments, p = 0.0041) and in the corpus callosum of KI mice (***C*****,** Student's t-test, n = 4 independent experiments, p = 0.0106). ***D*****,** Rab3-GAP1 levels did not change in KI astrocytes. ***E***, GTPase activity of purified GST-Rab3a was not affected by binding to mHtt (Student's t-test, n = 4 independent experiments, 30 min, p = 0.4807; 60 min, p = 0.9353; 90 min, p = 0.4071). *$p < 0.05$, **$p < 0.01$; ns, not significant.

Figure 3.5

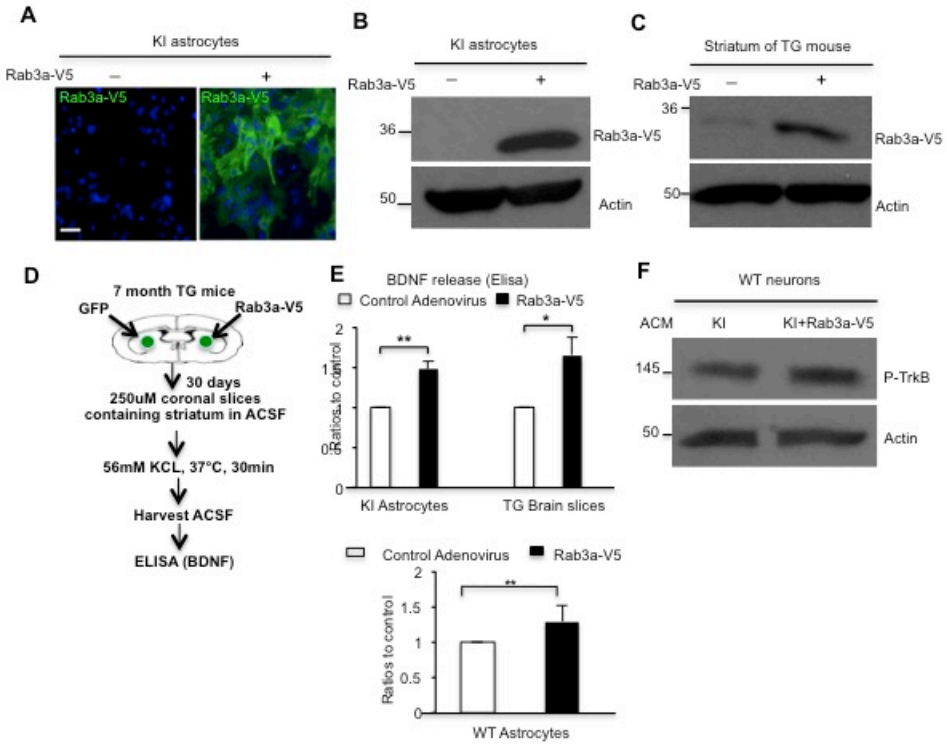
A
KI astrocytes
Rab3a-V5
–
+
Rab3a-V5
Rab3a-V5
B
KI astrocytes
Rab3a-V5
–
+
36
Rab3a-V5
50
Actin
C
Striatum of TG mouse
Rab3a-V5
–
+
36
Rab3a-V5
50
Actin
D
7 month TG mice
GFP
Rab3a-V5
30 days
250uM coronal slices
containing striatum in ACSF
56mM KCL, 37°C, 30min
Harvest ACSF
ELISA (BDNF)
E
BDNF release (Elisa)
Control Adenovirus
Rab3a-V5
Ratios to control
**
*
KI Astrocytes
TG Brain slices
Control Adenovirus
Rab3a-V5
**
Ratios to control
WT Astrocytes
F
WT neurons
ACM
KI
KI+Rab3a-V5
145
P-TrkB
50
Actin

Figure 3.5.

Overexpression of Rab3a rescues defective release of BDNF from HD astrocytes. ***A-B*****,** Overexpression of Rab3a in KI astrocytes by adenovirus infection was confirmed by immunostaining **(*A*)** and western blotting **(*B*)**. ***C*****,** Rab3a was overexpressed in the striatum of TG mice by injecting Rab3a-V5 adenovirus into the striatum. ***D-E***, ELISA results indicated that BDNF secretion was increased from cultured KI astrocytes infected with Rab3a-V5 adenovirus (Student's t-test, $n = 3$ independent experiments, $p = 0.0056$) or from Rab3a-V5 adenovirus-injected brain slices containing striatum of TG mice (Student's t-test, $n = 3$ independent experiments, $p = 0.0464$). WT astrocyte cultures showed the same results. ***F***, WT neurons were treated with astrocyte-conditioned medium (ACM) containing released BDNF from KI or Rab3a-overexpressed KI astrocytes. p-TrkB levels are increased in neurons treated with Rab3a-overexpressed KI ACM relative to those treated with KI ACM (Student's t-test, n = 5 independent experiments, $p = 0.0292$). *$p < 0.05$, **$p < 0.01$; ns, not significant.

Figure 3.6

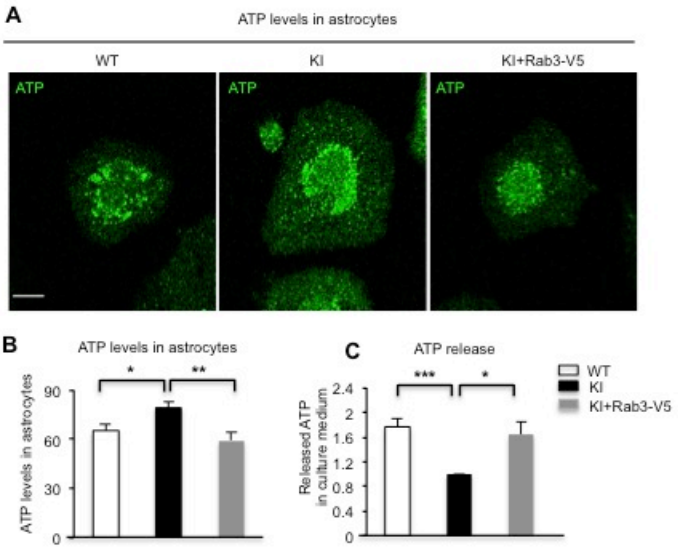
A
ATP levels in astrocytes
WT
KI
KI+Rab3-V5
ATP
ATP
ATP
B
ATP levels in astrocytes
ATP levels in astrocytes
90
60
30
0
*
**
C
ATP release
Released ATP in culture medium
2.4
2
1.6
1.2
0.8
0.4
0
***
*
WT
KI
KI+Rab3-V5

Figure 3.6.

Overexpression of Rab3a rescues the deficient release of ATP from HD astrocytes. ***A*,** Quinacrine staining was performed by incubating living cultured WT, KI, and Rab3a-overexpressed KI astrocytes for 15 min after treatment of phorbol 12-myristate 13-acetate (PMA). ***B*,** The quantitative results showed that ATP levels are higher in KI astrocytes than WT astrocytes after stimulation, and overexpression of Rab3a reduces ATP levels in astrocytes compared with KI astrocytes (Student's t-test; WT vs. KI, WT = 12 cells, KI = 14 cells, $p = 0.0204$; KI vs. KI+Rab3a-V5, KI = 14 cells, KI+Rab3a-V5 = 15 cells, $p = 0.0068$). ***C*,** Bioluminescence assay showed that ATP secretion was rescued from cultured KI astrocytes infected with Rab3a-V5 adenovirus (Student's t-test, $n = 5$ independent experiments, WT vs. KI, $p = 0.00006$; KI vs. KI+Rab3a-V5, $p = 0.0125$). *$p < 0.05$, **$p < 0.01$, *** $p < 0.001$. Scale bar, 10μm.

Figure 3.7

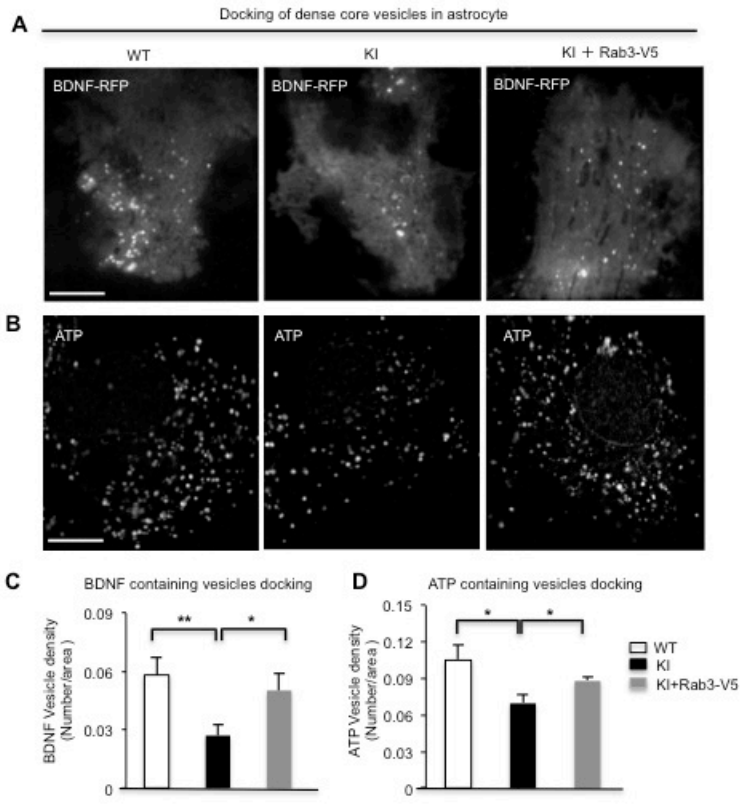
A
Docking of dense core vesicles in astrocyte
WT
KI
KI + Rab3-V5
BDNF-RFP
BDNF-RFP
BDNF-RFP
B
ATP
ATP
ATP
C
BDNF containing vesicles docking
BDNF Vesicle density (Number/area)
0.09
0.06
0.03
0
**
*
D
ATP containing vesicles docking
ATP Vesicle density (Number/area)
0.15
0.12
0.09
0.06
0.03
0
*
*
WT
KI
KI+Rab3-V5

Figure 3.7.

Defective docking of BDNF- and ATP-containing vesicles are rescued by Rab3a overexpression in HD astrocytes. ***A-D***, Total internal reflection fluorescence microscopy (TIRFM) revealing the docking of BDNF-containing vesicles (***A, C.*** Student's t-test; WT vs. KI, WT = 11 cells, KI = 16 cells, $p = 0.0043$; KI vs. KI+Rab3a-V5, KI = 16 cells, KI+Rab3a-V5 = 8 cells, $p = 0.0275$) and ATP-containing vesicles (***B, D.*** Student's t-test; WT vs. KI, WT = 16 cells, KI = 13 cells, $p = 0.0435$; KI vs. KI+Rab3a-V5, KI = 13 cells, KI+Rab3a-V5 = 15 cells, $p = 0.0226$) are compromised in KI astrocytes, which can be improved by overexpressing Rab3a. *$p < 0.05$, **$p < 0.01$. Scale bar, 10 μm.

Figure 3.8

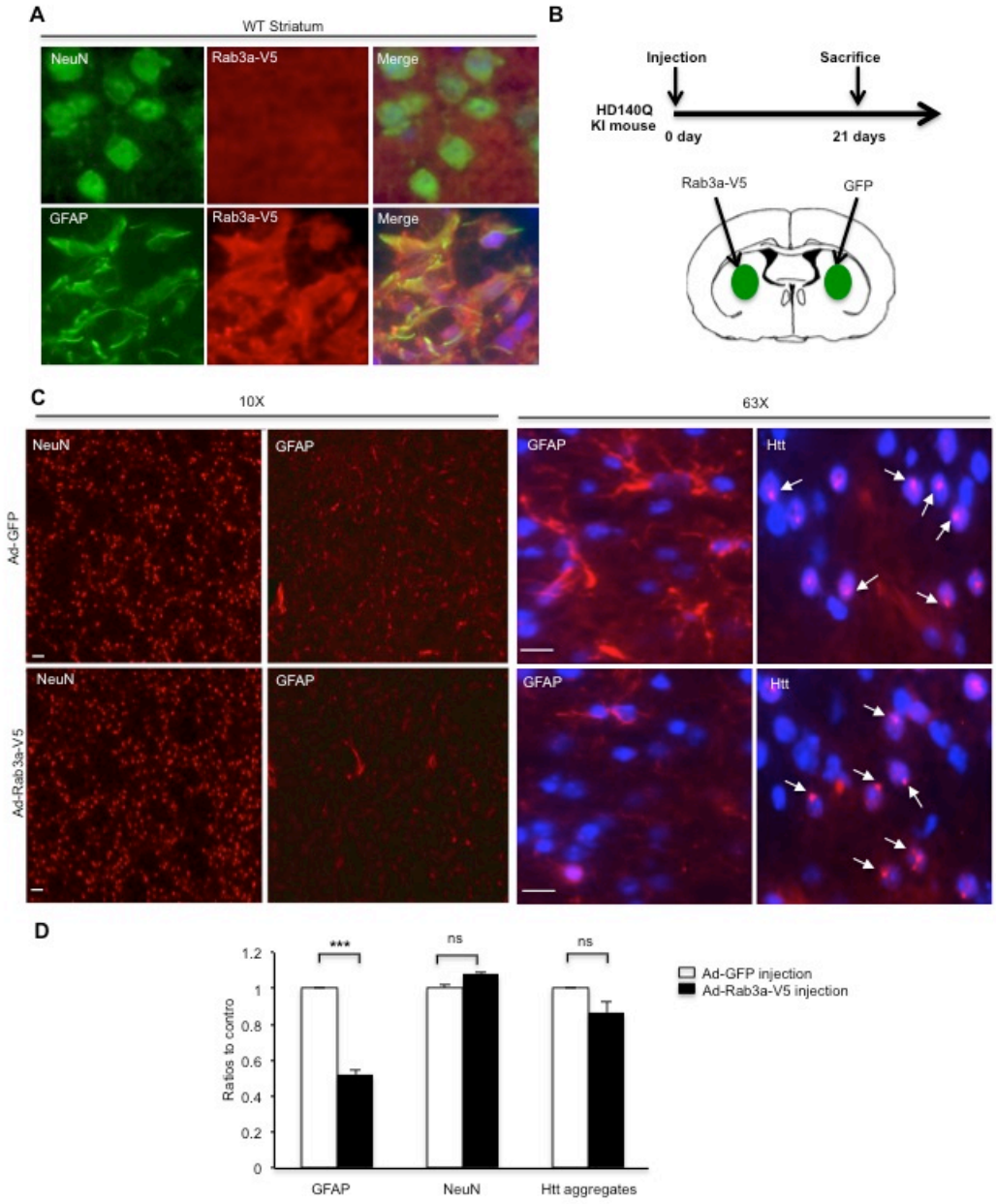
A
WT Striatum
NeuN
Rab3a-V5
Merge
GFAP
Rab3a-V5
Merge
B
Injection
Sacrifice
HD140Q
KI mouse
0 day
21 days
Rab3a-V5
GFP
C
10X
63X
Ad-GFP
Ad-Rab3a-V5
NeuN
GFAP
GFAP
Htt
D
***
ns
ns
Ratios to contro
1.2
1
0.8
0.6
0.4
0.2
0
Ad-GFP injection
Ad-Rab3a-V5 injection
GFAP
NeuN
Htt aggregates

Figure 3.8.

Overexpression of Rab3a reduces reactive astrocytes in the striatum of HD140Q KI mice. ***A***, Wild-type mice at 5-month-old were injected with Rab3a-V5 adenovirus into the left side of the striatum. After 21 days, immunofluorescent staining showed that Rab3a-V5 preferentially infected astrocytes in the striatum. ***B,*** The procedure of stereotaxic injection of 9-month-old HD140Q KI mice. ***C,*** Low magnification (10 X) micrographs showing NeuN and GFAP staining in adenoviral GFP and Rab3a-V5 injected striatum. High magnification (63 X) micrographs showing GFAP (red) or mutant Htt aggregates (arrows, red) staining in the merged images in which the nuclei are stained by Hoechst (blue). Scale bars: 10 mm. ***D,*** Quantitative analysis of the GFAP immunofluorescent density showing GFAP staining is significantly decreased in the Rab3a-V5 injection side compared with GFP injection side (Student's t-test, randomly selected 7-10 images per section, n = 8 sections per group, p = 7.51767E-13). The percentage of NeuN-positive cells and the number of mutant Htt aggregates per image are unchanged (Student's t-test, n = 600 cells per group, NeuN-positive cells, p = 0.1016; aggregates number, p = 0.1511). ***$p < 0.001$; ns, not significant.

Figure 3.9

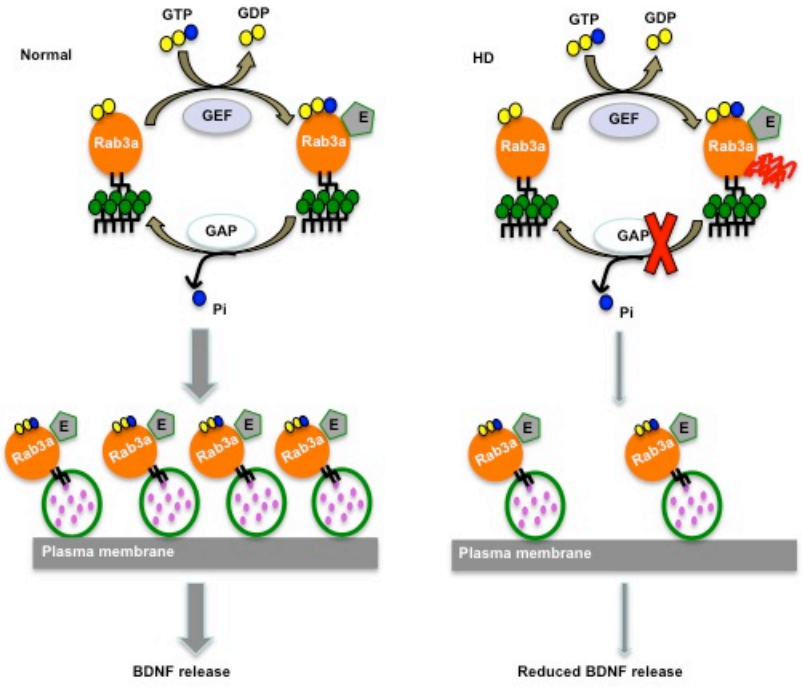
Normal
GTP
GDP
GEF
Rab3a
E
GAP
Pi
Plasma membrane
BDNF release
HD
GTP
GDP
GEF
Rab3a
E
GAP
Pi
Plasma membrane
Reduced BDNF release

Figure 3.9.

Proposed model for the decreased dense core vesicles released from HD astrocytes. Rab3a GTP/GDP exchange is essential for docking of dense core vesicles in astrocytes. In HD, the binding of mHtt to GTP-Rab3a keeps GTP-Rab3a from associating with Rab3-GAP1, disrupts Rab3a GTP/GDP exchange, inhibits docking of dense core vesicles, and results in the decreased release of secreted molecules, such as BDNF.

Chapter 4

Mutant Huntingtin Inhibits αB-crystallin Expression and Impairs Exosome Secretion From Astrocytes

This chapter presents work as: Yan Hong, Ting Zhao, Xiao-Jiang Li, and Shi-Hua Li. (submitted to The Journal of Neuroscience)

Yan Hong performed all of the experiments in this chapter. Yan Hong and Ting Zhao performed confocal microscopy together. Xiao-Jiang Li and Shi-Hua Li helped with the experimental design. Xiao-Jiang Li played a key role in the preparation of the manuscript.

4.1 **Abstract**

Exosomes, which are secreted from multiple types of cells including astrocytes and carry proteins and genetic materials, play important roles in cell-cell communication under physiological and pathophysiological conditions. Since mutant huntingtin (mHtt) with an expanded polyglutamine repeat in its N-terminal region can accumulate in glial cells to affect multiple cellular functions in Huntington disease (HD), it remains unknown whether mHtt is present in astrocytic exosomes or affects their generation or secretion. We found that mHtt is not present in astrocytic exosomes but can decrease exosome secretion from astrocytes in HD140Q knock-in (KI) mice. The decreased secretion from cultured astrocytes is caused by the expression of N-terminal mHtt that is able to accumulate in the nuclei and form aggregates. Consistently, there is a significant decrease in exosome secretion in the HD KI mouse striatum that showed abundant nuclear mHtt aggregates. Conversely, injection of astrocytic exosomes into the striatum of HD KI mice can reduce the density of mHtt aggregates. mHtt in astrocytes decreased the expression of αB-crystallin, a small heat shock protein that is enriched in astrocytes and mediates exosome secretion, by reducing the association of Sp1 with the enhancer of the αB-crystallin gene to affect its transcription. Importantly, overexpression of αB-crystallin rescues defective exosome release from HD astrocytes and reactive astrocytes as well as mHtt aggregates in the striatum of HD KI mice. Our results demonstrate that mHtt reduces the expression of αB-crystallin in astrocytes to decrease exosome secretion in the HD brains, contributing to non-cell-autonomous neurotoxicity in HD.

4.2 Introduction

Huntington's disease (HD) is a fatal, autosomal dominant, inherited neurodegenerative disorder that is caused by an expanded polyglutamine in the N-terminal region of huntingtin (Ross and Tabrizi, 2011; Bates et al., 2015). Although neuronal cells are preferentially degenerated in HD, the function of glial cells is also affected by mutant huntingtin (mHtt) (Hsiao and Chern, 2010; Lee et al., 2013). For example, mHtt reduces expression levels of EAAT2 (GLT-1) and potassium ion channel (Kir4.1) in astrocytes, which consequently increases neuronal excitotoxicity (Shin et al., 2005; Bradford et al., 2009; Tong et al., 2014). Our recent studies show that mHtt also decreases BDNF secretion by compromising exocytosis of dense-core vesicles in astrocytes (Hong et al., 2016). These findings suggest that mHtt may impair multiple functions in astrocytes.

Recent studies have found that astrocytes also secrete exosomes to support the normal function and survival of neuronal cells (Taylor et al., 2007; Guitart et al., 2016). Exosomes are small membranous vesicles (40-100 nm) secreted by multiple cell types and can be isolated from conditioned cell culture media or body fluids. Functions of exosomes include exchanging signals with neighboring cells, removing unwanted proteins, and transfer of pathogens between cells. Exosomes contain different types of mRNA, miRNA, and proteins, which are dependent on the host cells that produce exosomes (Théry, 2011; Jarmalavičiūtė and Pivoriūnas, 2016). Exosomes from neuronal cells have been found to spread misfolded proteins between cells, a mechanism underlying the spread of toxic proteins in the brain (Bellingham et al., 2012; Wang et al., 2017). However, exosomes from glial cells can carry neuroprotective molecules to prevent neurondegeneration (Hajrasouliha et al., 2013; Haney et al., 2013; Zhao et al., 2014; Guitart et al., 2016; Xin et al., 2017). For example, astrocyte-derived exosomes

carry neuroprotective cargoes, such as HSP70 and HspB1, to execute neuroprotective function (Taylor et al., 2007; Nafar et al., 2016). Whether mHtt is present in astrocytic exsomes to spread mHtt or affects astrocytic exosome biogenesis and/or release remains to be investigated.

Using primary astrocyte cultures from the HD 140Q knock-in (KI) mouse model that express full-length mHtt at the endogenous level, we found that mHtt is not present in astrocyte-derived exosomes, suggesting that mHtt is not transferred by astrocytic exosomes. Instead, the secretion of exosomes from HD astrocytes is affected. αB-crystallin, a small heat shock protein enriched in astrocytes and oligodendrocytes, is known to mediate exosome secretion (Gangalum et al., 2016). We found that αB-crystallin is deficient in HD astrocytes because mHtt affects its transcription. More importantly, overexpression of αB-crystallin improved exosome secretion from HD astrocytes and also ameliorated the neuropathology in HD KI mice. Our findings demonstrate for the first time that mHtt impairs exosome secretion, and also suggest a new mechanism underlying non-cell-autonomous neurotoxicity of mHtt.

4.3 Results

mHtt is not present in exosomes secreted by cultured astrocytes

It has been reported that mHtt may spread from cell to cell (Pecho-Vrieseling et al., 2014; Jeon et al., 2016; Zhang et al., 2016). To examine whether mHtt is a cargo of astrocyte-derived exosomes, we isolated exosomes from the culture medium of primary astrocytes from HD140Q knock-in (KI) mice following the established centrifugation protocol of exosome isolation (Théry et al., 2006). Briefly, we harvested culture medium of 30 days-old primary astrocytes and centrifuged it at a series of low- and high-speeds to isolate

exosomes (**Fig. 4.1*A***). Electron microscopy of the exosome fraction showed CD9 immunogold staining, which is a marker of exosomes, in the exosomes at the proper size (40-100 nm) (**Fig. 4.1*B***). Western blotting showed that exosome markers, such as Alix, Flotillin-1 and Hsc70, but not Grp78 (ER marker) and GM 130 (Golgi marker), are in the exosome fraction, indicating the purity of exosomes (**Fig. 4.1*C***). It has been reported that proteins associated with certain neurodegenerative disorders, such as APP and α-synuclein, are present in exosomes that are released from neurons (Xiao et al., 2017; Bieri et al., 2017). We also isolated exosomes from cultured HD KI neurons. Interestingly, we did not detect mHtt in the exosomes released from either astrocytes or neurons (**Fig. 4.1*D***), suggesting that exosomes would not transfer mHtt between cells in the HD brains. By comparing exosomes released from astrocytes and neurons that have the same quantity of proteins in their lysates, we found that astrocytes secreted more exosomes with more Hsc70 (**Fig. 4.1*E***). It has been shown that exosomes isolated from plasma could be directly injected into the mouse brain and are able to diffuse from the injected site (Zheng et al., 2017). To assess the protective effect of exosomes isolated from astrocytes, we injected astrocytic exosomes into the striatum of HD KI mice. Seven days after the injection, we observed a significant decrease in mHtt aggregate density in the injected site (**Fig. 4.2**), perhaps because exosomes-carrying Hsc70 and other molecules help the clearance of misfolded and aggregated proteins.

mHtt reduces exosome secretion from cultured astrocytes

Given that astrocytic exosomes are protective and that mHtt can impair the release of dense-core vesicles from cultured astrocyte (Hong et al., 2016), we wanted to examine whether mHtt affects the secretion of astrocytic exosomes. We therefore isolated

exosomes from WT and HD KI astrocyte culture medium. Western blotting showed that two exosome markers, Alix and Flotilin-1, are equally present in the lysates of WT and KI astrocytes. However, both Alix and Flotilin-1 are decreased in the isolated exosomes from HD KI astrocytes as compared with WT astrocytes (**Fig. 4.3*A***). Quantitative analysis of the ratio of Alix or Flotillin-1 in HD KI exosomes to that in WT exosomes showed 56.4 % and 45.3% reduction, respectively, in HD KI exosomes (**Fig. 4.3*B***). We also performed MTS cell proliferation assay to examine the cell viability and found no significant changes between WT and HD KI astrocytes. These results suggest that mHtt does not affect the biogenesis of exosome proteins, but rather impairs exosome secretion from astrocytes.

N-terminal fragments of mHtt impair exosome secretion from cultured astrocytes

Since smaller N-terminal mHtt is much more toxic than longer mHtt fragments (Davies et al., 1997; Schilling et al., 1999a; Slow et al., 2003; Gray et al., 2008), we wanted to investigate whether exosome secretion from astrocytes is affected in a fragment length-dependent manner. We transfected different N-terminal fragments (Htt-Exon1-20Q, -120Q; Htt-212aa-23Q, -150Q; Htt-508aa-23Q, -120Q) into WT astrocytes (**Fig. 4.4*A,B***). Western blotting results showed that in cell lysates, Alix and Flotillin-1 levels are equivalent between WT and mutant N-terminal Htt fragment-transfected astrocytes (**Fig. 4.4*C,E***). However, in exosomes derived from astrocytes transfected with different N-terminal Htt fragments, Alix and Flotillin-1 levels were significantly reduced when mutant Exon-1 Htt and Htt-212 fragments, but not the longer fragment (Htt-508), were expressed as compared with their WT counterparts (**Fig. 4.4*D,E***). These results indicate

that smaller N-terminal mHtt fragments were able to inhibit exosome secretion from astrocytes.

mHtt decreases exosome secretion from KI mouse striatum

Next, we wanted to know whether mHtt affects exosome secretion in the HD KI mouse brain. To examine exosome secretion in vivo, we isolated exosomes from the fresh mouse brain cortical tissues that were treated with papain to loosen the extracellular matrix and to release extracellular materials (Perez-Gonzalez et al., 2012; Polanco et al., 2016; Baker et al., 2016). The mild papain treatment does not break the cell membrane and thus prevents the contamination of the extracellular fluid with intracellular vesicles. Following a series of low- and high-speed centrifugations, exosomes derived from the cortex were further purified by a sucrose step gradient (**Fig. 4.5*A***). We found that fraction 3 (F3=0.95M sucrose) showed the highest levels of exosome markers (Alix, Flotillin-1), which is consistence with previous studies (**Fig. 4.5*B***; Perez-Gonzalez et al., 2012; Polanco et al., 2016). We therefore used fraction 3 as an exosome-enriched fraction to isolate exosomes from the cortex and striatum of 10-month-old WT or KI mice. Although Alix and Flotillin-1 in the cortex or the striatum lysates were not different between WT and HD KI mice, Alix and flotillin-1 levels were significantly decreased in the exosome fraction isolated from the HD KI striatum, but not the HD KI cortex compared with WT controls (**Fig. 4.5*C,D***). In HD KI mice, only N-terminal mutant Htt forms aggregates, and these aggregates have been found to be much more abundant in the striatum than in the cortex (Li et al., 2000; 2001). In the double immunofluorescence staining using antibodies to an astrocytic marker (GFAP) or neuronal marker (NeuN) and anti-Htt (mEM48), we found nuclear mHtt aggregates in both astrocytes and neurons in the

striatum of 10-month-old HD KI mouse (**Fig. 4.5*E***). As reported previously, neuronal aggregates are much larger and more abundant than glial Htt aggregates (Shin et al., 2007; Bradford et al., 2009), perhaps because glial cells are able to clear misfolded proteins more efficiently (Zhao et al., 2016; Tydlacka et al., 2008).

mHtt impairs αB-crystallin expression both in cultured astrocytes and in the striatum

The nuclear localization of mutant Htt in astrocytes led us to investigate whether mHtt affects the transcription of molecules that are important for the release of exosomes. It has been found that αB-crystallin, which mediates exosome secretion (Gangalum et al., 2016), is decreased in HD mouse models, such as R6/2 and BACHD mice (Zabel et al., 2002; Oliveira et al., 2016). By comparing the expression of αB-crystallin in cultured astrocytes and neurons, we found that αB-crystallin is much more abundant in astrocytes (**Fig. 4.6*A***). This marked difference led us to examine whether αB-crystallin is also decreased in the HD KI mouse model that expresses full-length Htt at the endogenous level. We used real-time PCR to examine mRNA levels of αB-crystallin in cultured KI astrocytes and found that the level of αB-crystallin mRNA is not changed at 28 days, but is decreased at 35 days compared with WT astrocytes (**Fig. 4.6*B***). Consistently, western blotting revealed that the level of αB-crystallin protein was also decreased at 35 days in cultured KI astrocytes as compared with WT astrocytes and other heat shock proteins (**Fig. 4.6*C,D***). Next, we examined αB-crystallin levels in the striatum of HD KI mice to see whether the pretein is altered during the progression of the disease. The striatum was isolated from HD KI mice at different ages (3-, 8- and 10-month-old) and lysed for

western blotting analysis. αB-crystallin was not altered until 10 months and showed a decrease when compared with the WT control (**Fig. 4.6*E***). The age-dependent decrease in αB-crystallin is consistent with the age-dependent accumulation of N-terminal Htt fragments and the formation of Htt aggregates in the KI mouse striatum.

Sp1 mediates αB-crystallin expression in astrocytes

Although αB-crystallin is decreased in HD mouse brains (Zabel et al., 2002; Oliveira et al., 2016), the mechanism underlying this decrease has not been elucidated. Since mRNA levels of αB-crystallin are reduced in KI astrocytes, we hypothesized that mHtt inhibits αB-crystallin transcription by affecting its promoter activity. Sp1 was found to regulate the activity of αB-crystallin by binding to its enhancer to activate its promoter (Swamynathan et al., 2007). Based on the fact that N-terminal mHtt binds Sp1 in astrocytes and affects the Sp1-dependent transcription of GLT-1 (Bradford et al., 2009), we asked whether mHtt in HD KI astrocytes also reduces Sp1 occupancy of the αB-crystallin enhancer. Since mHtt's accumulation in the nuclei of astrocytes is age-dependent (Shin et al., 2005; Bradford et al., 2009), we performed a chromatin immunoprecipitation (ChIP) assay using 28- (KI_Y) and 35- (KI_O) days-old astrocyte cultures from HD KI mice to examine whether mHtt could reduce the association of Sp1 with the αB-crystallin enhancer in HD KI astrocytes. There was a greater reduction in the association of Sp1 with the enhancer of αB-crystallin in older (35 days) astrocytes (**Fig. 4.7*A***). However, the association of Sp1 with the αB-crystallin enhancer showed no difference between old (WT_O) and young WT (WT_Y) astrocytes. These results support the idea that αB-crystallin expression is only decreased in the older HD KI astrocytes.

If decreased αB-crystallin levels are due to deficient Sp1-mediated transcription in KI astrocytes, overexpression of Sp1 should rescue decreased αB-crystallin expression and also promote exosome secretion. We then generated Sp1-HA plasmids to overexpress the pretein in cultured astrocytes. After 48 hours transfection, western blotting verified that endogenous αB-crystallin is increased by Sp1 overexpression (**Fig. 4.7*B***). Moreover, flotillin-1 is increased in the purified exosomes from Sp1-overexpressed KI astrocytes compared with the control plasmid-transfected KI astrocytes (**Fig. 4.7*C,D***). These results suggest that the abnormal association of mHtt with Sp1 can reduce Sp1-mediated αB-crystallin expression, leading to defective exosome secretion from astrocytes.

αB-crystallin overexpression rescues defective exosome secretion from KI astrocytes

Since Sp1 can mediate the expression of a number of genes, it would be important to ask if direct expression of αB-crystallin can rescue exosome release from KI astrocytes. We therefore generated αB-crystallin-HA plasmids to overexpress it in cultured KI astrocytes. Forty-eight hours after transfection, western blotting verified that expression of αB-crystallin-HA could significantly increase flotillin-1 in the exosome fraction (**Fig. 4.8*A***).

To further confirm the effect of αB-crystallin overexpression in vivo, we used αB-crystallin-V5 adenovirus for overexpression in the striatum of KI mice via stereotaxic injection. Expression of αB-crystallin-V5 was driven by the CMV promoter, which has high tropism toward astrocytes in the mouse brain (Hong et al., 2016; Iino et al., 2001; Yue et al., 2005). We isolated exosomes from the striatum of HD KI mice 30 days after stereotaxic injection. Western blotting confirmed the expression of transgenic αB-

crystallin with anti-V5 in the striatal lysates (**Fig. 4.8*B***). In these lysates, flotillin-1 was also slightly increased while Hsc70 remained unchanged as compared with the adenoviral-GFP control. We then purified the exosome fraction and found that both Hsc70 and flotillin-1 were significantly increased in exosomes after αB-crystallin overexpression (**Fig. 4.8*C***), suggesting an increase in the released exososmes.

We also noted that aggregated Htt on western blots, which appeared as a high MW smear, was decreased when transgenic αB-crystallin was expressed (**Fig. 4.8*B***). To confirm this, we performed double immunofluorescence staining of the striatum of HD KI mice after they had been injected with an adenoviral vector or adenoviral αB-crystallin. EM48 immunostaining clearly showed a reduction in Htt aggregates in the αB-crystallin-injected striatum (**Fig. 4.8*D***). In HD KI mouse brains, the increased staining of GFAP reflects reactive astrocytes in the absence of neuronal loss (Yu et al., 2003), which is an early pathology of HD. There was also a reduction of reactive astrocytes by transgenic αB-crystallin (**Fig. 4.8*E***). Quantitative analysis of the density of EM48-labeled aggregates and GFAP-positive astrocytes confirmed that overexpression of αB-crystallin could decrease mHtt aggregates and reactive astrocytes, which also support the idea that αB-crystallin-mediated exosome secretion is protective against HD neuropathology.

Discussion

Exosomes are specific extracellular vesicles that are secreted from multiple types of cells into biological fluids (Pisitkun et al., 2004; Caby et al., 2005; Vella et al., 2008). Our findings suggest that exososmes secreted from astrocytes are protective against HD

pathology and that mHtt can inhibit the release of exosomes from astrocytes, revealing a previously uncovered mechanism for non-cell-autonomous neurotoxicity in HD.

Exosomes can transfer lipids, proteins, and RNAs between cells to play important roles in cell-cell communication under physiological and pathophysiological conditions (Théry et al., 2002; Colombo et al., 2014; Maas et al., 2017; Levy, 2017). Emerging evidence has indicated that a number of proteins related to neurodegenerative disorders, including prion disease, Parkinson's disease and Alzheimer's disease (AD), are present in exosomes and may be transported by exosomes between cells (Coleman and Hill, 2015). Transfected mHtt in cultured cells was also reported to transfer to neighbors in cell culture (Costanzo et al., 2013). In addition, injection of exsomes released from fibroblasts of HD patients into newborn mouse brains triggered the manifestation of an HD phenotype (Jeon et al., 2016). However, it remains unknown whether endogenous exosomes contain mHtt. By examining exosomes isolated from HD KI astrocytes and neurons, we have found no evidence for the presence of mHtt in exosomes from these two types of brain cells. It seems that disease proteins are differentially carried by exosomes and their transport between cells is dependent on the nature of the proteins. Huntingtin is a much large protein than Tau and alpha-synuclein, which are smaller and might be easily packed into exosomes. It is also possible that a very minimal amount of mHtt is present in exosomes, and if so, the undetectable amount of mHtt in exososmes is unlikely to have a meaningful impact on HD neuropathology.

Our findings suggest that exosomes are more likely to execute a protective function in the HD brains. We generated several lines of evidence to support this idea. First, injection of exosomes into the HD KI mouse brain led to reduced HD-like

neuropathology. Second, exosome secretion in the HD KI mouse brain is decreased with aging and correlates with the increased formation of mHtt aggregates. Third, mHtt inhibits αB-crystallin expression to reduce exosome secretion, whereas overexpression of αB-crystallin could reverse this defect and the related neuropathology. These findings are consistent with emerging evidence that astrocyte-derived exosomes carrying neuroprotective cargo, such as heat shock proteins, could contribute to neuronal survival (Taylor et al., 2007; Nafar et al., 2016). For example, exosomes derived from adipose-derived stem cells could significantly decrease mHtt aggregates in cultured neuronal cells from R6/2 mice (Lee et al., 2016; Didiot et al., 2016; Lee et al., 2017).

The more interesting finding in our studies is that we identified that mHtt inhibits the expression of αB-crystallin to affect the release of exosomes from astrocytes and that this defect contributes to HD neuropathology. αB-crystallin plays a crucial role in several neurodegenerative disorders. For example, αB-crystallin can prevent amyloid fibril formation and reduces the toxicity of amyloid-β peptide in cells (Hochberg et al., 2014). The protective role of αB-crystallin in HD is also supported by the finding that expressing an mhtt fragment in the lens of mice lacking αB-crystallin markedly accelerated the onset and severity of mhtt aggregation (Muchowski et al., 2008). Decreased αB-crystallin levels were found in two HD mouse models, R6/2 and BACHD mice (Zabel et al., 2002; Oliveira et al., 2016), but the mechanism underlying this reduction has not been investigated. Our finding that mHtt reduces the expression of αB-crystallin to reduce exosome secretion is consistent with several known facts. First, αB-crystallin is mainly found in glial cells, but not neurons (Imura et al., 1999; Wyttenbach et al., 2004). Second, αB-crystallin transcription is regulated by Sp1, whose function

could be impaired by mHtt via abnormal protein interaction (Dunah et al., 2002; Li et al., 2002; Chen-Plotkin et al., 2006; Bradford et al., 2009). Third, only N-terminal Htt fragments are able to accumulate in the nucleus, which can lead to gene transcription dysregulation and mHtt aggregations in an age-dependent manner. Consistently, we found that αB-crystallin is also decreased in 10-month-old KI mice in which N-terminal mHtt has obviously accumulated in the nuclei of striatal cells to form aggregates.

The finding that mHtt affects the secretion of astrocytic exosomes also offers a new mechanistic insight into HD pathology, especially the non-cell-autonomous neurotoxicity of mHtt. It is well known that mHtt preferentially affects neurons in the striatum (Ross and Tabrizi, 2011; Bates et al., 2015). This preferential neurodegeneration has been thought to be due to different and multiple pathological pathways, including cell-autonomous or non-cell-autonomous disease processes (Ross and Tabrizi, 2011; Bates et al., 2015; Lee et al., 2013). Increasing evidence also indicates that mHtt affects multiple functions of glial cells to promote neurodegeneration (Hsiao and Chern, 2010; Lee et al., 2013). Of these adverse effects of mHtt in glial cells, transcriptional dysregulation appears to be a major mechanism for the toxic effect of mHtt in glial cells (Shin et al., 2005; Bradford et al., 2009; Tong et al., 2014; Huang et al., 2015). By examining exosomes released from astrocytes, we provide new evidence for the critical role of astrocytes in HD pathogenesis. Since mHtt is not found in the astrocytic exosomes, improving exosome secretion from astrocytes may be a potential therapeutic strategy for HD.

Figure 4.1

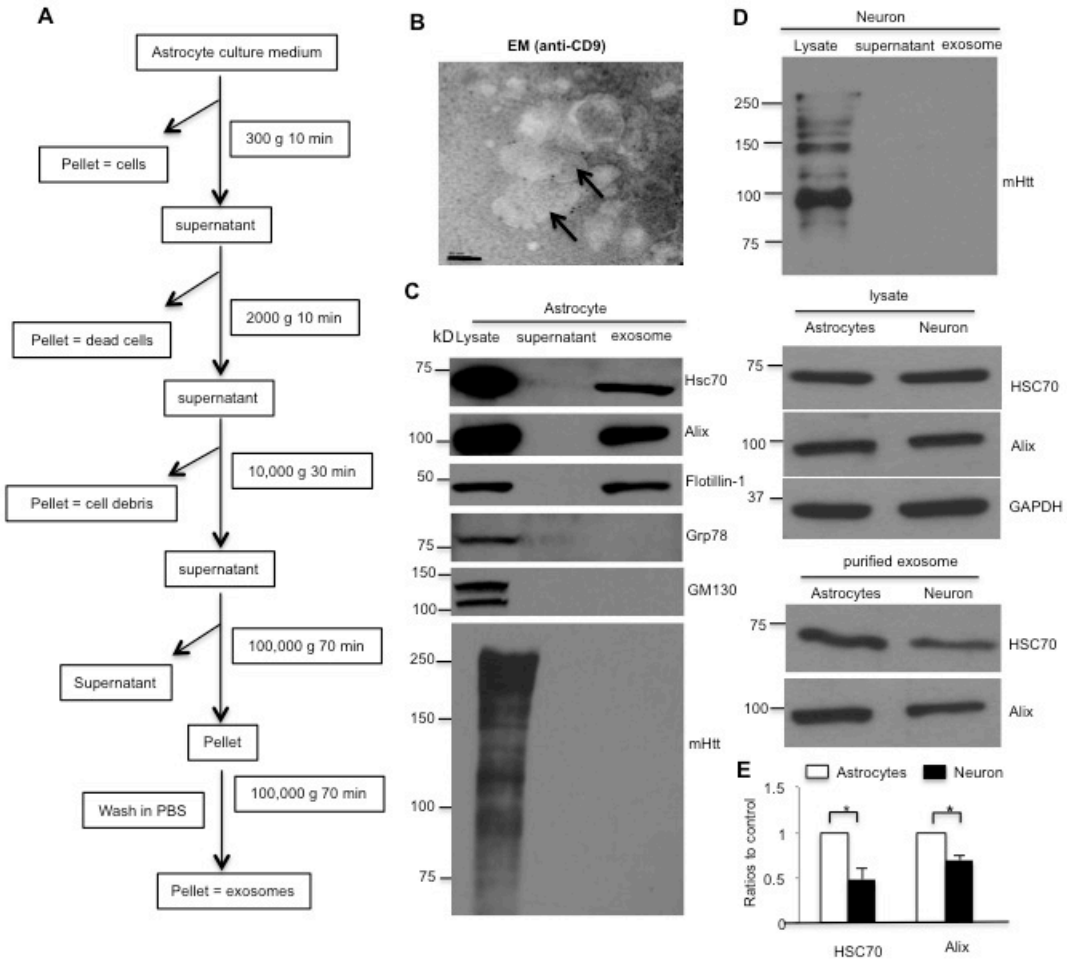
A
Astrocyte culture medium
300 g 10 min
Pellet = cells
supernatant
2000 g 10 min
Pellet = dead cells
supernatant
10,000 g 30 min
Pellet = cell debris
supernatant
100,000 g 70 min
Supernatant
Pellet
100,000 g 70 min
Wash in PBS
Pellet = exosomes
B
EM (anti-CD9)
C
Astrocyte
kD Lysate supernatant exosome
75
Hsc70
100
Alix
50
Flotillin-1
75
Grp78
150
100
GM130
250
150
100
75
mHtt
D
Neuron
Lysate supernatant exosome
250
150
100
75
mHtt
lysate
Astrocytes Neuron
75
HSC70
100
Alix
37
GAPDH
purified exosome
Astrocytes Neuron
75
HSC70
100
Alix
E
Astrocytes
Neuron
Ratios to control
1.5
1
0.5
0
HSC70
Alix

Figure 4.1.

mHtt is not present in the exosome released by cultured astrocytes. *A,* Experimental scheme of the exosome purification from astrocyte culture medium (CM). Sequential centrifugations of the CM eventually yield the supernatant and exosome pellet fractions. *B,* Immunoelectron microscopic images of the exosome fraction that was stained with anti-CD9 antibody and secondary antibody conjugated with 10-nm gold nanoparticles. Scale bars: 50 nm. *C,* Western blotting analysis of the whole cellular lysates, supernatant and exosome fraction using antibodies against the proteins indicated. Alix, Flotillin-1, and Hsc70 were detected in the exosome fraction, but Grp78 and GM130 were not. 1C2 immunoblotting revealed that Htt is not found in the astrocytic exosome fraction. *D-E,* Western blotting with 1C2 antibody showed that Htt is also absent in neuronal exosomes. Although Hsc70 and Alix were found to be at equivalent levels in astrocytic and neuronal lysates, they are more abundant in astrocytic exosomes than in neuronal exosomes (Student's t-test, $n = 4$ independent experiments). $*p < 0.05$.

Figure 4.2

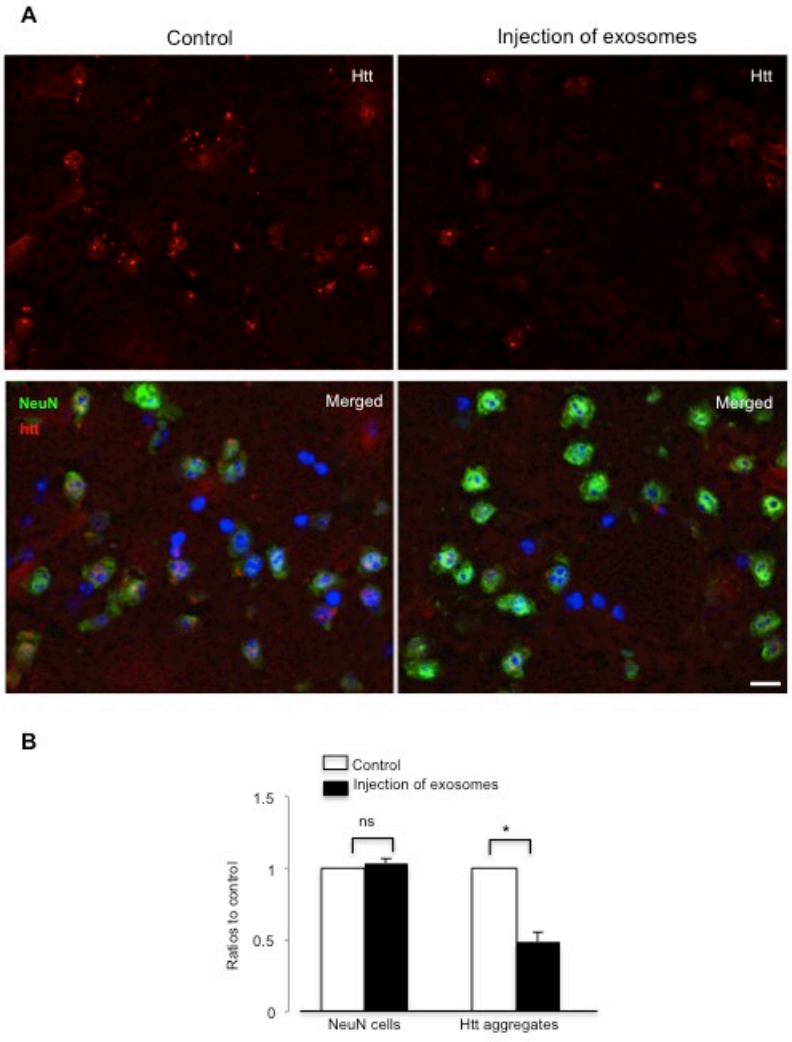
A
Control
Injection of exosomes
Htt
Htt
NeuN
htt
Merged
Merged
B
Control
Injection of exosomes
1.5
1
0.5
0
Ratios to control
ns
*
NeuN cells
Htt aggregates

Figure 4.2.

Astrocytic exosomes reduce mHtt aggregates in the striatum of HD KI mice. A, High magnification (63 X objective) micrographs showing immunostained mHtt aggregates (red; upper panel) and mHtt aggregates (red) merged with NeuN (green) and nuclei stained by Hoechst (blue) (lower panel) in the striatum of 9-month-old HD KI mice. Scale bars: 5 μm. *B,* Quantitative analysis showing a significantly decreased number of mHtt aggregates in the site injected with astrocytic exosomes compared with the PBS-injected site. The percentage of NeuN-positive cells per image is unchanged (Student's t-test, randomly selected 7-10 images per section, n = 8 sections per group).

Figure 4.3

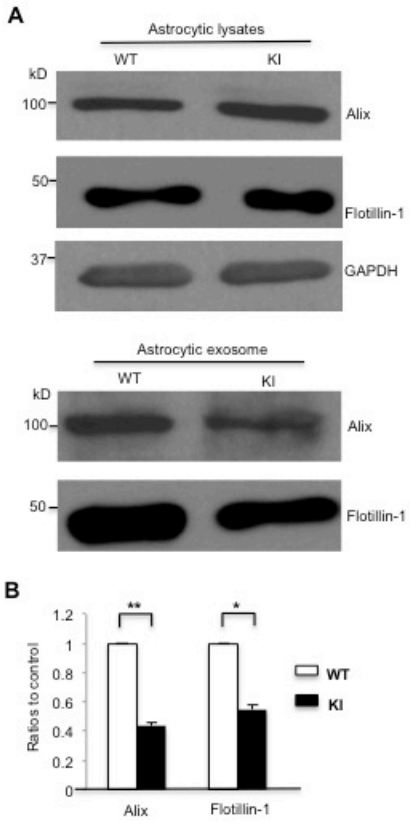
A
Astrocytic lysates
WT
KI
kD
100
Alix
50
Flotillin-1
37
GAPDH
Astrocytic exosome
WT
KI
kD
100
Alix
50
Flotillin-1
B
**
*
1.2
1
0.8
0.6
0.4
0.2
0
Ratios to control
WT
KI
Alix
Flotillin-1

Figure 4.3.

Exosome secretion is decreased from HD KI primary astrocyte cultures. *A,* Western blotting showing the same amount protein levels of Alix or Flotillin-1 in the lysates of WT and HD KI astrocytes, respectively, but decreased Alix and Flotillin-1 levels in the exosomes derived from HD KI astrocytes. *B,* Quantifying ratios of Alix and Flotillin-1 levels in exosomes to those in astrocyte lysates (Student's t-test, $n = 6$ independent experiments). *$p < 0.05$, **$p < 0.01$.

Figure 4.4

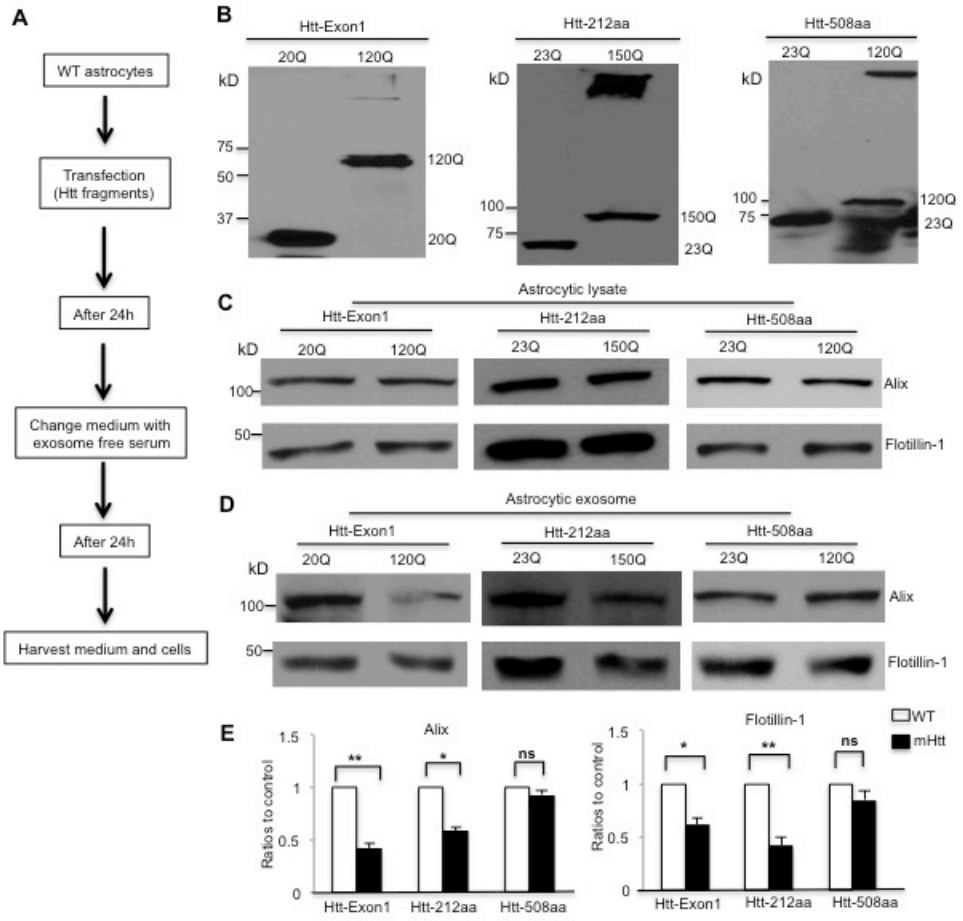
A
WT astrocytes
Transfection (Htt fragments)
After 24h
Change medium with exosome free serum
After 24h
Harvest medium and cells
B
Htt-Exon1
20Q
120Q
kD
75
50
37
120Q
20Q
Htt-212aa
23Q
150Q
kD
100
75
150Q
23Q
Htt-508aa
23Q
120Q
kD
100
75
120Q
23Q
C
Astrocytic lysate
Htt-Exon1
Htt-212aa
Htt-508aa
kD
20Q
120Q
23Q
150Q
23Q
120Q
100
50
Alix
Flotillin-1
D
Astrocytic exosome
Htt-Exon1
Htt-212aa
Htt-508aa
kD
20Q
120Q
23Q
150Q
23Q
120Q
100
50
Alix
Flotillin-1
E
Alix
Ratios to control
1.5
1
0.5
0
**
*
ns
Htt-Exon1
Htt-212aa
Htt-508aa
Flotillin-1
Ratios to control
1.5
1
0.5
0
*
**
ns
Htt-Exon1
Htt-212aa
Htt-508aa
WT
mHtt

Figure 4.4.

N-terminal fragments of mHtt impair exosome secretion from cultured astrocytes. *A-B,* Htt fragments including Exon1 (Htt-Exon1 20Q, 120Q), N-terminal 212 amino acids (Htt-212aa 23Q, 150Q) and N-terminal 508 amino acids (Htt-508aa 23Q, 120Q) were transfected into WT astrocytes. Western blotting with an Htt antibody (mEM48) showed the expression of different Htt fragments in cultured WT astrocytes. *C-D*, Alix and flotillin-1 protein levels were unchanged in the lysates of each mutant N-terminal fragment-transfected astrocytes compared with their WT counterparts. However, the pretein levels were decreased in exosomes derived from astrocytes transfected with Htt-Exon1-120Q and Htt-212aa-150Q, but not Htt-508aa-120Q. *E,* Quantifying ratios of Alix and Flotillin-1 in exosomes to those in astrocytic lysates in each mHtt transfection. (Student's t-test, $n = 4$ independent experiments for each fragment). *$p < 0.05$, **$p < 0.01$, *** $p < 0.001$, ns, not significant.

Figure 4.5

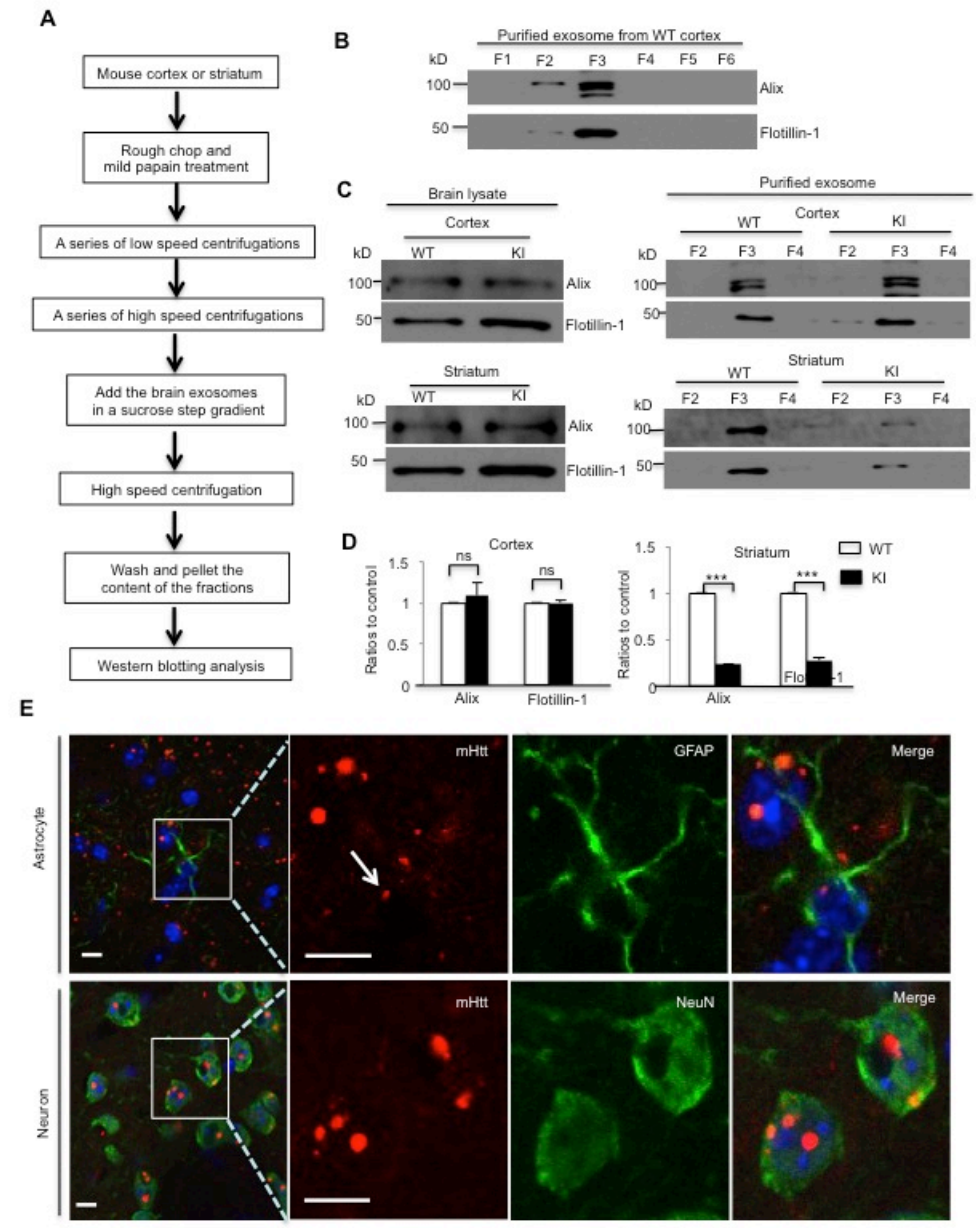
A
Mouse cortex or striatum
Rough chop and mild papain treatment
A series of low speed centrifugations
A series of high speed centrifugations
Add the brain exosomes in a sucrose step gradient
High speed centrifugation
Wash and pellet the content of the fractions
Western blotting analysis
B
Purified exosome from WT cortex
kD
F1 F2 F3 F4 F5 F6
100
50
Alix
Flotillin-1
C
Brain lysate
Cortex
WT KI
Striatum
Purified exosome
D
Cortex
Striatum
ns
***
Ratios to control
WT
KI
Alix
Flotillin-1
E
Astrocyte
Neuron
mHtt
GFAP
NeuN
Merge

Figure 4.5.

mHtt decreases exosome secretion from HD KI mouse striatum. *A,* Brain exosome isolation experimental flow chart. *B,* Western blotting showing that exosome markers, Alix and Flotillin-1, are mainly present in fraction 3. *C,* In the cortex or the striatum lysates from WT and KI mice, Alix and flotillin-1 were equivalent. However, Alix and flotillin-1 levels were significantly decreased in the exosome fraction derived from the HD KI striatum, but not the HD KI cortex compared with WT controls. *D,* Quantifying ratios of Alix and Flotillin-1 in exosomes to those in the cortex or striatal lysates in fraction 3 (Student's t-test, WT & KI n= 4 mice in each genotype). *E,* Immunostaining showing nuclear mHtt aggregates in both astrocytes and neurons in 10-month-old HD KI striatum. mHtt (Red) was probed by 1C2 antibody. GFAP (green, upper panel) represents astrocytes, and NeuN (green, lower panel) indicates neurons. *** $p < 0.001$, ns, not significant.

Figure 4.6

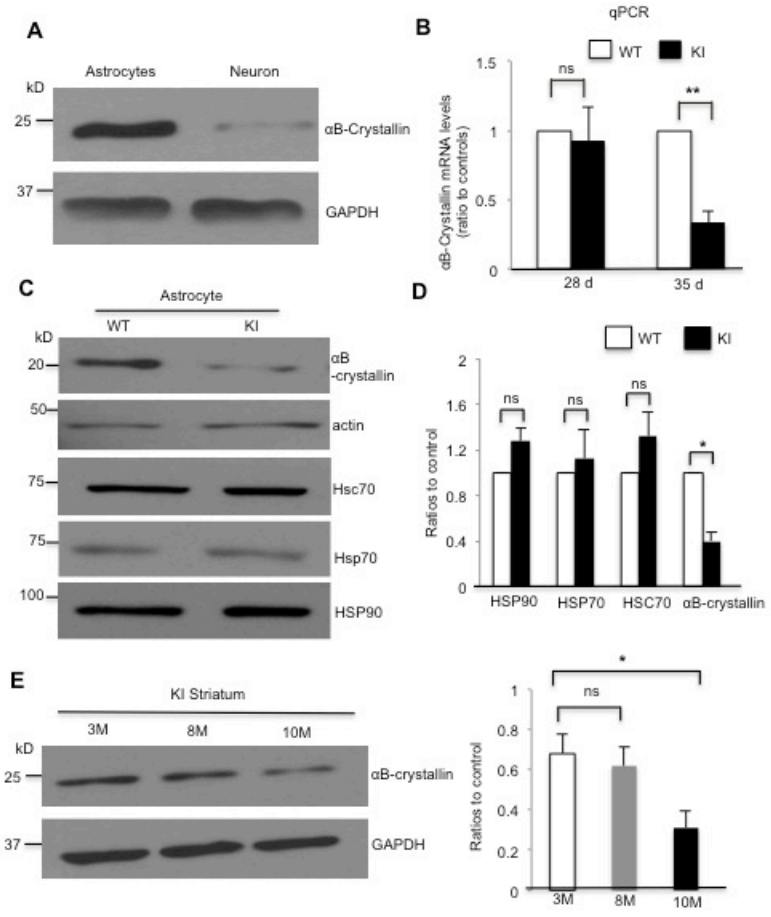
A
Astrocytes
Neuron
kD
25
αB-Crystallin
37
GAPDH
B
qPCR
WT
KI
ns
**
αB-Crystallin mRNA levels (ratio to controls)
1.5
1
0.5
0
28 d
35 d
C
Astrocyte
WT
KI
kD
20
αB -crystallin
50
actin
75
Hsc70
75
Hsp70
100
HSP90
D
WT
KI
ns
ns
ns
*
Ratios to control
2
1.6
1.2
0.8
0.4
0
HSP90
HSP70
HSC70
αB-crystallin
E
KI Striatum
3M
8M
10M
kD
25
αB-crystallin
37
GAPDH
*
ns
Ratios to control
1
0.8
0.6
0.4
0.2
0
3M
8M
10M

Figure 4.6.

mHtt impairs αB-Crystallin expression in both cultured astrocytes and the striatum. *A,* Western blotting showing that αB-crystallin is enriched in the lysates of cultured astrocytes but deficient in cultured neurons. *B,* qRT-PCR results revealing a significant reduction in αB-crystallin mRNA in HD KI astrocytes at 35 days of culture, but not at 28 days compared with WT astrocytes (Student's t-test, $n = 6$ independent experiments). *C-D,* Western blotting revealing decreased αB-crystallin in cultured HD KI astrocytes at 35 days of culture compared with WT astrocytes. Hsp70, Hsc70, and Hsp90 levels are similar in KI and WT astrocytes (Student's t-test, $n = 6$ independent experiments). *E,* Western blotting showing decreased αB-crystallin levels in the striatum of 10-month-old HD KI mice relative to 3 and 8-month-old KI mice (Student's t-test, $n = 3$ mice in each age). *$p < 0.05$, **$p < 0.01$, ns, not significant.

Figure 4.7

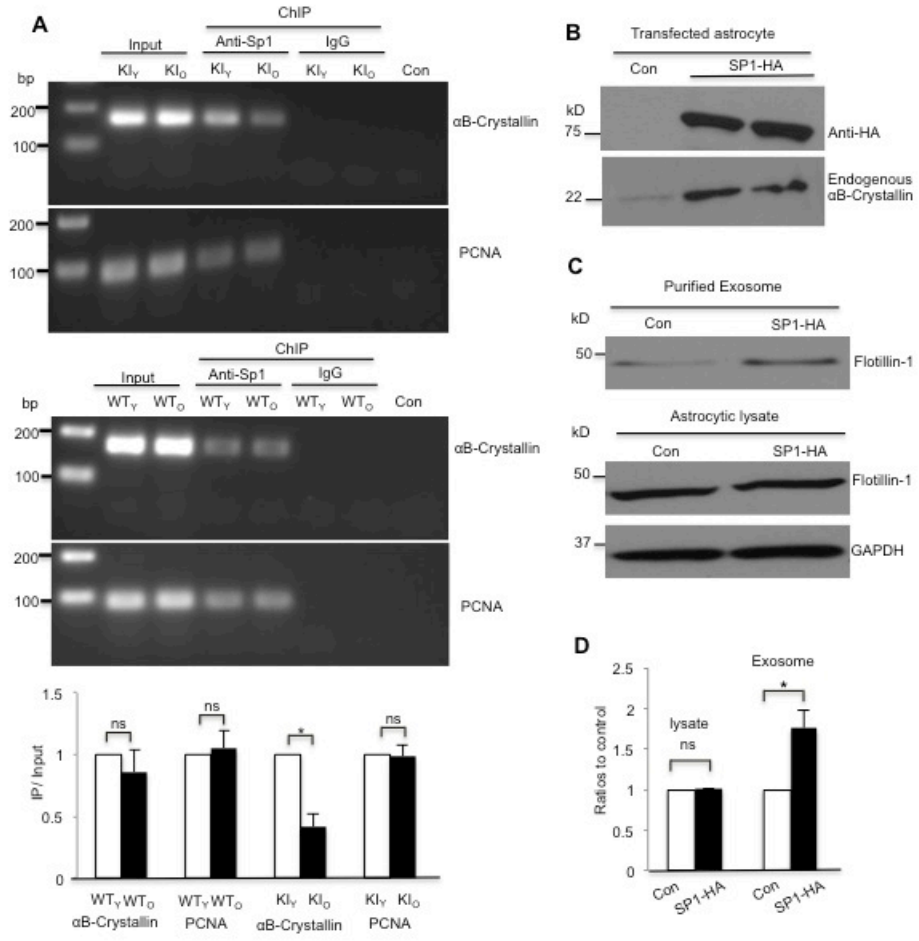
A
ChIP
Input
Anti-Sp1
IgG
bp
200
100
αB-Crystallin
PCNA
Con
B
Transfected astrocyte
Con
SP1-HA
kD
75
22
Anti-HA
Endogenous αB-Crystallin
C
Purified Exosome
50
Flotillin-1
Astrocytic lysate
37
GAPDH
D
Exosome
lysate
ns
*
Ratios to control
IP / Input
1.5
1
0.5
0

Figure 4.7.

Sp1 mediates αB-crystallin expression in astrocytes. *A,* ChIP assay results showing decreased association of Sp1 with the αB-crystallin enhancer in 35-day KI (KI_O) astrocytes compared with 25-day KI (KI_Y) astrocytes. No significant difference between 35-day (WT_O) and 25-day WT (WT_Y) astrocytes was found. Proliferating cell nuclear antigen (PCNA) served as a control. Rabbit anti-Sp1 and IgG were used for immunoprecipitation (Con indicates no template). Quantification of the ratios of PCR products from immunoprecipitated (IP) to input (Student's t-test, $n = 4$ independent experiments). *B,* Transfection of mouse Sp1-HA into HD KI astrocytes increased endogenous αB-crystallin expression (Student's t-test, $n = 4$ independent experiments). *C-D,* Flotillin-1 was unchanged in astrocytic lysates, but was increased in exosomes derived from Sp1-transfected HD KI astrocytes relative to control plasmid transfection (Student's t-test, $n = 6$ independent experiments). *$p < 0.05$, ns, not significant.

Figure 4.8

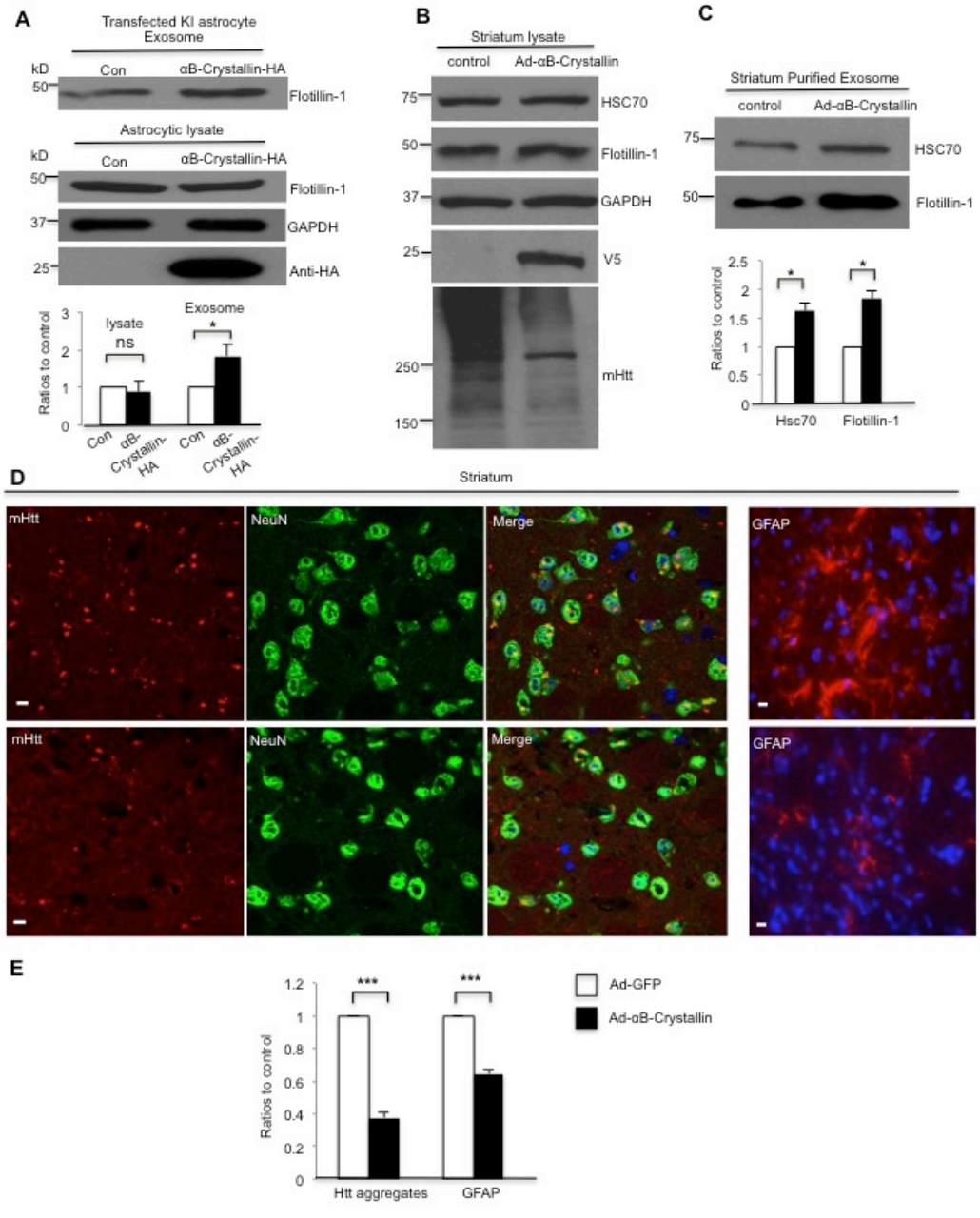
A
Transfected KI astrocyte Exosome
kD
Con
αB-Crystallin-HA
50
Flotillin-1
Astrocytic lysate
kD
Con
αB-Crystallin-HA
50
Flotillin-1
37
GAPDH
25
Anti-HA
Ratios to control
lysate
ns
Exosome
*
Con
αB-Crystallin-HA
Con
αB-Crystallin-HA
B
Striatum lysate
control
Ad-αB-Crystallin
75
HSC70
50
Flotillin-1
37
GAPDH
25
V5
250
150
mHtt
Striatum
C
Striatum Purified Exosome
control
Ad-αB-Crystallin
75
HSC70
50
Flotillin-1
Ratios to control
*
*
Hsc70
Flotillin-1
D
mHtt
NeuN
Merge
GFAP
mHtt
NeuN
Merge
GFAP
E
Ratios to control
***
***
Ad-GFP
Ad-αB-Crystallin
Htt aggregates
GFAP

Figure 4.8.

Overexpression of αB-crystallin rescues defective exosome secretion from KI astrocytes. *A,* Mouse αB-Crystallin-HA plasmid was transfected into WT astrocytes. Flotillin-1 was unchanged in the astrocytic lysates, but was increased in exosomes derived from αB-crystallin-overexpressing HD KI astrocytes compared with exosomes from astrocytes that received a control plasmid transfection (Student's t-test, $n = 4$ independent experiments). *B-C,* Western blotting verified αB-crystallin-V5 expression *in vivo*. HSC70 and flotillin-1 were increased in exosomes purified, but not lysates, from the αB-crystallin-V5 injected striatum compared with an adenoviral-GFP control injection. mHtt aggregates were decreased in the αB-crystallin-V5-injected region (Student's t-test, $n = 4$ independent experiments). *D,* High magnification (63 X objective) micrographs showing GFAP staining and mHtt aggregates (red), which are also shown in the merged images with NeuN (green) and nuclei stained by Hoechst (blue), in the striatum of 10-month-old HD mice. Scale bars: 5 μm. *E,* Quantitative analysis of the GFAP immunofluorescence density showing that GFAP staining and the number of mHtt aggregates were significantly decreased in the αB-crystallin-V5-injected striatum compared with the control striatum (Student's t-test, randomly selected 7-10 images per section, n = 8 sections per group). *$p < 0.05$, *** $p < 0.001$, ns, not significant

Chapter 5

General Conclusions and Future Directions

5.1 Summary

In this study, we set out to define the role of mHtt in astrocytic secretion. In chapter 3, we focused on the effect of mHtt on dense-core vesicle secretion from astrocytes. BDNF, a neurotrophic factor packaged in dense-core vesicles, is essential for neuronal development, survival and function. Previous studies demonstrated that BDNF is decreased in the brains of HD patients and animal models. The decreased BDNF in neuronal cells is due to defective BDNF transcription and decreased axonal transport from cortical neurons to the striatum (Gauthier et al., 2004). Glial cells, particularly astrocytes, can also synthesize and release BDNF via exocytosis to support the neighboring neurons. Since striatal neurons are unable to synthesize BDNF, striatal astrocyte-derived BDNF is another important trophic support for the survival of striatal neurons. However, whether mHtt affects astrocytic BDNF biogenesis and secretion remains unknown. A recent study demonstrates that overexpression of mHtt in cultured astrocytes impairs BDNF transcription by sequestering BDNF transcriptional factors into mHtt aggregates (Wang et al., 2012). Given that very few mHtt aggregates are found in astrocytes in the HD brains that express mHtt at the endogenous level (Shin et al., 2005), it is necessary to examine whether mHtt at the endogenous level affects BDNF production and/or release in astrocytes.

In this study, we used both full-length HD 140Q knock-in (KI) and GFAP-Htt transgenic (TG) mouse models to investigate the effect of mHtt on astrocytic BDNF. In these mouse models, full-length mHtt with 140Q is expressed at the endogenous levels in KI mice (Menalled et al., 2003), and N-terminal Htt (1–208 aa) with 160Q is expressed at levels similar to endogenous Htt in TG mice (Bradford et al., 2009). We found that both

TG and KI astrocytes in culture release less BDNF than control wild-type (WT) astrocytes. To further verify this finding, we measured BDNF release from brain slices of TG mice in which mHtt expression is restricted to astrocytes. We found essentially the same result that brain slices from TG mice release less BDNF than slices from WT mice. Thus, our results indicate that mHtt at endogenous levels impairs BDNF release from astrocytes.

We then sought to explore the mechanism underlying the decreased BDNF secretion from HD astrocytes. First, we examined BDNF mRNA and protein levels by qRT-PCR and Western blotting, respectively, and found that mHtt does not affect BDNF synthesis in cultured astrocytes. Next, since BDNF synthesis was unchanged, we hypothesized that BDNF secretion deficiency might be due to decreased exocytosis of BDNF-containing vesicles. Rab3a, a member of the Rab family, is highly enriched in the brain and mediates release of secretory vesicles, including synaptic vesicles and dense-core vesicles (Tsuboi and Fukuda, 2006). Although Rab3a is expressed in astrocytes (Maienschein et al., 1999), its function in astrocytes remains elusive. We found that knocking down Rab3a causes decreased secretion of BDNF and ATP, another cargo in dense-core vesicles, from astrocytes, indicating that Rab3a plays an essential role in dense-core vesicle secretion from astrocytes. Importantly, we found that more degraded mHtt fragments than full-length mHtt is associated with Rab3a by coimmunoprecipitation assay and in vitro binding assay. In addition, we found that mHtt also binds to GTP-Rab3a, which is an active form of Rab3a for exocytosis, suggesting that the association between mHtt and Rab3a may contribute to the suppressed BDNF secretion from HD astrocytes.

The ability to associate/dissociate GTP and GDP is essential for the function of Rab3a in dense-core vesicle docking (van Weering et al., 2007). We found that GTP-Rab3a protein levels are increased in KI astrocytes, indicating that mHtt inhibits the conversion of GTP-Rab3a. It has been reported that Rab3-GAP1 binds GTP-Rab3a to accelerate the conversion from the active GTP-bound form to the inactive GDP-bound form (Burstein et al., 1993). We found that mHtt does not impair Rab3-GAP1 expression levels, but significantly reduces the association between GTP-Rab3a and Rab3-GAP1 in KI astrocytes compared with WT astrocytes. Importantly, BDNF secretion is increased both from cultured HD astrocytes and from HD brain slices by Rab3a overexpression. Since BDNF is not the only cargo in dense-core vesicles, we also examined ATP secretion and showed the same results as BDNF.

Since disruption of GTP/GDP-Rab3a exchange is reported to cause defective docking of dense-core vesicles in mammalian chromaffin cells (van Weering et al., 2007), we next examined whether the disrupted GTP/GDP-Rab3a exchange by mHtt influences docking of BDNF-containing dense-core vesicles in HD astrocytes by TIRF microscopy. The numbers of docked BDNF vesicles were significantly decreased in cultured KI astrocytes compared with WT astrocytes, and the impaired docking could be rescued by overexpressing Rab3a in KI astrocytes.

Finally, we examined whether overexpression of Rab3a would decrease HD-related pathology in vivo. We injected Rab3a-V5 adenovirus and GFP adenovirus into different sides of the striatum in the same animal for 30 days. We found that Rab3a overexpression could selectively rescue reactive astrocytes in the striatum of HD KI mice, but it did not decrease mHtt aggregates. Based on above findings, we propose that

mHtt binds Rab3a to affect its GTP/ GDP exchange and impairs the docking of dense-core vesicles in HD astrocytes, resulting in decreased release of BDNF.

In chapter 4, we focused on the effect of mHtt on astrocytic exosome secretion. Exosomes are cellular vesicles that have recently been studied in a variety of diseases. Exosomes are small membranous vesicles secreted by multiple cell types, carrying proteins and genetic materials and playing important roles in cell-cell communication under physiological and pathophysiological conditions. Exosomes from neuronal cells have been shown to spread misfolded proteins between cells, a mechanism underlying the spread of toxic proteins in the brain (Bellingham et al., 2012; Wang, et al., 2017). Emerging evidence shows that exosomes from glial cells carry neuroprotective molecules to prevent neurodegeneration (Hajrasouliha et al., 2013; Haney et al., 2013; Zhao et al., 2014; Guitart et al., 2016; Xin et al., 2017). It is necessary to examine whether mHtt is present in astrocytic exosomes to spread mHtt, and whether and how mHtt affects exosome biogenesis and /or release in astrocytes.

It has been reported that mHtt may spread from cell to cell (Pecho-Vrieseling et al., 2014; Jeon et al., 2016; Zhang et al., 2016), and proteins associated with certain neurodegenerative disorders, such as APP and α-synuclein, are present in exosomes that are released from neurons (Xiao et al., 2017; Bieri et al., 2017). However, it has not been investigated whether mHtt is present in exosomes when it is expressed as full-length protein at the endogenous level. To examine whether mHtt is a cargo of astrocytic and neuronal exosomes, we isolated exosomes from the culture medium of primary cultures from KI mice and did not detect mHtt in the exosomes released from either astrocytes or neurons, suggesting that exosomes would not transfer mHtt between cells in the HD

brains. By comparing exosomes released from astrocytes and neurons, we found that astrocytes secreted more exosomes containing more Hsc70. We next injected astrocytic exosomes into the striatum of HD KI mice and observed a significant decrease in mHtt aggregate density in the injected site, perhaps because exosomes-carrying Hsc70 and other molecules help the clearance of misfolded and aggregated proteins.

Given that astrocytic exosomes are protective and that mHtt can impair the release of dense-core vesicles from astrocyte cultures, we investigated how mHtt affects the secretion of exosomes from astrocytes. We found that mHtt does not affect exosome biogenesis, but rather impairs exosome secretion from astrocytes, and also found that smaller N-terminal mHtt fragments (Htt-Exon1-120Q and Htt-212aa-150Q) are able to inhibit exosome secretion from astrocytes. To examine mHtt's effects on exosomes in vivo, we isolated exosomes from the cortex and the striatum of 10-month-old WT or HD KI mice. Interestingly, mHtt does not affect exosome biogenesis in either the cortex or the striatum, but impairs exosome secretion only from the striatum. In HD KI mice, only N-terminal mHtt forms aggregates, and these aggregates have been found to be much more abundant in the striatum than in the cortex. We performed double immunofluorescence staining and indeed found that nuclei mHtt aggregates in both astrocytes and neurons in the striatum of 10-month-old HD KI mouse, which might explain why mHtt only impairs exosome release from the striatum at this age.

The nuclear localization of mHtt in astrocytes led us to investigate whether mHtt affects the transcription of molecules that are important for the release of exosomes. It has been reported that αB-crystallin is decreased in HD transgenic mouse models. We found that both αB-crystallin mRNA and protein levels are decreased in KI astrocytes

and the striatum of HD KI mice in an age-dependent manner, which is consistent with the age-dependent accumulation of N-terminal Htt fragments and the formation of Htt aggregates in the KI mouse striatum. Since mRNA levels of αB-crystallin are decreased in KI astrocytes, we hypothesized that mHtt inhibits αB-crystallin transcription by reducing its promoter activity. Sp1 was found to regulate the activity of αB-crystallin by binding to its enhancer to activate its promoter (Swamynathan et al., 2007). We performed a ChIP assay and found a greater reduction in the association of Sp1 with the enhancer of the αB-crystallin gene in KI astrocytes in an age-dependent manner, which supports the idea that αB-crystallin expression is only decreased in older KI astrocytes.

Finally, we examined whether αB-crystallin overexpression could rescue defective exosome secretion. Our results show that overexpression of αB-crystallin increases exosome secretion from both KI astrocytes and the striatum of HD KI mice. Importantly, αB-crystallin overexpression rescues reactive astrocytes and decreases mHtt aggregates, indicating that αB-crystallin-mediated exosome secretion is protective against HD neuropathology.

Taken together, our findings demonstrate that mHtt impairs astrocytic secretion, and uncover new pathological pathways that affect the critical support of glial cells to neurons in the HD brain.

5.2 Future direction

The continuation of this project could proceed in many ways. Since HD is characterized by selective neurodegeneration that occurs in the striatal medium spiny neurons, one of the future directions would be to determine whether and how mHtt-impaired astrocyte

secretion contributes to the selective neurodegeneration in HD. Since striatal neurons cannot synthesize BDNF, exogenous BDNF that is derived from cortical neurons as well as local striatal astrocytes is critical for their survival. Therefore, decreased BDNF release from HD astrocytes, which we found, might contribute to the selective vulnerability of the striatal neurons. In chapter 3, we measured GTP-Rab3a activity in the absence of Rab3-GAP1 in WT and KI astrocyte lysate and found that mHtt in KI lysates does not directly affect the GTPase activity of Rab3a. In the future study, we need to measure GTP-Rab3a activity in the presence of Rab3-GAP1 in WT and KI astrocyte lysate to confirm that mHtt impairs GTP-Rab3a hydrolysis. We also will measure GTP-Rab3a hydrolysis in the present of Rab3-GAP1 in different brain regions of WT and KI mice to examine whether mHtt preferentially impairs GTP-Rab3a hydrolysis in the striatum.

We also found that mHtt impairs the secretion of astrocytic exosomes that contain neuroprotective cargoes, which might also lead to the preferential degeneration of striatal medium spiny neurons, given that mHtt impairs exosome secretion from the striatum but not the cortex of 10-month-old HD KI mice. However, the mechanisms underlying this differential effect on exosome release in different brain regions by mHtt expression remain to be understood. It is possible that exosome secretion from striatal astrocytes is more susceptible to impairment by mHtt expression. Future studies should investigate whether the secretion of astrocytic exosome from the striatum is less than that from other brain regions in HD KI mice compared with WT mice. We will generate adenoviral vector to express the exosome marker Alix-GFP under GFAP promoter (Ad-GFAP-Alix-GFP), and inject this virus into the striatum and other brain regions of WT and HD KI mice by stereotaxic injection. After 21 to 30 days, we will isolate exosomes from

different brain regions of WT and HD KI mice. Since astrocytic exosomes are labeled with GFP, we will use fluorescence activated cell sorting (FACS) to isolate astrocytic exosomes from different brain regions and perform western blotting to compare Alix expression levels in different brain regions of WT and HD KI mice. Given that N-terminal mHtt reduces Sp1-mediated αB-crystallin transcription in primary astrocytes in an age-dependent manner, which caused a deficiency of exosome secretion, future studies can investigate whether mHtt induces dysregulation of αB-crystallin expression in astrocytes in HD KI mice in a brain region-dependent manner. To this end, we need to culture astrocytes from different brain regions, such as the cortex and the striatum, of HD KI mice to compare the nuclear accumulation of mHtt fragments and exosome release. This investigation will examine whether αB-crystallin levels are lower in striatal astrocytes than astrocytes from other regions by qRT-PCR and Western blotting. If so, we will perform the CHIP assay to determine whether disrupted association of Sp1 with the αB-crystallin enhancer by mHtt preferentially occurs in striatal astrocytes.

In addition to using primary cultures, we can cross HD KI mice with GFAP-GFP mice to specifically label astrocytes with GFP, and then use FACS to isolate astrocytes from different brain regions of HD KI mice. Enriched astrocytes from different brain regions would be subjected to qRT-PCR for comparing transcriptional levels of αB-crystallin, as well as to the CHIP assay for detecting the association between the αB-crystallin enhancer and Sp1. On the other hand, we will also examine Sp1 expression levels and activity among astrocytes from the striatum and other brain regions using the aforementioned methodology, which may provide additional clues to the nature of the selective decrease in exosome secretion from astrocytes.

Another future research direction is to investigate whether mHtt also affects the secretion of other molecules from astrocytes. Astrocytes are housekeepers in the CNS and secrete a variety of classic neurotransmitters, neuromodulators, and metabolic and trophic factors. They communicate with neurons and other glial cells through the release of signaling molecules. Our current study demonstrates that mHtt impairs BDNF and ATP release, suggesting that mHtt might affect other factors, such as glial cell-derived neurotrophic factor (GDNF) and ciliary neurotrophic factor (CNTF), which are essential for neuronal survival and function. In the future, we can culture primary astrocytes and harvest conditioned medium to screen for the release of these factors by ELISA and establish the mechanisms underlying the altered secretion of these molecules.

5.3 Conclusions

Our study demonstrates the important impact of mHtt on astrocytic secretion, and suggests that astrocytes could be a potential therapeutic target for HD treatment. Our findings demonstrate that mHtt at the endogenous levels decreases the secretion of BDNF-containing dense-core vesicles from astrocytes by disrupting the conversion of GTP-Rab3a into GDP-Rab3a and that overexpressing Rab3a can rescue this deficient BDNF release and early neuropathology in the HD KI mouse brain, suggesting that astrocytic Rab3a is a potential therapeutic target in treating HD. Our findings also demonstrate that mHtt impairs the secretion of astrocytic exosomes by decreasing αB-crystallin, a protein that is expressed mainly in glial cells and mediates exosome secretion. Overexpression of αB-crystallin could alleviate the deficient release of exosomes and neuropathology in HD KI mice, revealing a new pathological pathway that affects the critical support of glial cells to neurons in the HD brain. Elevating astrocytic

secretion of dense-core vesicles and exosomes might be not just for HD treatment, but also possibly for many other neurodegenerative diseases (**Fig. 5.1**).

Fig 5.1

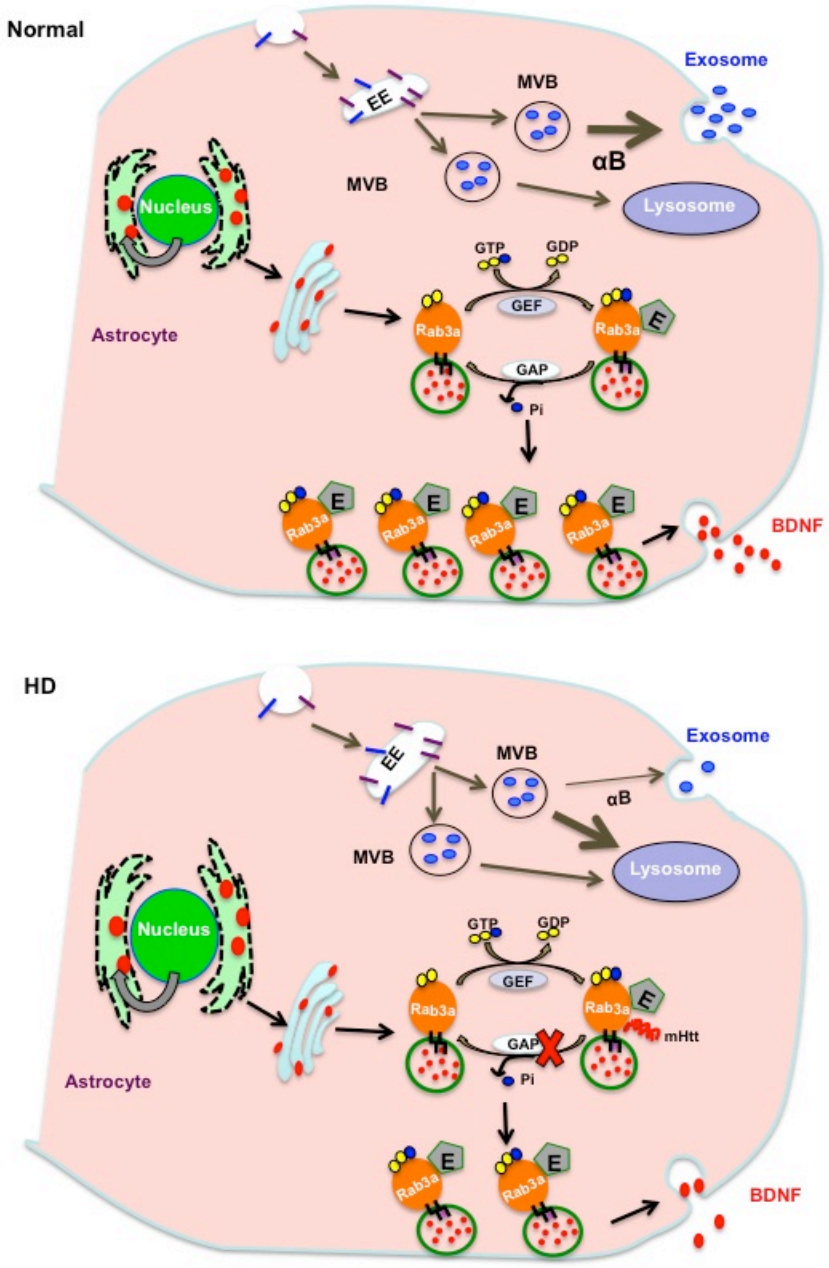
Normal
EE
MVB
Exosome
αB
MVB
Lysosome
Nucleus
GTP
GDP
GEF
Astrocyte
Rab3a
E
GAP
Pi
BDNF
HD
EE
MVB
Exosome
αB
MVB
Lysosome
Nucleus
GTP
GDP
GEF
Rab3a
E
mHtt
GAP
Astrocyte
Pi
BDNF

Figure 5.1

Proposed model for the decreased astrocytic secretion. In normal condition, astrocytes release neurotrophic factors such as BDNF and exosomes to support the normal function and survival of neuronal cells. However, in HD, mHtt decreases the secretion of BDNF by compromising exocytosis of dense-core vesicles in astrocytes. mHtt also reduces the expression of αB-crystallin in astrocytes to decrease exosome secretion in the HD brains.

References

Aid T, Kazantseva A, Piirsoo M, Palm K, Timmusk T (2007) Mouse and rat BDNF gene structure and expression revisited. *J. Neurosci Res* **85**, 525–535.

Airaksinen MS, and Saarma M (2002) The GDNF family: signalling, biological functions and therapeutic value. *Nat Rev Neurosci* **3**, 383-394.

Akopova I, Tatur S, Grygorczyk M, Luchowski R, Gryczynski I, Gryczynski Z, Borejdo J, Grygorczyk R (2012) Imaging exocytosis of ATP-containing vesicles with TIRF microscopy in lung epithelial A549 cells. *Purinergic Signal* **8**: 59-70

Allen NJ, Barres BA (2009) Neuroscience: Glia - more than just brain glue. *Nature* **457**: 675-7.

Baker S, Polanco JC, Götz J (2016) Extracellular Vesicles Containing P301L Mutant Tau Accelerate Pathological Tau Phosphorylation and Oligomer Formation but Do Not Seed Mature Neurofibrillary Tangles in ALZ17 Mice. *J Alzheimers Dis* **54**: 1207-1217.

Bal-Price A, Moneer Z, Brown GC (2002) Nitric oxide induces rapid, calcium-dependent release of vesicular glutamate and ATP from cultured rat astrocytes. *Glia* **40**, 312–323.

Bates GP, Dorsey R, Gusella JF, Hayden MR, Kay C, Leavitt BR, Nance M, Ross CA, Scahill RI, Wetzel R, Wild EJ, Tabrizi SJ (2015) Huntington disease. *Nat Rev Dis Primers* 1:15005.

Bankston AN, Mandler MD, Feng Y (2013) Oligodendroglia and neurotrophic factors in neurodegeneration. *Neuroscience bulletin* ***29***, 216-228.

Bartzokis G, Lu PH, Tishler TA, Fong SM, Oluwadara B, Finn JP, Huang D, Bordelon Y, Mintz J, Perlman S (2007) Myelin breakdown and iron changes in Huntington's disease: pathogenesis and treatment implications. *Neurochemical research* ***32***, 1655-1664.

Bauer S, Kerr BJ, Patterson PH (2007) The neuropoietic cytokine family in development, plasticity, disease and injury. *Nat Rev Neurosci* **8**, 221-232.

Behrens PF, Franz P, Woodman B, Lindenberg KS, Landwehrmeyer GB (2002) Impaired glutamate transport and glutamate-glutamine cycling: Downstream effects of the Huntington mutation. *Brain* **125**: 1908–1922.

Bellingham SA, Guo BB, Coleman BM, Hill AF (2012) Exosomes: vehicles for the transfer of toxic proteins associated with neurodegenerative diseases? *Front Physiol* **3**: 124.

Bhuin T, Roy JK (2015) Rab11 in disease progression. *Int J Mol Cell Med* **4**: 1-8

Bieri G, Gitler AD, Brahic M (2017) Internalization, axonal transport and release of fibrillar forms of alpha-synuclein. *Neurobiol Dis.* S0969-9961 (17) 30055-4

Bianco F, Perrotta C, Novellino L, Francolini M, Riganti L, Menna E, Saglietti L, Schuchman EH, Furlan R, Clementi E, Matteoli M, Verderio C (2009) Acid sphingomyelinase activity triggers microparticle release from glial cells. *EMBO J* **28**:

1043–1054.

Bloch J, Bachoud-Lévi AC, Déglon N, Lefaucheur JP, Winkel L, Palfi S, Nguyen JP, Bourdet C, Gaura V, Remy P, Brugières P, Boisse MF, Baudic S, Cesaro P, Hantraye P, Aebischer P, Peschanski M (2004) Neuroprotective gene therapy for Huntington's disease, using polymer-encapsulated cells engineered to secrete human ciliary neurotrophic factor: results of a phase I study. *Hum Gene Ther* ***15***: 968-975.

Bohanna I, Georgiou-Karistianis N, Sritharan A, Asadi H, Johnston L, Churchyard A, Egan G (2011) Diffusion tensor imaging in Huntington's disease reveals distinct patterns of white matter degeneration associated with motor and cognitive deficits. *Brain Imaging Behav* **5**: 171-80

Bradford J, Shin JY, Roberts M, Wang CE, Li XJ, Li S (2009) Expression of mutant huntingtin in mouse brain astrocytes causes age-dependent neurological symptoms. *Proc Natl Acad Sci U S A* **106**: 22480-22485.

Bradford J, Shin JY, Roberts M, Wang CE, Sheng G, Li S, Li XJ (2010) Mutant huntingtin in glial cells exacerbates neurological symptoms of Huntington disease mice. *J Biol Chem* **285**: 10653-61.

Brandstaetter H, Kruppa AJ, Buss F (2014) Huntingtin is required for ER-to-Golgi transport and for secretory vesicle fusion at the plasma membrane. *Dis Model Mech.* **7**: 1335-40.

Bucci C, Parton RG, Mather IH, Stunnenberg H, Simons K, Hoflack B, Zerial M (1992) The small GTPase rab5 functions as a regulatory factor in the early endocytic pathway. *Cell* **70**: 715–28.

Bucci C, Alifano P, Cogli L (2014) The role of rab proteins in neuronal cells and in the trafficking of neurotrophin receptors. *Membranes (Basel)* **4**: 642-77

Burstein ES, Brondyk WH, Macara IG, Kaibuchi K, Takai Y (1993) Regulation of the GTPase cycle of the neuronally expressed Ras-like GTP-binding protein Rab3A. *J Biol Chem* **268**: 22247-22250.

Bustos MA, Lucchesi O, Ruete MC, Mayorga LS, Tomes CN (2012) Rab27 and Rab3 sequentially regulate human sperm dense-core granule exocytosis. *Proc Natl Acad Sci U S A* **109**: E2057-66.

Caby MP, Lankar D, Vincendeau-Scherrer C, Raposo G, Bonnerot C (2005) Exosomal-like vesicles are present in human blood plasma. *Int Immunol* **17**: 879-87.

Canals JM, Pineda JR, Torres-Peraza JF, Bosch M, Martin-Ibanez R, Munoz MT, Mengod G, Ernfors P, Alberch J (2004) Brain-derived neurotrophic factor regulates the onset and severity of motor dysfunction associated with enkephalinergic neuronal degeneration in Huntington's disease. *J. Neurosci* **24**, 7727–7739.

Casanova JE, Wang X, Kumar R, Bhartur SG, Navarre J, Woodrum JE, Altschuler Y, Ray GS, Goldenring JR (1999) Association of Rab25 and Rab11a with the apical recycling system of polarized MadinDarby canine kidney cells. *Mol Biol Cell* **10**: 47-61

Cattaneo E, Zuccato C, Tartari M, (2005) Normal huntingtin function: an alternative approach to Huntington's disease. *Nat Rev Neurosci* **6**: 919 –930.

Chan CS, Surmeier DJ (2014) Astrocytes go awry in Huntington's disease. *Nat Neurosci* **17**, 641-642.

Chen-Plotkin AS, Sadri-Vakili G, Yohrling GJ, Braveman MW, Benn CL, Glajch KE, DiRocco DP, Farrell LA, Krainc D, Gines S, MacDonald ME, Cha JH (2006) Decreased association of the transcription factor Sp1 with genes downregulated in Huntington's disease. *Neurobiology of disease **22***, 233-241.

Cisbani G, Cicchetti F (2012) An in vitro perspective on the molecular mechanisms underlying mutant huntingtin protein toxicity. *Cell Death Dis* **3**: e382.

Coco S, Calegari F, Pravettoni, Pozzi D, Taverna E, Rosa P, Matteoli M, Verderio C (2003) Storage and release of ATP from astrocytes in culture. *J. Biol. Chem* **278**, 1354–1362.

Colombo M, Raposo G, Théry C (2014) Biogenesis, secretion, and intercellular interactions of exosomes and other extracellular vesicles. *Annu Rev Cell Dev Biol* **30**: 255-89.

Costanzo M, Abounit S, Marzo L et al (2013) Transfer of polyglutamine aggregates in neuronal cells occurs in tunneling nano- tubes. *J Cell Sci* **126**: 3678–3685.

Cotrina ML, Lin JH, Alves-Rodrigues A, Liu S, Li J, Azmi-Ghadimi H, Kang J, Naus CC, Nedergaard M (1998) Connexins regulate calcium signaling by controlling ATP release. *Proc. Natl. Acad. Sci. U. S. A.* **95**: 15735–15740.

Cox D, Lee DJ, Dale BM, Calafat J, Greenberg S (2000) A Rab11-containing rapidly recycling compartment in macrophages that promotes phagocytosis. *Proc Natl Acad Sci U S A* **97**: 680-5.

Crook ZR, Housman D (2011) Huntington's disease: can mice lead the way to treatment? *Neuron* 69, 423- 35

Dannies PS (1999) Protein hormone storage in secretory granules: mechanisms for concentration and sorting. *Endocr. Rev* **20**: 3–21.

Darchen F, Goud B (2000) Multiple aspects of Rab protein action in the secretory pathway: focus on Rab3 and Rab6. *Biochimie* **82**: 375-384.

Davies SW, Turmaine M, Cozens BA, DiFiglia M, Sharp AH, Ross CA, Scher- zingerE, WankerEE, MangiariniL, BatesGP (1997) Formationofneu- ronal intranuclear inclusions underlies the neurological dysfunction in mice transgenic for the HD mutation. *Cell* **90**: 537–548.

Didiot MC, Hall LM, Coles AH, Haraszti RA, Godinho BM, Chase K, Sapp E, Ly S, Alterman JF, Hassler MR, Echeverria D, Raj L, Morrissey DV, DiFiglia M, Aronin N, Khvorova A (2016) Exosome-mediated Delivery of Hydrophobically Modified siRNA for Huntingtin mRNA Silencing. *Mol Ther* **24**: 1836-1847.

Dieni S, Matsumoto T, Dekkers M, Rauskolb S, Ionescu MS, Deogracias R, Gundelfinger ED, Kojima M, Nestel S, Frotscher M, Barde YA (2012) BDNF and its pro-peptide are stored in presynaptic dense core vesicles in brain neurons. *J Cell Biol* **196**: 775-88.

DiFiglia M, Sapp E, Chase K, Schwarz C, Meloni A, Young C, Martin E, Vonsattel JP, Carraway R, Reeves SA (1995) Huntingtin is a cytoplasmic protein associated with vesicles in human and rat brain neurons. *Neuron* **14**:1075-1081.

DiFiglia M, Sapp E, Chase KO, Davies SW, Bates GP, Vonsattel JP, Aronin N (1997) Aggregation of huntingtin in neuronal intranuclear inclusions and dystrophic neurites in brain. *Science* **277**, 1990-1993.

Dragatsis I, Levine MS, Zeitlin, S (2000) Inactivation of Hdh in the brain and testis results in progressive neurodegeneration and sterility in mice. *Nat Genet **26***, 300- 306.

Driver-Dunckley E, CJ (2007) Huntington's Disease. In: Schapira AHV. *Neurology and Clinical Neuroscience* Vol 67

Duman RS, Voleti B (2012) Signaling pathways underlying the pathophysiology and treatment of depression: novel mechanisms for rapid-acting agents. *Trends Neurosci* **35**:

47-56.

Dunah AW, Jeong H, Griffin A, Kim YM, Standaert DG, Hersch SM, Mouradian MM, Young AB, Tanese N, Krainc D (2002) Sp1 and TAFII130 transcriptional activity disrupted in early Huntington's disease. *Science* **296**: 2238-43

Duyao M, Ambrose C, Myers R, Novelletto A, Persichetti F, Frontali M, Folstein S, Ross C, Franz M, Abbott M (1993) Trinucleotide repeat length instability and age of onset in Huntington's disease. *Nature genetics* **4**, 387-392.

Duyao MP, Auerbach AB, Ryan A, Persichetti F, Barnes GT, McNeil SM, Ge P, Vonsattel JP, Gusella JF, Joyner AL (1995) Inactivation of the mouse Huntington's disease gene homolog Hdh. *Science* **269**:407-410.

EI Khoury J, Luster AD (2008) Mechanisms of microglia accumulation in Alzheimer's disease: therapeutic implications. *Trends Pharmacol Sci* **29**:626–632

Ellerby HM, Hayden MR, Bredesen DE, Ellerby LM (2004) Specific caspase interactions and amplification are involved in selective neuronal vulnerability in Huntington's disease. *Cell Death Differ* **11**: 424-438.

Espey MG, Kustova Y, Sei Y, Basile AS (1998) Extracellular glutamate levels are chronically elevated in the brains of LP-BM5-infected mice: a mechanism of retrovirus-induced encephalopathy. *J Neurochem* **71**: 2079-87.

Estrada-Sánchez AM, Montiel T, Segovia J, Massieu L (2009) Glutamate toxicity in the striatum of the R6/2 Huntington's disease transgenic mice is age-dependent and correlates with decreased levels of glutamate transporters. *Neurobiol Dis* **34**:78-86.

Gangalum RK, Bhat AM, Kohan SA, Bhat SP (2016) Inhibition of the Expression of the Small Heat Shock Protein αB-Crystallin Inhibits Exosome Secretion in Human Retinal Pigment Epithelial Cells in Culture. *J Biol Chem* **291**:12930-42

Gauthier LR, Charrin BC, Borrell-Pagès M, Dompierre JP, Rangone H, Cordelières FP, De Mey J, MacDonald ME, Lessmann V, Humbert S, Saudou F (2004) Huntingtin controls neurotrophic support and survival of neurons by enhancing BDNF vesicular transport along microtubules. *Cell* **118**:127-138.

Giralt A, Carretón O, Lao-Peregrin C, Martín ED, Alberch J (2011) Conditional BDNF release under pathological conditions improves Huntington's disease pathology by delaying neuronal dysfunction. *Mol Neurodegener* **6**:71.

Gray M, Shirasaki DI, Cepeda C, Andre´ VM, Wilburn B, Lu XH, Tao J, Yamazaki I, Li SH, Sun YE, Li XJ, Levine MS, Yang XW (2008) Full- length human mutant huntingtin with a stable polyglutamine repeat can elicit progressive and selective neuropathogenesis in BACHD mice. *J Neurosci* **28**: 6182– 6195.

Group, T.H.s.D.C.R. (1993) A novel gene containing a trinucleotide repeat that is expanded and unstable on Huntington's disease chromosomes. The Huntington's Disease

Collaborative Research Group. *Cell* ***72***, 971-983.

Guitart K, Loers G, Buck F, Bork U, Schachner M, Kleene R. Guitart K, Loers G, Buck F, Bork U, Schachner M, Kleene R (2016) Improvement of neuronal cell survival by astrocyte-derived exosomes under hypoxic and ischemic conditions depends on prion protein. *Glia* **64**:896-910

Gutekunst CA, Li SH, Yi H, Mulroy JS, Kuemmerle S, Jones R, Rye D, Ferrante RJ, Hersch SM, Li XJ (1999) Nuclear and neuropil aggregates in Huntington's disease: relationship to neuropathology. *J Neurosci* **19**, 2522-2534.

Hajrasouliha AR, Jiang G, Lu Q, Lu H, Kaplan HJ, Zhang HG, Shao H (2013) Exosomes from retinal astrocytes contain antiangiogenic components that inhibit laser-induced choroidal neovascularization. *J Biol Chem* **288**: 28058-67

Haney MJ, Zhao Y, Harrison EB, Mahajan V, Ahmed S, He Z, Suresh P, Hingtgen SD, Klyachko NL, Mosley RL, Gendelman HE, Kabanov AV, Batrakova EV (2013) Specific transfection of inflamed brain by macrophages: a new therapeutic strategy for neurodegenerative diseases. *PLoS One* **8**:e61852.

Harper PS (1992) The epidemiology of Huntington's disease. *Hum Genet* **89**, 365-376.

Harjes P, Wanker EE (2003) The hunt for huntingtin function: interaction partners tell many different stories. *Trends Biochem Sci* **28**:425– 433.

Hassel B, Tessler S, Faull RL, Emson PC (2008) Glutamate uptake is reduced in

prefrontal cortex in Huntington's disease. *Neurochem Res* **33**: 232–237.

Hermel E, Gafni J, Propp SS, Leavitt BR, Wellington CL, Young JE, Hackam AS, Logvinova AV, Peel AL, Chen SF, Hook V, Singaraja R, Krajewski S, Goldsmith PC, Hertz L, Dringen R, Schousboe A, Robinson SR (1999) Astrocytes: glutamate producers for neurons. *J. Neurosci. Res* **57**, 417–428.

Hickey MA, Kosmalska A, Enayati J, Cohen R, Zeitlin S, Levine MS, Chesselet MF (2008) Extensive early motor and non-motor behavioral deficits are followed by striatal neuronal loss in knock-in Huntington's disease mice. *Neuroscience* **157**: 280-95.

Hong Y, Zhao T, Li XJ, Li S (2016) Mutant Huntingtin Impairs BDNF Release from Astrocytes by Disrupting Conversion of Rab3a-GTP into Rab3a-GDP. *J Neurosci* **36**, 8790-8801.

Hochberg GK, Ecroyd H, Liu C, Cox D, Cascio D, Sawaya MR, Collier MP, Stroud J, Carver JA, Baldwin AJ, Robinson CV, Eisenberg DS, Benesch JL, Laganowsky A. (2014) The structured core domain of αB-crystallin can prevent amyloid fibrillation and associated toxicity. *Proc. Natl. Acad. Sci. USA* **111**, 1562–1570.

Howells DW, Porritt MJ, Wong JY, Batchelor PE, Kalnins R, Hughes AJ, Donnan GA (2000) Reduced BDNF mRNA expression in the Parkinson's disease substantia nigra. *Exp Neurol* **166**:127-135

Hsiao HY, Chern Y (2010) Targeting glial cells to elucidate the pathogenesis of Huntington's disease. *Mol Neurobiol* **41**: 248-55.

Huang B, Wei W, Wang G, Gaertig MA, Feng Y, Wang W, Li XJ, Li S (2015) Mutant huntingtin downregulates myelin regulatory factor-mediated myelin gene expression and affects mature oligodendrocytes. *Neuron* **85**: 1212-26.

Huang EJ and Reichardt LF (2001) Neurotrophins: roles in neuronal development and function. *Annu Rev Neurosci* **24**, 677-736.

Iglesias R, Dahl G, Qiu F, Spray DC, Scemes E (2009) Pannexin 1: the molecular substrate of astrocyte "hemichannels". *J. Neurosci* **29**, 7092–7097.

Iino M, Goto K, Kakegawa W, Okado H, Sudo M, Ishiuchi S, Miwa A, Takayasu Y, Saito I, Tsuzuki K, Ozawa S (2001) Glia-synapse interaction through Ca2+-permeable AMPA receptors in Bergmann glia. *Science* **292**: 926-9.

Imura T, Shimohama S, Sato M, Nishikawa H, Madono K, Akaike A, Kimura J (1999) Differential expression of small heat shock proteins in reactive astrocytes after focal ischemia: possible role of beta-adrenergic receptor**.** *J Neurosci* **19**: 9768-79.

Jahn R and Fasshauer D (2012) Molecular machines governing exocytosis of synaptic vesicles. *Nature* **490**: 201-7.

Jarmalavičiūtė A, Pivoriūnas A (2016) Exosomes as a potential novel therapeutic tools

against neurodegenerative diseases. *Pharmacol Res* **113**: 816-822

Jeon I, Cicchetti F, Cisbani G, Lee S, Li E, Bae J, Lee N, Li L, Im W, Kim M, Kim HS, Oh SH, Kim TA, Ko JJ, Aubé B, Oueslati A, Kim YJ, Song J (2016) Human-to-mouse prion-like propagation of mutant huntingtin protein. *Acta Neuropathol* **132**: 577-92.

Kettenmann, H, Hanisch, U. K, Noda, M, Verkhratsky, A (2011) Physiology of microglia. *Physiol. Rev* **91**, 461–553.

Kim SU,and de Vellis J (2005) Microglia in health and disease. *J Neurosci Res* **81**, 302-313.

Klegeris A, McGeer EG, McGeer PL (2007) Therapeutic approaches to inflammation in neurodegenerative disease. *Curr Opin Neurol* **20**: 351–357.

Kremer B, Goldberg P, Andrew SE, Theilmann J, Telenius H, Zeisler J, Squitieri F, Lin B, Bassett A, Almqvist E (1994) A worldwide study of the Huntington's disease mutation. The sensitivity and specificity of measuring CAG repeats. *N Engl J Med **330***, 1401-1406.

Krämer-Albers EM, Bretz N, Tenzer S, Winterstein C, Mobius W, Berger H, Nave KA, Schild H, Trotter J (2007) Oligodendrocytes secrete exosomes containing major myelin and stress-protective proteins: trophic support for axons? *Proteomics Clin. Appl* **1**, 1446–1461.

Lachenal G, Pernet-Gallay K, Chivet M, Hemming J, Belly A, Bodon G, Blot B, Haase

G, Goldberg Y, Sadoul R (2011) Release of exosomes from differentiated neurons and its regulation by synap- tic glutamatergic activity. *Mol. Cell. Neurosci* **46**, 409–418.

Lee CY, Cantle JP, Yang XW (2013) Genetic Manipulations of Mutant Huntingtin in Mice: New Insights into HD Pathogenesis. *FEBS J* **280**: 4382-94.

Lee J, Fukumoto H, Orne J, Klucken J, Raju S, Vanderburg CR, Irizarry MC, Hyman BT, Ingelsson M (2005) Decreased levels of BDNF protein in Alzheimer temporal cortex are independent of BDNF polymorphisms. *Exp Neurol* **194**:91-96

Lee M, Liu T, Im W, Kim M (2016) Exosomes from adipose-derived stem cells ameliorate phenotype of Huntington's disease in vitro model. *Eur J Neurosci* **44**: 2114-9.

Lee ST, Im W, Ban JJ, Lee M, Jung KH, Lee SK, Chu K, Kim M (2017) Exosome-Based Delivery of miR-124 in a Huntington's Disease Model. *J Mov Disord* **10**: 45-52.

Levy E (2017) Exosomes in the Diseased Brain: First Insights from In vivo Studies. Front Neurosci 11: 142.

Liévens JC, Woodman B, Mahal A, Spasic-Boscovic O, Samuel D, Kerkerian-Le Goff L, Bates GP (2001) Impaired glutamate uptake in the R6 Huntington's disease transgenic mice. *Neurobiol Dis* **8**: 807–821.

Li H, Li SH, Johnston H, Shelbourne PF, Li XJ (2000) Amino-terminal fragments of mutant huntingtin show selective accumulation in striatal neurons and synaptic toxicity. *Nat Genet* **25**:385-9.

Li H, Li SH, Yu ZX, Shelbourne P, Li XJ (2001) Huntingtin aggregate-associated axonal degeneration is an early pathological event in Huntington's disease mice. *J Neurosci* **21**: 8473-81.

Li SH, Cheng AL, Zhou H, Lam S, Rao M, Li H, Li XJ (2002) Interaction of Huntington disease protein with transcriptional activator Sp1. *Molecular and cellular biology **22***, 1277-1287.

Li SH and Li XJ (2004) Huntingtin-protein interactions and the pathogenesis of Huntington's disease. *Trends Genet* **20**:146-154.

Li, S, and Li, XJ (2006) Multiple pathways contribute to the pathogenesis of Huntington disease. *Mol Neurodegener* **1**, 19.

Li X, Sapp E, Chase K, Comer-Tierney LA, Masso N, Alexander J, Reeves P, Kegel KB, Valencia A, Esteves M, Aronin N, Difiglia M (2009) Disruption of Rab11 activity in a knock-in mouse model of Huntington's disease. *Neurobiol Dis* **36**:374-83.

Lievens JC, Woodman B, Mahal A, Spasic-Boscovic O, Samuel D, Kerkerian-Le Goff L, Bates GP (2001) Impaired glutamate uptake in the R6 Huntington's disease transgenic mice. *Neurobiol Dis* **8**:807–821

Lobsiger CS and Cleveland DW (2007) Glial cells as intrinsic components of non- cell-autonomous neurodegenerative disease. *Nat Neurosci* **10**, 1355-1360.

Lu B (2003) BDNF and activity-dependent synaptic modulation. *Learn. Mem*. **10**, 86–98.

Lu B, Pang PT, Woo NH (2005) The yin and yang of neurotrophin action. *Nat Rev Neurosci* **6**: 603-614.

Maas SL, Breakefield XO, Weaver AM (2017) Extracellular Vesicles: Unique Intercellular Delivery Vehicles. *Trends Cell Biol* 27:172-188.

Maienschein V, Marxen M, Volknandt W, Zimmermann H (1999) A plethora of presynaptic proteins associated with ATP-storing organelles in cultured astrocytes. *Glia* **26**: 233-244

Martelli AM, Baldini G, Tabellini G, Koticha D, Bareggi R, Baldini G (2000) Rab3A and Rab3D control the total granule number and the fraction of granules docked at the plasma membrane in PC12 cells. *Traffic* **1**: 976-986.

Menalled LB, Sison JD, Dragatsis I, Zeitlin S, Chesselet MF (2003) Time course of early motor and neuropathological anomalies in a knock-in mouse model of Huntington's disease with 140 CAG repeats. *J Comp Neurol* **465**: 11-26.

Miyamoto N, Maki T, Shindo A, Liang AC, Maeda M, Egawa N, Itoh K, Lo EK, Lok J, Ihara M, Arai K (2015) Astrocytes Promote Oligodendrogenesis after White Matter

Damage via Brain-Derived Neurotrophic Factor. *J Neurosci* **35**:14002-14008.

Molofsky AV, Krencik R, Ullian EM, Tsai HH, Deneen B, Richardson WD, Barres BA, Rowitch DH (2012) Astrocytes and disease: a neurodevelopmental perspective. *Genes Dev* **26**:891-907

Muchowski PJ, Ramsden R, Nguyen Q, Arnett EE, Greiling TM, Anderson SK, Clark JI (2008) Non-invasive measurement of protein aggregation by mutant huntingtin fragments or alpha-synuclein in the lens. *J. Biol. Chem* **283**, 6330–6336.

Nafar F, Williams JB, Mearow KM (2016) Astrocytes release HspB1 in response to amyloid-β exposure in vitro. *J Alzheimers Dis* **49**: 251-63.

Nasir J, Floresco SB, O'Kusky JR, Diewert VM, Richman JM, Zeisler J, Borowski A, Marth JD, Phillips AG, Hayden MR (1995) Targeted disruption of the Huntington's disease gene results in embryonic lethality and behavioral and morphological changes in heterozygotes. *Cell* **81**:811-823.

Oliveira AO, Osmand A, Outeiro TF, Muchowski PJ, Finkbeiner S (2016) αB-Crystallin overexpression in astrocytes modulates the phenotype of the BACHD mouse model of Huntington's disease. *Hum Mol Genet* **25**:1677-89

Palgi M, Lindstrom R, Peranen J, Piepponen TP, Saarma M, Heino TI (2009) Evidence that DmMANF is an invertebrate neurotrophic factor supporting dopaminergic neurons. *Proc Natl Acad Sci U S A* ***106***, 2429-2434.

Pal A, Severin F, Lommer B, Shevchenko A, Zerial M (2006) Huntingtin-HAP40 complex is a novel Rab5 effector that regulates early endosome motility and is upregulated in Huntington's disease. *J Cell Biol* **172**: 605–18.

Pangrsic T, Potokar M, Stenovec M, Kreft M, Fabbretti E, Nistri A, Pryazhnikov E, Khiroug L, Giniatullin R, Zorec R (2007) Exocytotic release of ATP from cultured astrocytes. *J Biol Chem* **282**: 28749-28758.

Parpura V, Basarsky T, Liu F, Jeftinija K, Jeftinija S, Haydon P (1994) Glutamate-mediated astrocyte–neuron signalling. *Nature* **369**, 744–747.

Parpura V and Zorec R (2010) Gliotransmission: Exocytotic release from astrocytes. *Brain Res Rev* **63**: 83-92.

Pasantes Morales H and Schousboe A (1988) Volume regulation in astrocytes: a role for taurine as an osmoeffector. *J. Neurosci. Res* **20**, 503–509.

Pecho-Vrieseling E, Rieker C, Fuchs S, Bleckmann D, Esposito MS, Botta P, Goldstein C, Bernhard M, Galimberti I, Müller M, Lüthi A, Arber S, Bouwmeester T, van der Putten H, Di Giorgio FP (2014) Transneuronal propagation of mutant huntingtin contributes to non-cell autonomous pathology in neurons. *Nat Neurosci* **17**:1064-72.

Pekny M, Pekna M, Messing A, Steinhäuser C, Lee JM, Parpura V, Hol EM, Sofroniew MV, Verkhratsky A (2016) Astrocytes: a central element in neurological diseases. *Acta Neuropathol* **131**: 323-45.

Perez-Gonzalez R, Gauthier SA, Kumar A, Levy E (2012) The exosome secretory pathway transports amyloid precursor protein carboxyl-terminal fragments from the cell into the brain extracellular space. *J Biol Chem* **287**:43108-15.

Perez-Navarro E, Canudas AM, Akerund P, Alberch J, Arenas E (2000) Brain-derived neurotrophic factor, neurotrophin-3, and neurotrophin-4/5 prevent the death of striatal projection neurons in a rodent model of Huntington's disease. *J Neurochem* **75**, 2190-2199.

Pisitkun T, Shen RF, Knepper MA (2004) Identification and proteomic profiling of exosomes in human urine. *Proc Natl Acad Sci U S A* **101**:13368-73.

Polanco JC, Scicluna BJ, Hill AF, Götz J (2016) Extracellular Vesicles Isolated from the Brains of rTg4510 Mice Seed Tau Protein Aggregation in a Threshold-dependent Manner. *J Biol Chem* **291**:12445-66.

Potolicchio I, Carven GJ, Xu X, Stipp C, Riese RJ, Stern LJ, Santambrogio L (2005) Proteomic analysis of microglia-derived exosomes: metabolic role of the aminopeptidase CD13 in neuropeptide catabolism. *J Immunol* **175**: 2237-43.

Power D, Srinivasan S, Gunawardena S (2012) In-vivo evidence for the disruption of Rab11 vesicle transport by loss of huntingtin. *Neuroreport* **23**: 970-7.

Pryazhnikov E and Khiroug L (2008) Sub-micromolar increase in [Ca2+]i triggers delayed exocytosis of ATP in cultured astrocytes. *Glia* **56**, 38–49.

Quesseveur G, David DJ, Gaillard MC, Pla P, Wu MV, Nguyen HT, Nicolas V, Auregan

G, David I, Dranovsky A, Hantraye P, Hen R, Gardier AM, Déglon N, Guiard BP (2013) BDNF overexpression in mouse hippocampal astrocytes promotes local neurogenesis and elicits anxiolytic-like activities. *Transl Psychiatry* **3**: e253.

Rekas A, Adda CG, Andrew Aquilina J, Barnham KJ, Sunde M, Galatis D, Williamson NA, Masters CL, Anders RF, Robinson CV, Cappai R, Carver JA (2004) Interaction of the molecular chaperone alphaB-crystallin with alpha-synuclein: effects on amyloid fibril formation and chaperone activity. *J. Mol.Biol* **340**: 1167–1183.

Ren M, Xu G, Zeng J, De Lemos-Chiarandini C, Adesnik M, Sabatini DD (1998) Hydrolysis of GTP on rab11 is required for the direct delivery of transferrin from the pericentriolar recycling compartment to the cell surface but not from sorting endosomes. *Proc Natl Acad Sci U S A* **95**: 6187-92.

Rosas HD, Lee SY, Bender AC, Zaleta AK, Vangel M, Yu P, Fischl B, Pappu V, Onorato C, Cha JH, Salat DH, Hersch SM (2009) Altered white matter mi- crostructure in the corpus callosum in Huntington's disease: implications for cortical "disconnection". *Neuroimage* **49**:2995-3004.

Ross CA and Tabrizi SJ (2011) Huntington's disease: from molecular pathogenesis to clinical treatment. *Lancet Neurol* **10**: 83-98.

Sahlender DA, Roberts RC, Arden SD, Spudich G, Taylor MJ, Luzio JP, Kendrick-Jones J, Buss F (2005) Optineurin links myosin VI to the Golgi complex and is involved in Golgi organization and exocytosis. *J. Cell Biol* **169**, 285–295.

Sargsyan SA, Monk PN, Shaw PJ (2005) Microglia as potential contributors to motor neuron injury in amyotrophic lateral sclerosis. *Glia* **51**:241–253

Saxena S and Caroni P (2011) Selective neuronal vulnerability in neurodegenerative diseases: from stressor thresholds to degeneration. *Neuron* **71**: 35-48.

Schilling G, Becher MW, Sharp AH, Jinnah HA, Duan K, Kotzuk JA, Slunt HH, Ratovitski T, Cooper JK, Jenkins NA, Copeland NG, Price DL, Ross CA, Borchelt DR (1999a) Intranuclear inclusions and neuritic aggregates in transgenic mice expressing a mutant N-terminal fragment of huntingtin. *Hum Mol Genet* **8**:397– 407.

Schilling G, Wood JD, Duan K, Slunt HH, Gonzales V, Yamada M, Cooper JK, Margolis RL, Jenkins NA, Copeland NG, Takahashi H, Tsuji S, Price DL, Borchelt DR, Ross CA. (1999b). Nuclear accumulation of truncated atrophin-1 fragments in a transgenic mouse model of DRPLA. *Neuron **24***, 275-286.

Schlüter OM, Schmitz F, Jahn R, Rosenmund C, Südhof TC (2004) A complete genetic analysis of neuronal Rab3 function. *J Neurosci* **24**: 6629-6637.

Simmons DA, Casale M, Alcon B, Pham N, Narayan N, Lynch G (2007) Ferritin accumulation in dystrophic microglia is an early event in the development of Huntington's disease. *Glia* **55**:1074–1084

Shin JY, Fang ZH, Yu ZX, Wang CE, Li SH, Li XJ (2005) Expression of mutant huntingtin in glial cells contributes toneuronal excitotoxicity. *J Cell Biol* **171**:1001-1012.

Slow EJ, van Raamsdonk J, Rogers D, Coleman SH, Graham RK, Deng Y, Oh R, Bissada N, Hossain SM, Yang YZ, Li XJ, Simpson EM, Gutekunst CA, Leavitt BR, Hayden MR (2003) Selective striatal neuronal loss in a YAC128 mouse model of Huntington disease. *Hum Mol Genet* **12**:1555– 1567.

Soukup GR, Sperfeld AD, Uttner I, Karitzky J, Ludolph AC, Kassubek J, Schreiber H (2009) Frontotemporal cognitive function in X-linked spinal and bulbar muscular atrophy (SBMA): a controlled neuropsychological study of 20 patients. *J Neurol* **256**, 1869-1875.

Stenmark H, Parton RG, Steele-Mortimer O, Lutcke A, Gruenberg J, Zerial M (1994) Inhibition of rab5 GTPase activity stimulates membrane fusion in endocytosis. *Embo J* **13**: 1287–96.

Swamynathan SK, Piatigorsky J (2007) Regulation of the mouse alphaB-crystallin and MKBP/HspB2 promoter activities by shared and gene specific intergenic elements: the importance of context dependency. *Int J Dev Biol* **51**:689-700.

Szatkowski M, Barbour B, Attwell D (1990) Non-vesicular release of glutamate from glial cells by reversed electrogenic glutamate uptake. *Nature* **348**, 443–446.

Tabrizi SJ, Workman J, Hart PE, Mangiarini L, Mahal A, Bates G, Cooper JM, Schapira AH (2000) Mitochondrial dysfunction and free radical damage in the Huntington R6/2 transgenic mouse. *Ann Neurol* **47**:80–86.

Takahashi T, Kikuchi S, Katada S, Nagai Y, Nishizawa M, Onodera O (2008) Soluble polyglutamine oligomers formed prior to inclusion body formation are cytotoxic. *Hum*

Mol Genet **17**, 345-356.

Takai Y, Sasaki T, Shirataki H, Nakanishi H (1996) Rab3A small GTP-binding protein in Ca^{2+}-dependent exocytosis. *Genes to Cells* **1**: 615-632.

Tai YF, Pavese N, Gerhard A, Tabrizi SJ, Barker RA, Brooks DJ, Piccini P (2007) Microglial activation in presymptomatic Huntington's disease gene carriers. *Brain* **130**:1759–1766

Tasset I, Sánchez-López F, Agüera E, Fernández-Bolaños R, Sánchez FM, Cruz-Guerrero A, Gascón-Luna F, Túnez I (2012) NGF and nitrosative stress in patients with Huntington's disease. *J Neurol Sci **315***, 133-136.

Taylor AR, Robinson MB, Gifondorwa DJ, Tytell M, Milligan CE (2007) Regulation of heat shock protein 70 release in astrocytes: role of signaling kinases. *Dev. Neurobiol* **67**, 1815–1829

Théry C, Zitvogel L, Amigorena S (2002) Exosomes: composition, biogenesis and function. *Nat Rev Immunol* **2**:569-79

Théry C, Amigorena S, Raposo G, Clayton A (2006) Isolation and characterization of exosomes from cell culture supernatants and biological fluids. *Curr Protoc Cell Biol* Chapter 3:Unit 3.22.

Théry C (2011) Exosomes: secreted vesicles and intercellular communications. *F1000 Biol Rep* **3**:15.

Tong X, Ao Y, Faas GC, Nwaobi SE, Xu J, Haustein MD, Anderson MA, Mody I, Olsen ML, Sofroniew MV, Khakh BS (2014) Astrocyte Kir4.1 ion channel deficits contribute to neuronal dysfunction in Huntington's disease model mice. *Nat Neurosci* **17**: 694-703.

Toro D, Canals JM, Ginés S, Kojima M, Egea G, Alberch J (2006) Mutant huntingtin impairs the post-Golgi trafficking of brain-derived neurotrophic factor but not its Val66Met polymorphism. *J Neurosci* **26**: 12748-57.

Tsuboi T and Fukuda M (2006) Rab3A and Rab27A cooperatively regulate the docking step of dense-core vesicle exocytosis in PC12 cells. *J Cell Sci* **119**: 2196-2203.

Tsunemi T, Ashe TD, Morrison BE, Soriano KR, Au J, Roque RA, Lazarowski ER, Damian VA, Masliah E, La Spada AR (2012) PGC-1alpha rescues Huntington's disease proteotoxicity by preventing oxidative stress and promoting TFEB function. *Sci. Transl. Med* **4,** 142ra197.

Turmaine M, Raza A, Mahal A, Mangiarini L, Bates GP, Davies SW (2000) Nonapoptotic neurodegeneration in a transgenic mouse model of Huntington's disease. *Proc Natl Acad Sci U S A* **97**, 8093-8097.

Tydlacka S, Wang CE, Wang X, Li S, Li XJ (2008) Differential activities of the ubiquitin-proteasome system in neurons versus glia may account for the preferential accumulation of misfolded proteins in neurons. *J Neurosci* **28**: 13285-95.

Ullrich O, Reinsch S, Urbé S, Zerial M, Parton RG (1996) Rab11 regulates recycling

through the pericentriolar recycling endosome. *J Cell Biol* **135**: 913-24.

Van Weering JR, Toonen RF, Verhage M (2007) The Role of Rab3a in Secretory Vesicle Docking Requires Association/Dissociation of Guanidine Phosphates and Munc18-1. *PLoS ONE* **2**: e616.

Vella LJ, Greenwood DL, Cappai R, Scheerlinck JP, Hill AF (2008) Enrichment of prion protein in exosomes derived from ovine cerebral spinal fluid. *Vet Immunol Immunopathol* **124**: 385-93.

Wang CE, Tydlacka S, Orr AL, Yang SH, Graham RK, Hayden MR, Li S, Chan AW, Li XJ (2008) Accumulation of N-terminal mutant huntingtin in mouse and monkey models implicated as a pathogenic mechanism in Huntington's disease. *Human molecular genetics* **17**, 2738-2751.

Wang L, Lin F, Wang J, Wu J, Han R, Zhu L, Zhang G, DiFiglia M, Qin Z (2012) Truncated N-terminal huntingtin fragment with expanded-polyglutamine (htt552-100Q) suppresses brain-derived neurotrophic factor transcription in astrocytes. *Acta Biochim Biophys Sin* **44**: 249-258.

Wang Y, Balaji V, Kaniyappan S, Krüger L, Irsen S, Tepper K, Chandupatla R, Maetzler W, Schneider A, Mandelkow E, Mandelkow EM (2017) The release and trans-synaptic transmission of Tau via exosomes. *Mol Neurodegener* **12**: 5

Waudby CA, Knowles TP, Devlin GL, Skepper JN, Ecroyd H, Carver JA, Welland ME,

Christodoulou J, Dobson CM, Meehan S (2010) The interaction of αB-crystallin with mature α-synuclein amyloid fibrils inhibits their elongation. *Biophys. J* **98**, 843–851.

Weber JJ, Sowa AS, Binder T, Hübener J (2014) From pathways to targets: understanding the mechanisms behind polyglutamine disease. *Biomed Res Int* 701758.

Westergaard N, Drejer J, Schousboe A, Sonnewald U (1996) Evaluation of the importance of transamination versus deamination in astrocytic metabolism of [U-13C] glutamate. *Glia* **17**, 160–168.

Wilcke M, Johannes L, Galli T, Mayau V, Goud B, Salamero J (2000) Rab11 regulates the compartmentalization of early endosomes required for efficient transport from early endosomes to the trans-golgi network. *J Cell Biol* **151**:1207-20.

Wolfram-Aduan A, Altemus M, Wickwire JH, Sandstrom MI (2014) Presymptomatic glutamate levels in prefrontal cortex in the Hdh (CAG150) mouse model of Huntington's disease. *J Huntingtons Dis* **3**:387-99

Wu X, Chen PS, Dallas S, Wilson B, Block ML, Wang CC, Kinyamu H, Lu N, Gao X, Leng Y, Chuang DM, Zhang W, Lu RB, Hong JS (2008) Histone deacetylase inhibitors up-regulate astrocyte GDNF and BDNF gene transcription and protect dopaminergic neurons. *Int J Neuropsychopharmacol* **11**:1123-1134

Wyttenbach A (2004) Role of heat shock proteins during polyglutamine neurodegeneration. *J. Mol. Neurosci* **23**, 69–95

Xiao T, Zhang W, Jiao B, Pan CZ, Liu X, Shen L (2017) The role of exosomes in the pathogenesis of Alzheimer' disease. *Transl Neurodegener* **6**:3

Xin H, Wang F, Li Y, Lu QE, Cheung WL, Zhang Y, Zhang ZG, Chopp M (2017) Secondary Release of Exosomes From Astrocytes Contributes to the Increase in Neural Plasticity and Improvement of Functional Recovery After Stroke in Rats Treated With Exosomes Harvested From MicroRNA 133b-Overexpressing Multipotent Mesenchymal Stromal Cells. *Cell Transplant* **26**: 243-257.

Yang W, Wang G, Wang CE, Guo X, Yin P, Gao J, Tu Z, Wang Z, Wu J, Hu X, Li S, Li XJ (2015) Mutant alpha-synuclein causes age-dependent neuropathology in monkey brain. *J Neurosci* **35**: 8345-58

Yano H, Baranov SV, Baranova OV, Kim J, Pan Y, Yablonska S, Carlisle DL, Ferrante RJ, Kim AH, Friedlander RM (2014) Inhibition of mitochondrial protein import by mutant huntingtin. *Nature neuroscience **17**,* 822-831.

Yu ZX, Li SH, Evans J, Pillarisetti A, Li H, Li XJ (2003) Mutant huntingtin causes context-dependent neurodegeneration in mice with Huntington's disease. *J Neurosci* **23**: 2193-202.

Yue Q, Groszer M, Gil JS, Berk AJ, Messing A, Wu H, Liu X (2005) PTEN deletion in Bergmann glia leads to premature differentiation and affects laminar organization. *Development* **132**: 3281-91

Zabel C, Chamrad DC, Priller J, Woodman B, Meyer HE, Bates GP, Klose J (2002) Alterations in the mouse and human proteome caused by Huntington's disease. *Mol Cell Proteomics* **1**: 366-75.

Zeitlin S, Liu JP, Chapman DL, Papaioannou VE, Efstratiadis A (1995) Increased apoptosis and early embryonic lethality in mice nullizygous for the Huntington's disease gene homologue. *Nat Genet* **11**:155-163.

Zhao T, Hong Y, Li S, Li XJ (2016) Compartment-Dependent Degradation of Mutant Huntingtin Accounts for Its Preferential Accumulation in Neuronal Processes. *J Neurosci* **36**: 8317-8328.

Zhang X, Abels ER, Redzic JS, Margulis J, Finkbeiner S, Breakefield XO (2016) Potential Transfer of Polyglutamine and CAG-Repeat RNA in Extracellular Vesicles in Huntington's Disease: Background and Evaluation in Cell Culture. *Cell Mol Neurobiol*. **36**: 459-70.

Zhao Y, Haney MJ, Gupta R, Bohnsack JP, He Z, Kabanov AV, Batrakova EV (2014) GDNF-transfected macrophages produce potent neuroprotective effects in Parkinson's disease mouse model. *PLoS One* **9**:e106867

Zheng T, Pu J, Chen Y, Mao Y, Guo Z, Pan H, Zhang L, Zhang H, Sun B, Zhang B (2017) Plasma Exosomes Spread and Cluster Around β-Amyloid Plaques in an Animal Model of Alzheimer's Disease. *Front Aging Neurosci* **9**:12

Zoghbi HY and Orr HT (2000 Glutamine repeats and neurodegeneration. *Annu Rev Neurosci* **23**, 217-247.

Zuccato C, Ciammola A, Rigamonti D, Leavitt BR, Goffredo D, Conti L, MacDonald ME, Friedlander RM, Silani V, Hayden MR, Timmusk T, Sipione S, Cattaneo E (2001) Loss of huntingtin-mediated BDNF gene transcription in Huntington's disease. *Science* **293**: 493-498.

Zuccato C, Tartari M, Crotti A, Goffredo D, Valenza M, Conti L, Cataudella T, Leavitt BR, Hayden MR, Timmusk T, Rigamonti D, Cattaneo E (2003) Huntingtin interacts with REST/NRSF to modulate the transcription of NRSE-controlled neuronal genes. *Nat Genet* **35**: 76–83.

Zuccato C, Liber D, Ramos C, Tarditi A, Rigamonti D, Tartari M, Valenza M, Cattaneo E (2005) Progressive loss of BDNF in a mouse model of Huntington's disease and rescue by BDNF delivery. *Pharmacol Res* **52**: 133-139.

Zuccato C and Cattaneo E (2007) Role of brain-derived neurotrophic factor in Huntington's disease. *Progress in Neurobiology* **81**: 294-330.